

**Role of eNOS and Nrf2 in
the vascular effects of
(-)-epicatechin**

[Die Rolle von eNOS und Nrf2 bei den vaskulären Effekten von
(-)-Epicatechin]

Inaugural-Dissertation
zur Erlangung des Doktorgrades
der Mathematisch-Naturwissenschaftlichen Fakultät
der Heinrich-Heine-Universität Düsseldorf

vorgelegt von

Tomasz Krenz

aus Lukow, Polen

Düsseldorf, 2014

Aus der Klinik für Kardiologie, Pneumologie und Angiologie des
Universitätsklinikums der Heinrich-Heine-Universität, Düsseldorf

Gedruckt mit der Genehmigung der
Mathematisch-Naturwissenschaftlichen Fakultät der
Heinrich-Heine-Universität Düsseldorf

Referent: Univ.-Prof. Dr. med. Malte Kelm

Koreferent: Univ.-Prof. Dr. rer. nat. Eckhard Lammert

Tag der mündlichen Prüfung 03.02.2014

Hiermit erkläre ich ehrenwörtlich, dass ich die vorliegende Dissertation selbständig angefertigt habe und keine anderen als die angegebenen Quellen und Hilfsmittel benutzt habe.

Diese Dissertation wurde weder in gleicher noch in ähnlicher Form in einem anderen Prüfungsverfahren vorgelegt. Außerdem erkläre ich, dass ich bisher noch keine weiteren akademischen Grade erworben oder zu erwerben versucht habe.

Düsseldorf, den 06.01.2014

Tomasz Krenz

Abstract

The mechanisms by which dietary flavanols mediate their vascular effects are not well understood. Accumulating data support the evidence that flavanol-rich foods like cocoa are able to improve endothelium-dependent vasorelaxation in healthy subjects, as well as in pathological conditions. Proposed mechanisms include an increase in nitric oxide (NO)-bioavailability by direct activation of the endothelial NO synthase (eNOS) or by affecting the redox state of vascular cells. (-)-Epicatechin is the most abundant flavanol monomer in cocoa and seems to be the active component responsible for those effects. However a direct link between the eNOS/NO signaling pathway and vascular response to (-)-epicatechin *in vivo* has never been demonstrated so far. The transcription factor nuclear factor (erythroid-derived 2)-like 2 (Nrf2) is a key master switch controlling the expression of enzymes involved in the regulation of the cellular redox state, is activated by electrophilic compounds, and it is a potential *in vivo* target of (-)-epicatechin or its circulating metabolites.

This work aimed at investigating the role of eNOS and Nrf2 in the vascular response to (-)-epicatechin in living mice. This study provides novel evidence that both eNOS and Nrf2 are required to improve vascular function by (-)-epicatechin *in vivo* and indeed are targets of circulating (-)-epicatechin metabolites in vascular tissue. The underlying mechanisms include an activation of eNOS by phosphorylation and increased NO-bioavailability as assessed by increases in the secondary messenger cyclic guanosine monophosphate (cGMP), and activation of cGMP-dependent kinase (PKG)-dependent vasodilator-stimulated phosphoprotein (VASP) phosphorylation, along with regulation of glutathione (GSH) levels and Nrf2-dependent expression of antioxidant response genes and redox state in the heart and in the lung of the mice. These effects are absent by administration of NOS inhibitors, and in mice lacking eNOS (eNOS^{-/-}) or Nrf2 (Nrf^{-/-}). In addition, novel potential pathways targeted by (-)-epicatechin were identified in vascular tissue by global transcriptional profiling, including regulation of the xenobiotic defense pathway controlled by the aryl hydrocarbon receptor (AhR) as well as calcium signaling/handling in the smooth muscle cell. In conclusion both, increased NO production by eNOS and reduced NO consumption by Nrf2 mediated antioxidant defense can increase NO-bioactivity in the vascular wall.

Zusammenfassung

Die Mechanismen für die vaskulären Effekte von Nahrungsflavanolen sind weitgehend unbekannt. Immer mehr Daten deuten darauf hin, dass flavanolreiche Nahrungsmittel, wie beispielsweise Kakao in der Lage sind die endothelabhängige Gefäßfunktion im Menschen unter physiologischen und pathophysiologischen Bedingungen zu verbessern. Es wird angenommen, dass eine Erhöhung der Stickstoffmonoxid (NO) Verfügbarkeit durch Aktivierung der endothelialen NO Synthase (eNOS), und eine Regulation des Redoxsystems vaskulärer Zellen zu den zugrundeliegenden Mechanismen gehören. (-)-Epicatechin ist die häufigste monomere Flavanol Substanz im Kakao und scheint als solche aktiv für die Effekte von Flavanolen verantwortlich zu sein. Allerdings wurde der direkte Zusammenhang zwischen der eNOS/NO Signalkaskade und der (-)-Epicatechin vermittelten vaskulären Antwort noch nicht gezeigt. Der Transkriptionsfaktor *nuclear factor (erythroid-derived 2)-like 2* (Nrf2) ist ein Master-Regulator für die Kontrolle des zellulären Redoxstatus durch Regulation der Expression beteiligter Enzyme. Nrf2 kann durch elektrophile Substanzen aktiviert werden, potentiell auch durch (-)-Epicatechin oder entsprechende zirkulierende Metabolite.

Das Ziel dieser Arbeit war es daher die Rolle von eNOS und Nrf2 in der Gefäßantwort auf (-)-Epicatechin in vivo zu untersuchen. Diese Arbeit zeigt, dass sowohl eNOS als auch Nrf2 notwendig sind, um die Gefäßfunktion in vivo zu erhöhen, und dass diese Faktoren an den Mechanismen im vaskulären Gewebe beteiligt sind. Zu den zugrundeliegenden Mechanismen gehören: Eine Aktivierung der eNOS durch Erhöhung der Phosphorylierung; Eine Erhöhung der NO Verfügbarkeit gemessen als Erhöhung des sekundären Botenstoffes zyklisches Guanosinmonophosphat (cGMP) und Aktivierung der cGMP-abhängigen Proteinkinase (PKG), gezeigt als Erhöhung der vasodilatator-stimulierten Phosphoprotein (VASP) phosphorylierung. Darüber hinaus wurde eine Regulation des Redoxsystems im kardiovaskulären Gewebe wie dem Herzen und der Lunge als Erhöhung der Glutathion (GSH) Level nachgewiesen. Wichtig ist, dass diese Effekte in eNOS^{-/-} und Nrf^{-/-} Mäusen, und mit NOS-Inhibition nicht länger nachweisbar waren. Des weitern was es durch Microarray Analysen in dieser Arbeit möglich neue potentielle Signalwege für die vaskulären Effekte von (-)-Epicatechin zu

Zusammenfassung

identifizieren, darunter Signalkaskaden zum Abbau xenobiotischer Substanzen unter Kontrolle des Aryl-Hydrocarbon-Rezeptors (AhR), sowie die Regulation der Kalzium-Homöostase in vaskulären, glatten Muskelzellen. Zusammenfassend sind eine Erhöhung der NO Produktion durch eNOS und ein erniedrigter NO Abbau durch die Nrf2 vermittelte antioxidative Antwort maßgeblich für Erhöhung der NO Verfügbarkeit in der Gefäßwand.

Table of Contents

ABSTRACT	III
ZUSAMMENFASSUNG	IV
TABLE OF CONTENTS	VI
FIGURE INDEX	IX
TABLE INDEX	X
ABBREVIATIONS	XI
INTRODUCTION	1
Flavanols and cardiovascular health	1
Cardiovascular disease and endothelial dysfunction	1
Flavanols and control of endothelial function: a role of eNOS ?	3
The vascular NO pool	5
Flavanols and vascular function	6
Regulation of vascular antioxidant state by dietary flavanols	7
In vivo assessment of endothelial function	10
AIM OF THE STUDY	13
MATERIALS AND METHODS	15
Materials	15
Mice	17
Genotyping	18
Collection of mice blood and organs	18
Experimental setup	19
Oral administration of (-)-epicatechin to mice	19
Inhibition of nitric oxide synthase (NOS)- and cyclooxygenase (COX)	19
Treatment with vasoactive drugs	20
In vivo measurements in mice	21
LDPI Measurements	21
Ultrasound Measurements	22
Assessment of PORH	24

Table of Contents

Surgical excision of the femoral artery	25
Assessment of blood pressure	26
Biochemical analysis	26
Western Blot	26
cGMP	27
GSH	28
Molecular biological analysis	28
Real Time PCR	28
Microarray analysis	29
Analytical analysis	30
Measurement of nitrate and nitrite	30
Measurement of (-)-epicatechin metabolites	30
Statistical Analyses	31
RESULTS	32
1. Plan of the study and experimental setup	32
2. Proof of concept: (-)-Epicatechin is rapidly absorbed and metabolised in living mice	33
3. (-)-Epicatechin increases vascular reactivity in mice in vivo	34
3.1: Establishment of in vivo methods for assessment of vascular function: ultrasound and LDPI	34
3.1.1: Vasoactive molecules modulate the vascular diameter and mean perfusion in the hindlimb.	34
3.1.2: Post-occlusive reactive hyperemia (PORH) in the hindlimb of the mouse	37
3.1.3: Validation of PORH in mouse hindlimb assessed by LDPI	39
3.1.4: Endogenous vasodilators modulate the PORH response	41
3.1.5: PORH response decreases with age in mice.	42
3.2: Oral (-)-epicatechin increases vascular function in living mice	44
3.2.1: (-)-Epicatechin increases vascular function in an eNOS-dependent fashion	44
3.2.2: (-)-Epicatechin increases vascular function in a Nrf2-dependent fashion	47
4: Molecular mechanisms (I) – (-)-Epicatechin activates eNOS mediated NO-signaling	50
4.1: (-)-Epicatechin activates eNOS in the vasculature in vivo by increasing phosphorylation	50
4.2: Increased eNOS activity leads to an increase in vascular NO-bioactivity	52
4.2.1: The increase in vascular NO-bioactivity is eNOS dependent	52
4.2.2: The increase in vascular NO-bioactivity in Nrf2 dependent	54
4.3: Effect of (-)-epicatechin on systemic NO-bioavailability.	55
5. Molecular mechanisms (II) – effects of (-)-epicatechin on tissue redox state (GSH)	56
5.1: (-)-Epicatechin increases redox state in tissues of the cardiovascular system	56
5.2: The increase in redox state in tissues of the cardiovascular system is Nrf2 dependent	58
5.3: (-)-Epicatechin regulates the expression of antioxidant genes in cardiovascular tissues	59
6. Identification of novel targets of (-)-epicatechin in vascular tissue by microarray analysis	61
6.1: Transcriptional profiling of genes in an (-)-epicatechin dose-response model	61
6.2: Functional analysis of genes constitutively induced or suppressed by (-)-epicatechin	64

Table of Contents

6.3: Analysis of pathways constitutively regulated by low and high dose (-)-epicatechin	67
6.4: Novel potential targets of (-)-epicatechin – AhR and Xenobiotic metabolism	69
6.5: Novel potential targets of (-)-epicatechin – Ca ⁺⁺ -signaling in vascular smooth muscle cells	71
7. Summary of main findings	74
DISCUSSION	75
Why assessing the effects of (-)-epicatechin in vivo in mice ?	75
Is eNOS required for the beneficial vascular effects of (-)-epicatechin in vivo?	76
Is maintenance of NO-bioavailability and redox state essential for the effects of (-)-epicatechin ?	78
Is Nrf2 required for the beneficial vascular effects of (-)-epicatechin in vivo?	81
What other mechanisms are involved in the vascular effects of (-)-epicatechin ?	86
Transcriptional profiling of genes in an (-)-epicatechin dose-response model	86
Novel (-)-epicatechin targets: vascular smooth muscle signalling and protection from toxic and oxidative stress	87
Establishing a mouse model for assessment of vascular function	92
What is the origin of the LDPI signal in mouse hindlimb?	92
Measurements of PORH: reproducibility and dependency on physiological stimuli.	93
Summary and Conclusion	95
Why is this study relevant for translational flavanol research ?	97
REFERENCES	99
ACKNOWLEDGMENT	111
CURRICULUM VITAE	113

Figure index

Fig. 1: Groups, structures, and examples of flavonoid substances and their food distribution.	2
Fig. 2: eNOS derived NO from the endothelium mediates vasodilation by regulation of sGC/cGMP signaling.	4
Fig. 3: eNOS and NO in the circulation.	5
Fig. 4: Potential effects of flavanols on NO-bioactivity.	14
Fig. 5: Set up and measurement principles of Laser Doppler perfusion imaging (LDPI).	22
Fig. 6: Measurement of pulse wave velocity (PWV).	23
Fig. 7: Induction of reactive hyperemic blood flow in mouse hindlimb.	25
Fig. 8: Experimental plan for the analysis of oral (-)-epicatechin effects in mice in vivo	32
Fig. 9: (-)-Epicatechin is absorbed and metabolized in mice.	33
Fig. 10: (-)-Epicatechin has a dose-dependent effect on vascular function	34
Fig. 11: Pharmacological modulation of vascular diameter and hindlimb perfusion.	36
Fig. 12: Physiological modulation of diameter change in the femoral artery by PORH.	37
Fig. 13: Physiological modulation of hindlimb perfusion by PORH.	38
Fig. 14: Course and slope of PORH assessed as FMD and changes in MPU.	39
Fig. 15: Validation of the PORH response as assessed by LDPI	40
Fig. 16: The hyperemic response is NOS and COX dependent.	41
Fig. 17: The degree of PORH decreases with age.	43
Fig. 18: (-)-Epicatechin increases FMD and accelerates PORH in vivo in an eNOS dependent fashion.	45
Fig. 19: (-)-Epicatechin increases vascular pulsatility in mice.	46
Fig. 20: (-)-Epicatechin does not improve FMD in <i>Nrf2</i> ^{-/-} mice in vivo.	48
Fig. 21: (-)-Epicatechin does not improve PORH in <i>Nrf2</i> ^{-/-} mice in vivo	49
Fig. 22: (-)-Epicatechin increases eNOS phosphorylation in the aorta.	51
Fig. 23: (-)-Epicatechin increases eNOS phosphorylation in the lung.	52
Fig. 24: (-)-Epicatechin activates the NO-stimulated cGMP – PKG pathway in aorta in a NOS dependent fashion.	53
Fig. 25: Effect of (-)-epicatechin on NO-bioavailability in <i>Nrf2</i> ^{-/-} mice.	54
Fig. 26: Effect of (-)-epicatechin on systemic NO-bioavailability.	55
Fig. 27: (-)-Epicatechin increases redox state in cardiovascular tissues.	57
Fig. 28: Effect of (-) epicatechin on redox state in <i>Nrf2</i> ^{-/-} mice.	58
Fig. 29: Protein expression of antioxidative genes in aorta after (-)-epicatechin treatment.	59
Fig. 30: Protein expression of genes involved in GSH metabolism in heart, lung and liver after (-)-epicatechin treatment.	60
Fig. 31: Strategy of comparative micro-array analysis to identify gene clusters regulated by (-)-epicatechin in vivo.	62
Fig. 32: Transcriptional profiling of targets dose-dependently regulated by (-)-epicatechin in mice in vivo.	63
Fig. 33: (-)-Epicatechin regulated pathways contributing to maintenance of vascular health by regulation of stress response and vascular functionality.	68
Fig. 34: mRNA expression of AhR in the aorta after 2 mg/kg and 10 mg/kg (-)-epicatechin treatment.	69
Fig. 35: Regulation of MLCK and MYPT in the aorta.	73
Fig. 36: Summary of the main results of this study.	74
Fig. 37: Network of (-)-epicatechin regulated genes involved in the NO- and Ca ⁺⁺ -mediated process of vascular muscle relaxation / contraction.	91
Fig. 38: (-)-Epicatechin increases vascular reactivity by regulation of eNOS/sGC/cGMP signaling and its effectors in smooth muscle cells.	96

Table index

Tab. 1: Chemicals	15
Tab. 2: Kits	16
Tab. 3: Equipment	16
Tab. 4: Instruments	17
Tab. 5: Software	17
Tab. 6: Antibodies for western-blot	26
Tab. 7: Primer for real time PCR	29
Tab. 8: Physiological parameter during administration of vasoactive drugs	37
Tab. 9: NOS-dependence of PORH by LDPI	42
Tab. 10: Blood pressure is not changed by (-)-epicatechin	47
Tab. 11: Level of nitrite and nitrate in plasma of Nrf2 knockout and wildtype mice after 2 mg/kg (-)-epicatechin treatment	56
Tab. 12: Top 20 most regulated genes in the aorta by 2 mg/kg and 10 mg/kg (-)-epicatechin determined by microarray analysis.	64
Tab. 13: Annotation Clustering of Genes constitutively induced or suppressed by 2 mg/kg (-)-epicatechin using DAVID Analysis	65
Tab. 14: Annotation Clustering of Genes constitutively induced or suppressed by 10 mg/kg (-)-epicatechin using DAVID Analysis	66
Tab. 15: Functional Clustering of Genes Constitutively regulated by 2 mg/kg and 10 mg/kg (-)-epicatechin using DAVID Analysis and KEGG pathway Analysis	67
Tab. 16: Summary of genes involved in Glutathione , Xenobiotic and Drug metabolism that are up- or down-regulated by 2 mg/kg and 10 mg/kg (-)-epicatechin in the aorta	70
Tab. 17: Summary of genes involved in Ca ⁺⁺ -signaling and vascular smooth muscle contraction that are up- or down-regulated by 2 mg/kg and 10 mg/kg (-)-epicatechin in the aorta	72

Abbreviations

Abbreviations

Abbreviations			
ACH	Acetylcholine	NRF2	Nuclear factor (erythroid-derived 2)-like 2
Akt	Protein kinase B	NRF2^{-/-}	NRF2 knockout mice
ANOVA	Analysis of variance	NTG	Nitroglycerine
approx.	Approximately	p	statistical probability value
ARNT	Aryl hydrocarbon Receptor Nuclear Translocator protein	PBS	Phosphate buffered saline
AUC	Area under curve	PCR	Polymerase Chain Reaction
BP	Blood pressure	PD	Diastolic pressure
BW	Body weight	PI₃K	Phosphatidylinositide 3-kinase
C57/BL6	Mice wildtype strain	PKA	Protein kinase A
Ca⁺⁺	Calcium	PKC	Protein kinase C
CAEC	Coronary artery endothelial cells	PKG	cGMP dependent kinase
CaM	Calmodulin	PLC	Phospholipase C
cAMP	Cyclic adenosine monophosphate	PS	Systolic pressure
cDNA	Complementary DNA	PORH	Post-occlusive reactive hyperemia
cGMP	Cyclic guanosine monophosphate	PWV	Pulse wave velocity
CV	Coefficient of variation	RASMC	Rat aortic smooth muscle cells
d	Diameter	RIPA	Radio immunoprecipitation assay
DAVID	Database for Annotation, Visualization and Integrated Discovery	RLT	Guanidine thiocyanate buffer
DNA	Deoxyribonucleic acid	RNA	Ribonucleic acid
dNTP	Deoxynucleotide	ROS	Reactive oxygen species
e.g.	<i>exempli gratia</i> - for example	RR	Respiration rate
EGCG	Epigallocatechin-3-gallate	RT	Reverse transcription
eNOS	Endothelial nitric oxide synthase	RX-NO	S-nitrosothiols + other nitroso species
eNOS^{-/-}	eNOS knockout mice	s.c.	Subcutaneous
etc.	Etcetera	SD	Standard Deviation
FAD	Flavin adenine dinucleotide	SEM	Standard error of mean
Fig.	Figure	Ser	Serine
FMD	Flow-mediated dilation	sGC	Soluble guanylate cyclase
FMN	Flavin mononucleotide	Tab.	Table
GSH	Glutathione	THB	Tetrahydropteridin
GSSG	Glutathione disulfide	VEGF	Vascular Endothelial Growth Factor
H₂O	Water	Wt	Wildtype
H₂O₂	Hydrogen Peroxide		
HepG2	hepatocellular carcinoma cell line	%	Percent
HPLC	High-performance liquid chromatography	°C	Degree Celsius
HR	Heart rate	cm	Centimetre
HUVEC	Human umbilical vein endothelial cells	C_t	Threshold cycle
i.e.	<i>id est</i> - that is	g	Gram
i.p.	Intraperitoneal	g	Gravity-force
i.v.	Intravenous	IU	International unit
IgG	Immunoglobulin G	h	Hour
IP₃R	Inositol trisphosphate receptor	kD	Kilodalton
IRAG	IP ₃ R-associated cGMP kinase substrate	kg	Kilogram
KEGG	Kyoto Encyclopedia of Genes and Genomes	M	Mol / l
L-Arg	L-Arginine	mg	Milligram
L-NNA	N ^ω -nitro-L-arginine	MHz	Megahertz
LANUV	<i>Landesamt für Natur, Umwelt und Verbraucherschutz</i>	min.	Minute
LDPI	Laser Doppler Perfusion Imaging	ml	Mililitre
MAPK	Mitogen-activated protein kinases	mm	Millimetre
max.	Maximum	mM	Millimol / l
min.	Minimum	mmHg	Millimeter of mercury
MLC	Myosin light chain	MPU	Mean perfusion units
mo	Month	ms	Millisecond
mRNA	Messenger RNA	nm	Nanometre
N	Number	pH	hydrogen ion concentration of a solution
NADPH	Nicotinamide adenine dinucleotide phosphate	pM	Picomol / l
NO	Nitric oxide	rpm	Rounds per minute
NO₂⁻	Nitrite	s	Second
NO₃⁻	Nitrate	V	Volt
NOS	Nitric oxide synthase	µg	Microgram
NOx	NO metabolites	µl	Microlitre
		µM	Micromol / l

Note: Gene names and chemicals are listed separately in the methods section

Introduction

Flavanols and cardiovascular health

Cardiovascular disease and endothelial dysfunction

Cardiovascular disease is a leading cause of death worldwide. Risk factors of modern life-style for experiencing an initial or recurrent cardiovascular event are obesity, lack of physical activity, smoking and alcohol consumption (Wang et al. 2009). Heart failure, coronary artery disease, hypertension and others are associated with endothelial dysfunction (Widlansky et al. 2003). A dysfunctional endothelium is characterized by a loss of endothelial control over vascular tone, impairment of endothelium-dependent vasorelaxation, alteration of the anticoagulant and anti-inflammatory properties leading to thrombosis, and vessel wall remodeling (impaired regulation of vascular growth) (Widlansky et al. 2003, Seals et al. 2011).

A growing number of therapeutic interventions known to decrease cardiovascular risk, including exercise, lipid lowering, smoking cessation, weight reduction, medication with angiotensin-converting enzyme inhibitors and statins and also dietary interventions, have been shown to improve endothelial function (Widlansky et al. 2003). The daily diet can play a major role in prevention of vascular disease initiation and progression (Eyre et al. 2004). Besides regulation of fat consumption, blood pressure and blood glucose levels current dietary recommendations include the consumption of fruits and vegetables (Lichtenstein et al. 2006) proven by epidemiological studies demonstrating a lower risk for cardiovascular disease (He et al. 2007) (Bhupathiraju et al. 2013). Despite the fact that they are low in calories and fat and have a favorable mineral ratio the mechanisms by which these diets mediate their beneficial effects on health still are not well understood (Dauchet et al. 2009).

There is epidemiological evidence that flavonoids mediate beneficial cardiovascular effects and lower the risk for vascular diseases and mortality (Mulvihill et al. 2010, McCullough et al. 2012, Toh et al. 2013). The group of flavonoids includes a number of various substances with different chemical properties including flavanols, flavonols, flavones, isoflavones, flavanones, and anthocyanins (Fig. 1). This can result in severe differences in their absorption, metabolism and bioactivities (Erdman et al. 2007). Moreover since the distribution of these flavonoids varies considerably in different

fruits and vegetables (Erdman et al. 2007) it is difficult to estimate an average dietary consumption in human.

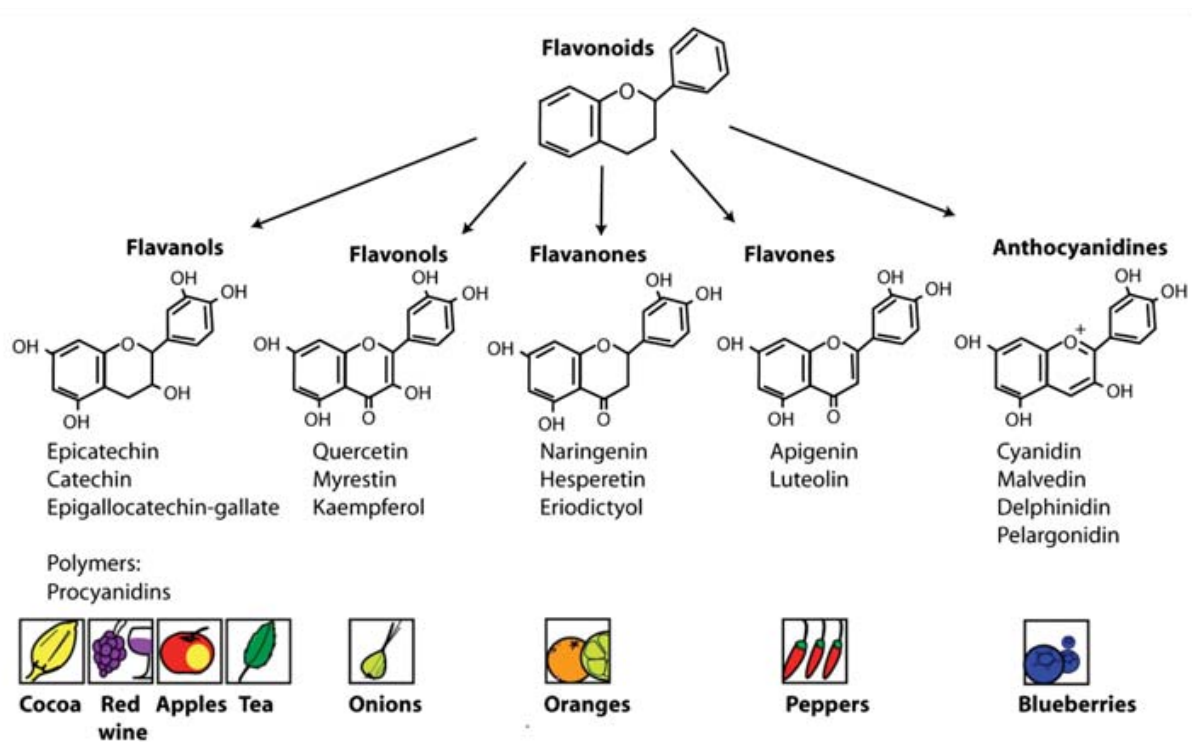


Fig. 1: Groups, structures, and examples of flavonoid substances and their food distribution. (Taken from Heiss and Kelm, 2010 (Heiss et al. 2010)).

The absorption and metabolism of cocoa flavanols and pure flavanol compounds such as (-)-epicatechin *in vivo* is studied in humans (Schroeter et al. 2006, Ottaviani et al. 2011) and also in animal models (Piskula et al. 1998, Baba et al. 2001, Donovan et al. 2006). There is evidence that the majority of circulating compounds found in blood are monomeric (-)-epicatechin compounds, which are methylated, glucuronidated, or sulfated (Schroeter et al. 2006, Ottaviani et al. 2011). However adsorption sites and kinetics are still not completely understood, tissue distribution and the metabolic and biological fate of flavanols, their monomeric compounds and respective metabolites are under active investigation. It is likely that the physiological effects are induced by fewer monomeric compounds. Among cocoa flavanols, the most abundant monomeric

compound is (-)-epicatechin (Gu et al. 2004, Heiss et al. 2010). It has been shown that administration of pure (-)-epicatechin, accounts for the beneficial effects of flavanols on endothelial function and the increase of circulating NO metabolites in humans (Schroeter et al. 2006) and is the single stereoisomer capable of mediating such significant vasodilatory responses (Ottaviani et al. 2011).

Flavanols and control of endothelial function: a role of eNOS ?

The health and functionality of the vascular system is strongly correlated to the functionality of the endothelium, which lines the luminal side of the vessels. The endothelial cell layer controls many biological events occurring either on the endoluminal or the interstitial side of the vasculature. Many processes including haemostasis, haematopoiesis, inflammatory reactions and immune response require close interactions between circulating cells or cytokines and the vascular endothelium (Mantovani et al. 1997). One of the most important signal transduction cascades is the release of a vasodilating factor by endothelial cells in response to blood flow mediated shear stress (Furchgott et al. 1980, Smiesko et al. 1993). The identification of this “endothelium-derived relaxing factor” as nitric oxide (NO) over 20 years ago is a milestone of cardiovascular research and was awarded with the nobel price in medicine (Furchgott et al. 1987, Ignarro et al. 1987, Palmer et al. 1987). One year later the source of this endothelial NO production was found to be the type 3 isoform of nitric oxide synthase or endothelial nitric oxide synthase (eNOS) (Palmer et al. 1988). Meanwhile the mechanism and signal transduction cascade leading to vasodilation by endothelial NO release is well investigated (Nausch et al. 2008, Morgado et al. 2012). Endothelial NOS derived NO is released from the vascular endothelium into vascular smooth muscle cells where it activates the enzyme soluble guanylate cyclase (sGC) and thereby production of the secondary messenger cyclic guanosine monophosphate (cGMP). Cyclic GMP increases the activity of a cGMP dependent protein kinase (PKG), which directly activates a myosin phosphatase and inhibits intracellular calcium (Ca^{++})

release leading to a decrease in the activity of a myosin kinase. Both lead to a reduced myosin phosphorylation state and thus to smooth muscle relaxation and vasodilation (Fig. 2). Moreover NO can exert its effects also through non cGMP/PKG-dependent mechanisms including changes in cAMP (cyclic adenosine monophosphate) -signaling (Cornwell et al. 1994, Bassil et al. 2006, Arejian et al. 2009) and interaction with endothelin receptor signaling (Lüscher et al. 1990, Redmond et al. 1996).

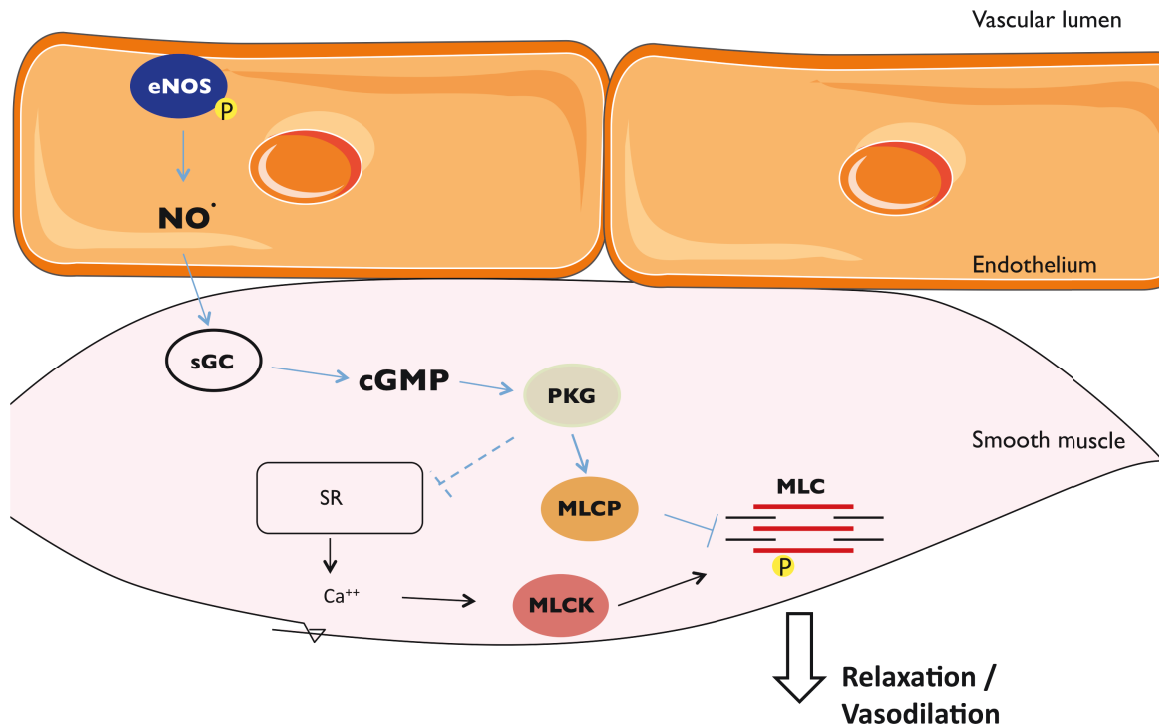


Fig. 2: eNOS derived NO from the endothelium mediates vasodilation by regulation of sGC/cGMP signaling.

eNOS = endothelial nitric oxide synthase, P = phosphorylation, NO = nitric oxide, sGC = soluble guanylate cyclase, cGMP = cyclic guanosine monophosphate, PKG = cGMP dependent protein kinase, SR = sarcoplasmic reticulum, Ca⁺⁺ = calcium, MLCP = myosin light chain phosphatase, MLCK = myosin light chain kinase, MLC = myosin light chain.

The vascular NO pool

Endothelial NOS-derived NO can migrate into the lumen of the vessel where it can further react to produce the circulating pool of NO metabolites (NO_2^- , NO_3^- , R-SNO, R-NNO) which transport NO-bioavailability in regions of the vasculature where eNOS expression is decreased (Rassaf et al. 2006). In addition the main blood cell subpopulations, including red blood cells (Cortese-Krott et al. 2012), carry an eNOS and thus actively contribute to the circulating NO pool (Cortese-Krott et al. 2012, Wood et al. 2013) (Fig.3).

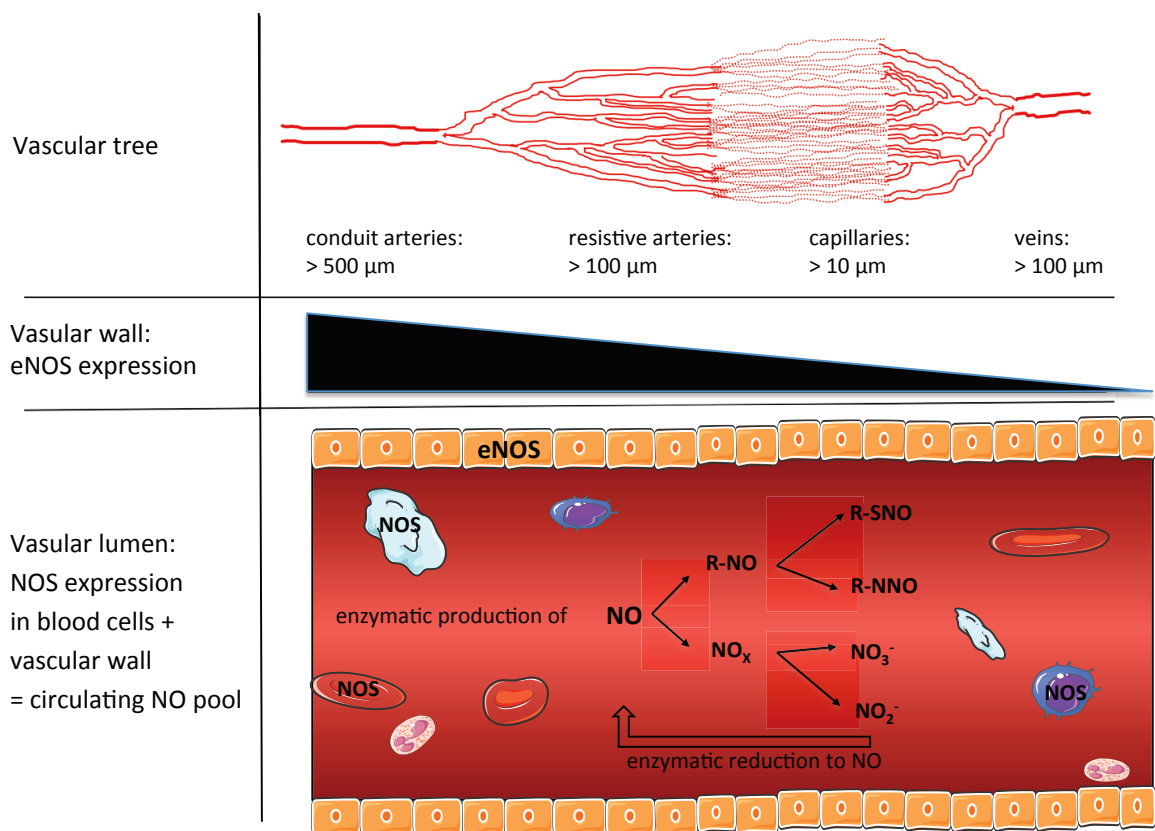


Fig. 3: eNOS and NO in the circulation.

Within the circulation eNOS is expressed in the vascular wall, but also in blood cells in the vascular lumen. Under normoxic conditions NO is produced enzymatically by NOS while reduction of nitrate (NO_3^-) and nitrite (NO_2^-) to NO takes place under low oxygen conditions. The sum of circulating NO species consist of oxidized and conjugated NO forms in the blood produced by endothelial cells of the vascular wall and blood cells. NOS = nitric oxide synthase, NO = nitric oxide, R-NO = covalently bound NO as nitrosothiol (R-SNO) or nitrosoamine (R-NNO).

The balanced production and release of vasodilators, most importantly eNOS derived NO maintains vascular homeostasis and regulates vascular tone. In addition to its vasodilating feature, endothelial NO has antiatherosclerotic properties, such as inhibition of platelet aggregation, leukocyte adhesion, smooth muscle cell proliferation, and expression of genes involved in atherogenesis (Li et al. 2000). Thus a decrease in NO-bioavailability (Kleinbongard et al. 2003, Heiss et al. 2006, Rassaf et al. 2006) and alterations in eNOS activity and expression are strongly associated with endothelial dysfunction and cardiovascular disease (Widlansky et al. 2003, Seals et al. 2011).

Flavanols and vascular function

The oral intake of cocoa flavanols and pure (-)-epicatechin has beneficial effects in particular on improvement of endothelium-dependent vascular function as has been shown by work conducted by our and other groups (Heiss et al. 2003, Schroeter et al. 2006, Heiss et al. 2007). Further an improvement of insulin sensitivity, a decrease in blood pressure (Hooper et al. 2012) and a reduced platelet aggregation (Ostertag et al. 2010) are reported for dietary cocoa flavanols. The pharmacology and mechanistic action of flavanols in vivo are not well understood, but they likely include a modulation of the immune response as shown for the cocoa compound procyanidin (Kenny et al. 2007), an activation of angiogenic cells by flavanol-rich cocoa drinks (Heiss et al. 2010). Most importantly cocoa flavanols and (-)-epicatechin enhance NO-bioavailability in health (Schroeter et al. 2006, Heiss et al. 2007, Loke et al. 2008) and state of increased cardiovascular risk including hypertension (Grassi et al. 2005), age (Holt et al. 2012) and smoking (Heiss et al. 2005, Heiss et al. 2007).

Importantly the oral intake of a pure (-)-epicatechin drink improved vascular function assessed as flow-mediated dilation (FMD) of the brachial artery in healthy male subjects with a maximum response after two hours (Schroeter et al. 2006). Also a longer intake of a high-flavanol drink containing (-)-epicatechin gradually increased FMD after one, three, five and seven days in healthy smokers (Heiss et al. 2007) and in healthy adults (Engler et al. 2004). Long-term improvement of FMD by cocoa flavanols

has also been shown in pathological state for patients with coronary artery disease (Heiss et al. 2010), diabetes (Balzer et al. 2008), obesity (Njike et al. 2011) and hypertension (Grassi et al. 2005).

The underlying mechanisms, which mediate the beneficial action of cocoa flavanols on vascular health are not well understood and are very poorly investigated in vivo. Proposed mechanisms include an increase in NO-bioavailability by direct activation of eNOS or by affecting the redox state of vascular cells. Endothelial NOS activity can be regulated by post-translational modifications, most importantly phosphorylation, but the enzyme can also be regulated on the transcriptional level (Forstermann et al. 1998). Studies mostly in cultured vascular endothelial cells suggest that red wine polyphenols (RWPs) and (-)-epicatechin are able to activate the eNOS enzyme (Leikert et al. 2002, Wallerath et al. 2003, Ndiaye et al. 2005, Ramirez-Sanchez et al. 2010, Ramirez-Sanchez et al. 2011). However, in vitro findings cannot be directly transferred to the in vivo situation because of the distinct limitations such as 1) lack of metabolism, 2) lack of systemic action and 3) lack of the direct interaction between vascular endothelium and vascular smooth muscle which is mandatory for vessel function. In human it is not possible to directly measure eNOS and NO-signaling to the vessels. The in vivo effect in rodents is poorly investigated and limited to studies in rats with RWPs (Andriambeloson et al. 1997, Benito et al. 2002, Agouni et al. 2009) and (-)-epicatechin (Gomez-Guzman et al. 2012) demonstrating elevated level of NO and cGMP in the aorta.

Regulation of vascular antioxidant state by dietary flavanols

The occurrence of endothelial dysfunction in pathophysiological state is not only correlated to reduced NO production but also to increased oxidative stress within the tissue. For instance, the decline in NO-bioavailability observed in a dysfunctional endothelium seems to be determined by an accelerated degradation of NO by reactive oxygen species (ROS) during oxidative stress, as well as by decreased activity or

expression of eNOS (Weseler et al. 2010, Seals et al. 2011). In the vasculature, oxidant molecules can originate from extracellular or intracellular sources and can be produced by enzymatic or non-enzymatic reactions. The blood is an excellent external carrier of oxidants and ROS as it is in permanent contact with vascular endothelial cells. Within the vascular wall intracellular sources are the mitochondrial respiratory chain and enzymes catalyzing oxidative reactions such as: Nicotinamide adenine dinucleotide phosphate oxidase (NAPDH), xanthine oxidase, lipoxygenase, myeloperoxidase and also uncoupled NOS (Sugamura et al. 2011).

However, in particular vascular cells are not defenseless and are able to protect the tissue against oxidative damage e.g. by deactivation of radical species (Sies 1993). One of the most abundant and important cellular antioxidants is the tripeptide glutathione (GSH) which synthesis is mainly controlled by gene regulation (Janssen-Heininger et al. 2013) , while the most important cellular sensor for pro-oxidative molecules is the transcription factor (erythroid-derived 2)-like 2 or Nrf2¹ (Zhu et al. 2008).

GSH exerts its antioxidant activity by directly scavenging free radicals and other ROS or as a cofactor in enzymatic reactions in which GSH is oxidized to form GSSG (GSH disulfide) (Sies 1999). The GSH-mediated antioxidant defense mechanism of endothelial cells includes several enzymes participating in the synthesis and metabolism of GSH: glutamate-cysteine ligase (GCL) and GSH synthetase mediate de novo synthesis of GSH while glutathione peroxidase (GPX), glutathione reductase (GSR) and glutathione-S-transferase (GST) metabolise GSH using H₂O₂ and NADPH as reducing agents (Sies 1993, Sies 1999).

In addition an adaptive response is activated to prevent further damage in eukaryotic cells. The redox-sensitive transcription factor Nrf2 activates protective proteins, which are able to prevent, deactivate and repair oxidative stress and oxidative damage. Most prominent targets of Nrf2 are phase II detoxifying enzymes including NAD(P)H quinone

¹ Gene ID: 4780 (homo sapiens), 18024 (mus musculus); Official name: nuclear factor, erythroid 2-like 2; Official symbol: NFE2L2 alias Nrf2 (*homo sapiens*), Nfe2l2 alias Nrf2 (*mus musculus*). According to the scientific consense this work uses Nrf2 when speaking of the functional protein.

oxidoreductase 1 (NQO1), heme oxygenase-1 (HO-1), GST and GCL, but also other antioxidants, proteasomes and drug metabolizing proteins (Kaspar et al. 2009, Baird et al. 2011). The transcriptional activity of Nrf2 can be induced by molecules, chemicals and compounds with electrophilic properties (Baird et al. 2011). Many of plant phytochemicals, which are abundantly contained in human diet possess such electrophilic chemical structures, including flavanols.

Besides the supposed effects on the NO-pathway a controversial discussion describes the antioxidant properties of flavanoids and their impact on cellular and tissue redox state. However investigations at non-physiological conditions *ex vivo* (Rice-Evans et al. 1996, Galleano et al. 2010) and the use of cell culture systems (Romeo et al. 2009, Martin et al. 2010, Rodriguez-Ramiro et al. 2011, Martin et al. 2013, Ruijters et al. 2013) including the reaction with medium additives (Long et al. 2010) contribute to strongly limit the impact of these results for interpretation of the physiological mechanisms.

Even though there is no direct evidence for antioxidant effects of cocoa and green tea polyphenols from controlled human interventional studies (Scheid et al. 2010, Ellinger et al. 2011), some studies report an increase in plasma antioxidant capacity and a decrease in plasma oxidation products associated with elevated plasma (-)-epicatechin concentrations (Rein et al. 2000, Wang et al. 2000). Furthermore an impact of (-)-epicatechin has been demonstrated on the redox-state in hepatic and neuronal cells *in vitro* (Martin et al. 2010, Martin et al. 2013) and in tissue of the rat *in vivo* (Litterio et al. 2012, Seymour et al. 2013). Whether or not these potential indirect antioxidant properties regulate the actual vascular functionality *in vivo* is not clear. Also the molecular mechanisms underlying these effects are not well understood.

As reported the transcription factor Nrf2 is a redox-sensitive sensor of oxidative stress and can be activated by numerous oxidative and electrophilic species, including reactive oxygen and nitrogen species, aldehydes and metals (Zhu et al. 2008, Baird et al. 2011). In this paradigm flavanol compounds may directly interact with Nrf2 due to their chemical structure and electrophilic properties. *In vitro* (-)-epicatechin is able to

activate Nrf2 in cultured neuronal cells (Shah et al. 2010). In vivo studies in mice and rats further support the contribution of Nrf2 to prevention of stroke damage and heart failure by (-)-epicatechin (Shah et al. 2010, Leonardo et al. 2013). However, the role of Nrf2 in the vascular effects of dietary (-)-epicatechin has never been investigated in vivo so far.

In vivo assessment of endothelial function

In human endothelial function is assessed as FMD of the brachial artery in the forearm (Pyke et al. 2005). The measurement of vascular function in living mice is challenging and not applied so far.

A wide range of animal models of cardiovascular disease is available, including hyperlipidemic mice and rats, spontaneously hypertensive rats, genetically modified mice lacking/overexpressing specific apolipoproteins, hypertensive mice lacking eNOS and surgical models of vessel lesion (Getz et al. 2012). However, there are only a limited number of methods available for measuring vascular reactivity and functionality in vivo in living animals. The molecular mechanisms responsible for modification of vascular function are classically studied in aortic rings isolated from animals, maintained in an organ bath, and pre-constricted with phenylephrine. Vasodilation is determined as a decrease in tension or increase in diameter during the addition of vasoactive substances (Furchgott et al. 1980) (Hutchison et al. 1999) (Zhu et al. 2003) (Woodman et al. 2000). This methodology was also applied to other vessels including femoral (Stoen et al. 2001), iliac (Cooke et al. 1991), mesenteric (Akata et al. 1995), and renal arteries (Ruiz-Nuno et al. 2004) from various species. The results obtained for these conduit arteries were similar and showed predominantly endothelium- and NOS-dependent vasodilation in response to acetylcholine, as well as similar dose-response curves for endothelium-independent vasodilators, e.g. nitroglycerine (NTG) (Ruiz-Nuno et al. 2004). The other frequently used method to determine vascular reactivity is the assessment of changes in perfusion pressure or flow in the coronary circulation of isolated hearts as a response to vasoactive

Introduction

substances (Kanatsuka et al. 1992, Godecke et al. 1998). A decrease in perfusion pressure or increase in flow predominantly reflects dilation of the resistance arteries. These ex vivo experiments have enabled very powerful reductionist approaches to the study of vascular reactivity although isolated vessel systems are greatly limited due to the absence of blood and their removal from the context of the whole organism (e.g., endocrine factors, hemodynamics, or nervous system). Moreover, they do neither allow assessment of experimental intra-individual effects nor longitudinal studies.

Similar to the assessment of perfusion flow in isolated systems in order to determine vascular reactivity, detection of tissue perfusion can also be used in vivo as a reliable readout for vascular function. Post occlusive reactive hyperemia (PORH) is the physiological increase of blood flow to the tissue following ischemia after transient arterial occlusion. PORH has also been applied for testing endothelial function of conduit vessels in humans, e.g. by measurement of FMD (Frick M 2002, Pyke et al. 2007), of venous occlusion plethysmography, or of skin microcirculation by laser Doppler flowmetry or imaging (Kubli et al. 2000, Keymel et al. 2010). Scanning laser doppler perfusion imaging (LDPI) has been applied in clinical settings to assess functional responses of the cutaneous microcirculation to vasoactive molecules or PORH in patients with endothelial dysfunction in hypertension (Farkas et al. 2004), peripheral arterial disease (Kluz et al. 2013), coronary artery disease (Keymel et al. 2010), diabetes (Jarnert et al. 2012), smoking (Petschke et al. 2006) (Fujii et al. 2013) or age (Algotsson et al. 1995). In swine and dog animal models LDPI was applied for measuring revascularization in wound healing (Mauskar et al. 2013) (Karayannopoulou et al. 2010), mucosal microcirculation (Kaner et al. 2013) or retinal capillary blood flow (Gelatt-Nicholson et al. 1999). In rodents and especially in mice LDPI is classically used to study angiogenesis and neovascularization after hindlimb ischemia (Long et al. 2013) (Sachdev et al. 2013) (Rivard et al. 1999, Limbourg et al. 2009), but it has never been applied for measuring reactive hyperemic responses in mice. Scanning LDPI is based on the physical phenomenon defined as the doppler effect, which is a change in the frequency of a wave occurring when the source and observer are in motion relative to each other. When laser light penetrates a tissue, it is backscattered and

Introduction

returns to its source without change of frequency. But if the laser light is backscattered by moving objects (i.e. blood cells) it undergoes a shift in frequency directly proportional to their concentration and velocity (Wardell et al. 1993). The measuring depth of the laser depends on the energy and wave length of the laser, on the measuring distance and, most importantly, on characteristics and vascularization of the tissue influencing its backscattering properties, including pigmentation, density, biophysical composition, presence of hairs, density and diameter of the vessels (macrocirculation, microcirculation, resistance vessels), amount of blood cells etc. (Jakobsson et al. 1993).

A direct measurement of FMD in animal models has been previously demonstrated in rats (Heiss et al. 2007) but was never applied in living mice. Similar PORH has never been assessed in mice *in vivo*.

Aim of the study

The mechanisms by which dietary flavanols mediate their vascular effects are not well understood. Accumulating data support the evidence that flavanol-rich foods like cocoa are able to improve endothelium-dependent vasorelaxation in healthy subjects, as well as in pathological conditions. Proposed mechanisms include an increase in nitric oxide (NO)-bioavailability by direct activation of the endothelial NO synthase or by affecting the redox state of vascular cells. (-) Epicatechin is the most abundant flavanol monomer in cocoa and seems to be the active component responsible for those effects. However a direct link between the eNOS/NO/cGMP signaling pathway and vascular response to (-)-epicatechin in vivo has never been demonstrated so far. The transcription factor nuclear factor (erythroid-derived 2)-like 2 (Nrf2) is a key master switch controlling the expression of enzymes involved in the regulation of the cellular redox state, and is activated by electrophilic compounds, and potentially (-)-epicatechin or its circulating metabolites.

This work aims at investigating the vascular effects of dietary (-)-epicatechin in vivo by raising following questions: 1) Is eNOS required for the beneficial vascular effects of (-)-epicatechin in vivo ? 2) are maintenance of NO-bioavailability and redox state essential for the effects of (-)-epicatechin ? 3) Is Nrf2 required for the beneficial vascular effects of (-)-epicatechin in vivo ? 4) What other potential targets/pathways in vascular tissue are activated and regulated by administration of (-)-epicatechin ?.

As a proof of concept adsorbtion and metabolism of (-)-epicatechin in mice will be assessed by analyzing plasma concentrations of (-)-epicatechin and its metabolites. To determine whether eNOS or Nrf2 are required for the beneficial vascular effects of (-)-epicatechin in vivo, vascular function will be assessed in mice treated with a NOS inhibitor, and in mice lacking eNOS (eNOS^{-/-}) or Nrf2 (Nrf2^{-/-}) by scanning LDPI and high-resolution ultrasound. To test whether eNOS dependent NO-bioactivity is regulated in vascular tissue eNOS expression, eNOS phosphorylation and cGMP level will be assessed in the aorta of the mice. To determine whether (-)-epicatechin regulates the redox state in vivo GSH-level and expression of antioxidant enzymes will be assessed in tissue of the cardiovascular system from wildtype and Nrf2^{-/-} mice. Finally to identify novel potential targets of (-)-epicatechin in the vasculature

Aim of the study

transcriptional profiling of global gene regulation will be performed in the aorta of the mice.

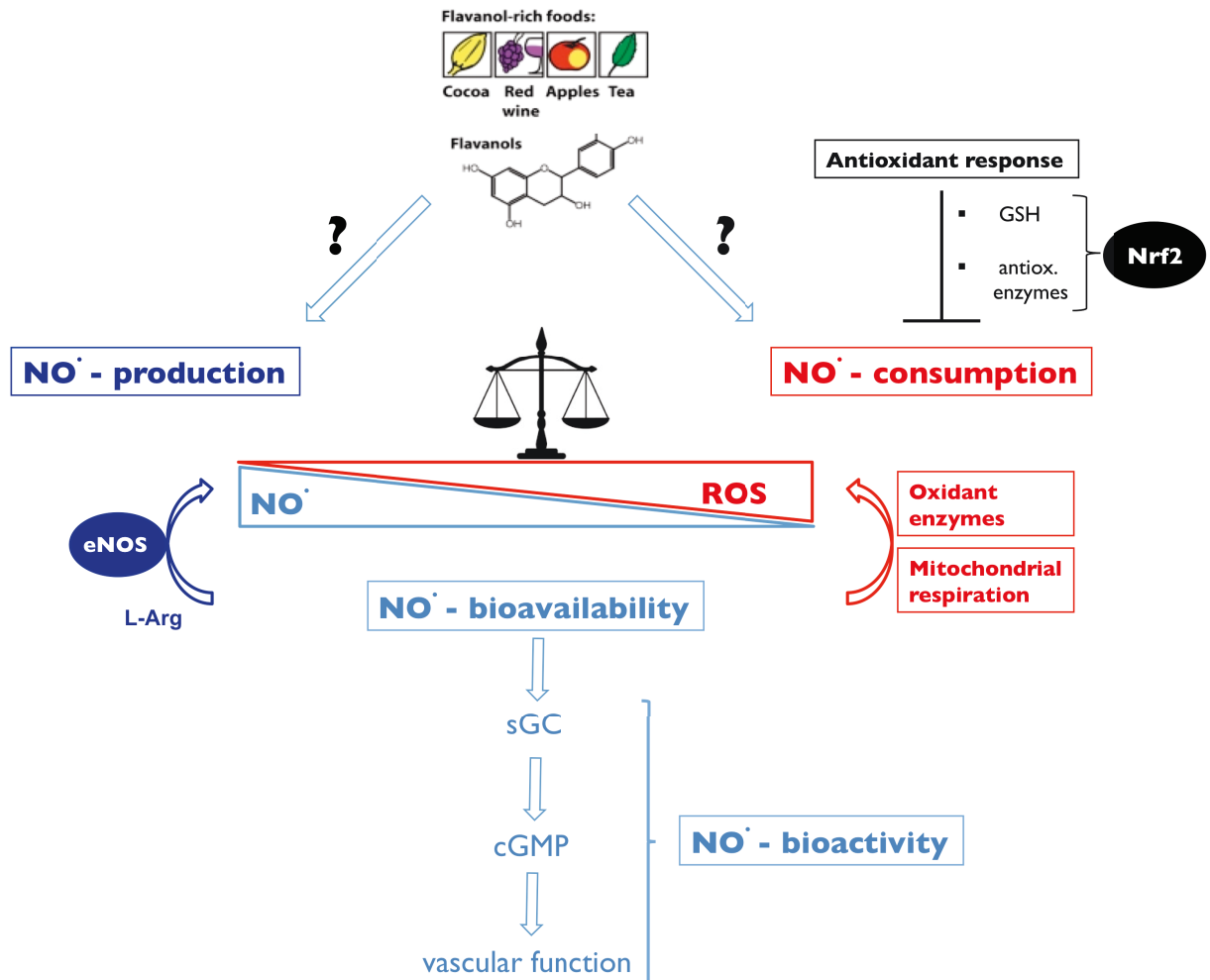


Fig. 4: Potential effects of flavanols on NO-bioactivity.

This work aims to investigate the *in vivo* effects of dietary flavanol treatment on vascular NO-bioactivity. The bioavailability within a system is dependent on the balance between NO production and NO consumption. The enzymes eNOS and the transcription factor Nrf2 regulate NO and ROS homeostasis and are potential targets of dietary flavanols.

Materials and Methods

Materials

Tab. 1: Chemicals		
1kb Plus DNALadder	Invitrogen	Carlsbad, USA
Acetic acid	Merck	New York, USA
Acetic anhydride	ArborAssays	Michigan, USA
Acetylcholine chloride	Sigma	St.Louis, USA
Adenosine	Sigma	St.Louis, USA
Aqua dest	Millipore	Darmstadt, Germany
Bicine	Sigma	St.Louis, USA
Bis-Tris	Sigma	St.Louis, USA
Blue Juice Gel Loading Buffer	Invitrogen	Carlsbad, USA
Bovine serum albumin (BSA)	Sigma	St.Louis, USA
Calciumchloride dihydrate	Sigma	St.Louis, USA
Diethyl ether	Merck	New York, USA
Dodecylsulfat * NaCl (SDS)	Roth	Karlsruhe, Germany
Drinking water for mice	San Benedetto	San, Benedetto, Italy
E-Gel® single comb gels with SYBR® Safe	Invitrogen	Carlsbad, USA
Epinephrine	Sigma	St.Louis, USA
Ethylenediaminetetraacetic acid (EDTA)	Roth	Karlsruhe, Germany
Heparin	Ratiopharm	Ulm, Germany
Hybond P Membran	GE healthcare	Little Chalfont, UK
Hydrochloric acid (HCL)	Merck	New York, USA
Indomethacin	Sigma	St.Louis, USA
Isoflurane	Abbott	Illinois, USA
MagicMark™ XP Western Protein Standard	Invitrogen	Carlsbad, USA
Mercaptoethanol	Sigma	St.Louis, USA
Methanol	Merck	New York, USA
Milkpowder Blotting grade	Sigma	St.Louis, USA
NaCl isotonic solution 0.9 %	Braun	Melsungen, Germany
Nitrogen, liquid (N ₂)	Linde AG	Munich, Germany
Nitrolingual®nitroglycerine	G. Pohl-Boskamp	Hohenlockstedt, Germany
nonyl phenoxypolyethoxyethanol (NP 40)	Sigma	St.Louis, USA
NuPAGE® Antioxidant	Invitrogen	Carlsbad, USA
NuPAGE® LDS Sample Buffer	Invitrogen	Carlsbad, USA
NuPAGE® MES running buffer	Invitrogen	Carlsbad, USA
NuPAGE® Novex® 3-8% tris-acetate Mini Gel	Invitrogen	Carlsbad, USA
NuPAGE® Reducing Agent	Invitrogen	Carlsbad, USA
NuPAGE® transfer buffer	Invitrogen	Carlsbad, USA
NuPAGE® Tris-acetate running buffer	Invitrogen	Carlsbad, USA
NuPAGE®Novex® 10% Bis-Tris Mini Gel	Invitrogen	Carlsbad, USA
Nw-Nitro-L-arginine	Sigma	St.Louis, USA
Oxygen gas (O ₂)	Linde AG	Munich, Germany
Phosphate buffered saline (PBS)	PAA	Pasching, Austria
Ponceau S solution	Sigma	St.Louis, USA
Potassium Dihydrogenphosphate	Sigma	St.Louis, USA
Potassium chloride	Merck	New York, USA
Protease-Phosphatase-Inhibitor Cocktail	Bio-Rad	Munich, Germany
Proteinase K	Qiagen	Hilden, Germany
S.N.I.F.F standard mice diet	Sterling	S.P.A, Italy
Sodium chloride (NaCl)	Sigma	St.Louis, USA
Sodium nitrate (NaNO ₃)	Sigma	St.Louis, USA
Sodium nitrite (NaNO ₂)	Sigma	St.Louis, USA
Sodium hydroxide (NaOH)	Merck	New York, USA
Sulfo Salicylic Acid (SSA)	Merck	New York, USA
Trichloroacetic acid (TCA)	Merck	New York, USA
Triethylamine	ArborAssays	Michigan, USA
Trishydroxymethylenaminomethan (Tris Base)	Merck	New York, USA
Tween 20 (Polyoxyethylene Sorbitan Monolaurate)	Sigma	St.Louis, USA
Ultrasound electrode cream - signa cream®	Parker	Fairfield, USA
Ultrasound gel - EcoGel100	Eco-Med-Pharma	Mississauga, Canada
Urethane	Sigma	St.Louis, USA
Veet® Hair Removal Cream	Reckitt Benckiser	Slough, UK

Materials and Methods

Tab. 2: Kits		
DC Protein Assay Kit	Bio-Rad	Munich, Germany
Glutathione kit DetectX	ArborAssays	Michigan, USA
Mouse GE 4x44K v2 Microarray Kit	Agilent Technologies	Santa Clara, USA
KAPA2G™ Robust PCR Kit	Peqlab	Erlangen, Germany
QuantiTect Reverse Transcription Kit	Qiagen	Hilden, germany
RNeasy Mini Kit	Qiagen	Hilden, germany
SuperSignal® West Phemto Chemiluminescent Substrate	Pierce	Bonn, Germany
SuperSignal® West Pico Chemiluminescent Substrate	Pierce	Bonn, Germany
TaqMan® Gene Expression Assays	Applied Biosystems	Foster City, USA
TaqMan® Gene Expression Master Mix	Applied Biosystems	Foster City, USA
Tab. 3: Equipment		
2100 Chip Bioanalyzer	Agilent Technologies	Santa Clara, USA
Autoinjector 719AL	Eicom	Dublin, Ireland
Centrifuge Mikro 200 R	Hettich	Tuttlingen, Germany
Centrifuge Rotina 38R	Hettich	Tuttlingen, Germany
E-Gel® iBase™ Power System	Invitrogen	Carlsbad, USA
FLUAStar Omega	BMG Labtech	Ortenberg, Germany
Gel Doc 2000	Bio-Rad	Munich, Germany
High-resolution ultrasound Vevo2100	Visual Sonics	Toronto, Canada
Homogenizer bin	Sartorius	Gorttingen, Germany
Homogenizer RW 16	IKA	Staufen, germany
ImageQuant LAS 4000	GE lifesciences	Little Chalfont, UK
Infra red light source	Beurer	Ulm, Germany
LCD light source KL 1500	Leica	Solms, Germany
Mastercycler gradient	Eppendorf	Hamburg, Germany
NanoDrop 2000	Thermo Scientific	Waltham, USA
NuPAGE® elektrophoresis system	Invitrogen	Carlsbad, USA
Operation table for rodents	Harvard Apparatus	Holliston, USA
Pperfusion pump	Isma Tec	Glattbrugg, Switzerland
PeriScan PIM 3 System	Perimed Instruments	Järfälla, Sweden
Pressure-volume catheter 1.4F SPR-839	Millar Instruments	Houston, USA
Prism 7900HT Sequence Detection System	Applied Biosystems	Foster City, USA
Razor Favorita II Typ GT109	Aesculap	Center Valley, USA
Reference pipets	Eppendorf	Hamburg, Germany
Shaking device 1040	Fisher Scientific	Hampton, USA
SpeedVac concentrator	Thermo Scientific	Waltham, USA
Special accuracy weighing machine	Sartorius	Gorttingen, Germany
Thermo mixer 5436	Eppendorf	Hamburg, Germany
Tissue Ruptor homogenizer	Qiagen	Hilden, germany
Ultrasound waterbath sonorex	Bandelin	Berlin-Lichterfelde, Germany
Vortex	VWR International	Radnor, USA
Waterbath E100	Lauda	Lauda-Königshofen, Germany
XCell SureLock™ Mini-Cell	Invitrogen	Carlsbad, USA

Materials and Methods

Tab. 4: Instruments		
chirurgical scissors, curved, 11.5 cm	FST	Heidelberg, Germany
fine anatomic pincette, curved, 100 mm	Aesculap	Center Valley, USA
fine scissors, curved, 8.5 cm	FST	Heidelberg, Germany
fine scissors, straight, 10.5 cm	FST	Heidelberg, Germany
fine scissors, straight, 8.5 cm	FST	Heidelberg, Germany
micro pincette, curve, 115 mm	Aesculap	Center Valley, USA
micro pincette, straight, 110 mm	Aesculap	Center Valley, USA
vascular occluder, 10 mm	KentScientific	Torrington, USA
Tab. 5: Software		
Brachial Analyser 5	mia-llc	Coralville, USA
DAVID Microarray analysis tool	Open source	
ECG Amplifier HSE Type 689	Harvard Apparatus	Holliston, USA
Graph Pad Prism 5	AD Instruments	Dunedin, New Zealand
Image J	Open source	
ImageQuant TL software	GE lifesciences	Little Chalfont, UK
LDPIWin3	Perimed Instruments	Järfälla, Sweden
Microsoft office	Microsoft	Albuquerque, USA
OMEGA control	BMG Labtech	Ortenberg, Germany
PowerChrom	eDAQ	Colorado Springs, USA
OMEGA DataAnalysis	BMG Labtech	Ortenberg, Germany
Sequence Detection Systems (SDS)	Applied Biosystems	Foster City, USA
SPSS	IBM	Armonk, USA
VEVO 2100 1.5	Visual Sonics	Toronto, Canada

Mice

All experimental procedures were conducted in conformity with the guidelines for the use of experimental animals, as given by the German “*Tierschutzgesetz*” and the “Guide for the Care and Use of Laboratory Animals” of the US National Institutes of Health and were approved by the *Landesamt für Natur, Umwelt und Verbraucherschutz* (LANUV) Nordrhein-Westfalen, Germany. Young (8±2 weeks) and elderly (6 months, 12 months, 24 months) male C57/BL6J mice were purchased from Janvier SAS (Le Genest, France) or bred in the animal facility of the Heinrich-Heine-University of Duesseldorf. Transgenic eNOS knockout mice with a C57/BL6J background (eNOS^{-/-}) and corresponding transgene negative littermates were kindly provided by A. Gödecke (Godecke et al. 1998). Heterozygous Nrf2 knock out mice (Nrf2^{+/-}) specified as knockout-B6.129P2-Nfe2l3^{tm1yIN} (No.RBRC01390) were obtained from RIKEN BioResource Center (Ibaraki, Japan, (Itoh et al. 1997)) and were

bred in the animal facility to obtain a population with Nrf2^{+/+}, Nrf2^{+/-} and Nrf2^{-/-} genetic background. Mice were kept in groups, at 19-21 °C in 50-60 % humidified atmosphere in a 12 h day/night rhythm. All mice were fed a standard diet ad libitum (SNIFF, S.P.A, Italy), with low content in NO₃⁻ and NO₂⁻. For all physiological in vivo measurements mice were anesthetized with isoflurane (3 % induction and 1.8-2 % maintenance). For final anesthesia 1 mg/g body weight urethane was administered intraperitoneal (i.p.).

Genotyping

The genotype of transgenic animals was determined and confirmed by RT-PCR using custom designed primers. For genotyping of the mice fresh or freshly frozen biopsies were used from the tail or ear. To isolate genomic DNA the tissue was lysed in 300 µl 50 mM NaOH for 40 minutes at 95 °C. The lysates were neutralized with 25 µl 1M Tris-HCl pH 4.5 and centrifuged at 14.000 rpm at 4°C for 10 minutes. The supernatant containing genomic DNA was directly used for PCR or stored at -20 °C. For the detection of the wildtype or disrupted Nrf2 allele HPLC-grade oligonucleotides purchased from Eurofinsgenomics (Luxemburg) were used: Nrf2: 5'-TGGACGGGACTATTGAAGGCTG-3', Nrf2: 5'-GCCGCCTTTTCAGTAGATGGAGG-3', lacZ: 5'-GCGGATTGACCGTAATGGGATAGG-3'. The DNA was amplified using the KAPA2G™ Robust PCR Kit, a ready master mix containing Hot Start polymerase and dNTPs (peqlab, Erlangen, Germany), following the manufacturer's instructions. Briefly, for one PCR reaction 5.5 µl H₂O, 12.5 µl TaqMix and 2 µl of each primer were added to 1 µl of template. A standard PCR program (step 1: 95°C, 15 sec.; step 2: 60°C, 15 sec.; step 3: 72°C, 15 sec.) was run with the primer mix, water and the KAPA2G™ Robust PCR Kit. Respective bands were identified on a commercial prestained 2 % agarose E-Gel® system from Invitrogen (Carsbad, USA).

Collection of mice blood and organs

For final collection of blood samples up to 1.5 ml blood was drawn from anesthetized, heparinized mice (40.000 IU/kg heparin i.p.) via heart puncture with closed chest using a 1 ml nozzle with Ø 0.2 mm cannula and collected into heparin (50 µL) tubes. To

separate plasma blood was centrifuged at 3000 g for 2 min. at 4 °C and the supernatant was directly shock frozen in liquid nitrogen before storage at -80 °C. For explanations of the organs the abdominal and thoracic cavities were opened by ventral incision, the *vena cava* was cut and the organs were perfused via heart injection with ice cold PBS until the lung and liver was cleared of blood. After harvesting heart, lung and liver the complete aorta including ascending, descending and abdominal part was carefully removed in one piece into ice cold PBS, carefully stripped of adventicia or blood coagulate and directly frozen in liquid nitrogen prior to storage at -80 °C. In case of transgenic animals a tail biopsy was harvested for a re-genotyping procedure.

Experimental setup

Oral administration of (-)-epicatechin to mice

A dose of 2 mg/kg and 10 mg/kg (-)-epicatechin (Sigma-Aldrich, St.Louis, USA) was administrated by enteral gavage feeding or ad libitum in drinking water. For acute treatment mice were fed a low flavanol diet for one week and fastened overnight. A single dose of 150 µl (-)-epicatechin was administrated. The solution was prepared by dissolving (-)-epicatechin in ethanol (stock: 20 µg/µl) and dilution to a final concentration of 0.4 µg/µl in drinking water. Mice were measured and sacrificed after one hour. For longer-term administration a daily drinking volume of 5 ml per mouse per day was defined and the required amount of a 100 mM (29 mg/ml) (-)-epicatechin stock solution was calculated and added in 100 ml drinking water. The water was changed daily for five days. Respective vehicle preparations with ethanol and water were used in control groups. The dietary treatment of mice with (-)-epicatechin had no effect on the body weight or daily drinking volume of the mice.

Inhibition of nitric oxide synthase (NOS)- and cyclooxygenase (COX)

NOS-inhibition was accomplished by administration of 1.6 mg/ml (=270 mg/kg/d) N ω -nitro-L-arginine (L-NNA) in 100 ml drinking water for six days (Stock: 160 mg/ml in 1 M

HCL). When (-)-epicatechin effects were investigated L-NNA was added simultaneously to the drinking water. Indomethacine was used for chronic inhibition of COX for six days in a concentration of 30 µg/ml (=5 mg/kg/d) dissolved in 100 ml drinking water. Corresponding vehicle controls were used in separate animal groups. All chemicals were purchased by Sigma-Aldrich.

Treatment with vasoactive drugs

All stock solutions were freshly prepared on the experimental day with warm (37 °C) saline as a vehicle. The effects of injection of the vehicle control were tested in the same groups of animals before injecting the vasoactive substances. Measurements were performed in n = 4 animals, as indicated.

Nitroglycerin (NTG). NO-dependent and endothelium-independent vasodilation was induced by bolus intraperitoneal (i.p.) administration of 12 mg/kg NTG in 100 µl vehicle (0.9% NaCl) (stock: 1 mg/ml, G.Pohl-Boskamp, Hohenlockstedt, Germany). Readings were taken immediately after injection as described.

Adenosine. To pharmacologically mimic the blood flow increase during reactive hyperemia, a 0.1 mg/kg bolus dose of adenosine was administered in 100 µl vehicle (stock 10^{-4} mol/l; Sigma-Aldrich) into the tail vein.

Epinephrine. To induce vasoconstriction, a local subcutaneous injection of 0.7 mg/kg epinephrine was used in 100 µl vehicle (stock 10^{-3} mol/l; Sigma-Aldrich) into the upper thigh.

Acetylcholine (ACH). To induce endothelium-dependent vasodilation, 0.07 mg/kg acetylcholine in 100 µl vehicle (stock 10^{-4} mol/L; Sigma-Aldrich) was injected into the tail vein.

In vivo measurements in mice

LDPI Measurements

In order to determine perfusion in mouse hindlimb scanning laser doppler perfusion imaging (LDPI) measurements were performed by using a PeriScan PIM 3 System (Perimed-Instruments, Järfälla, Sweden) provided with a monochromatic 670-690 nm wavelength laser with standard fiber separation (0.25 mm). Mice were anesthetized with isoflurane (3 % induction and 2 % maintenance) and were positioned and fixed on a heated platform (set to 39°C, body temperature approx. 36-37 °C) lying on the back (Fig. 5). The hindlimb was prepared for measurements by clearing the inner thigh of hair using depilation cream. The scanning head is adjusted to a measuring distance of 10 cm (as assessed by the laser). A 5x3 cm scanning area is rapidly scanned (1 image/sec) and the signal is quantified as arbitrary perfusion units (MPU = Mean Perfusion Units). Measurements were started after a 15 min. equilibration period and after achieving stable baseline values. Image analysis was performed off-line using the LDPIwin software (Perimed-Instruments). As depicted in Fig. 5C, the scanning LDPI signal is mainly dependent on the penetration depth of the laser and on the blood flow in the vessels encountered by the laser within the tissue. The femoral artery was found at 0.4 cm penetration depth, as visualized by high-resolution ultrasound (Fig. 5C, middle). In its proximity the perfusion map obtained by scanning the area showed a discrete region with very high signal (Fig. 5C, bottom), which was quantified as MPU.

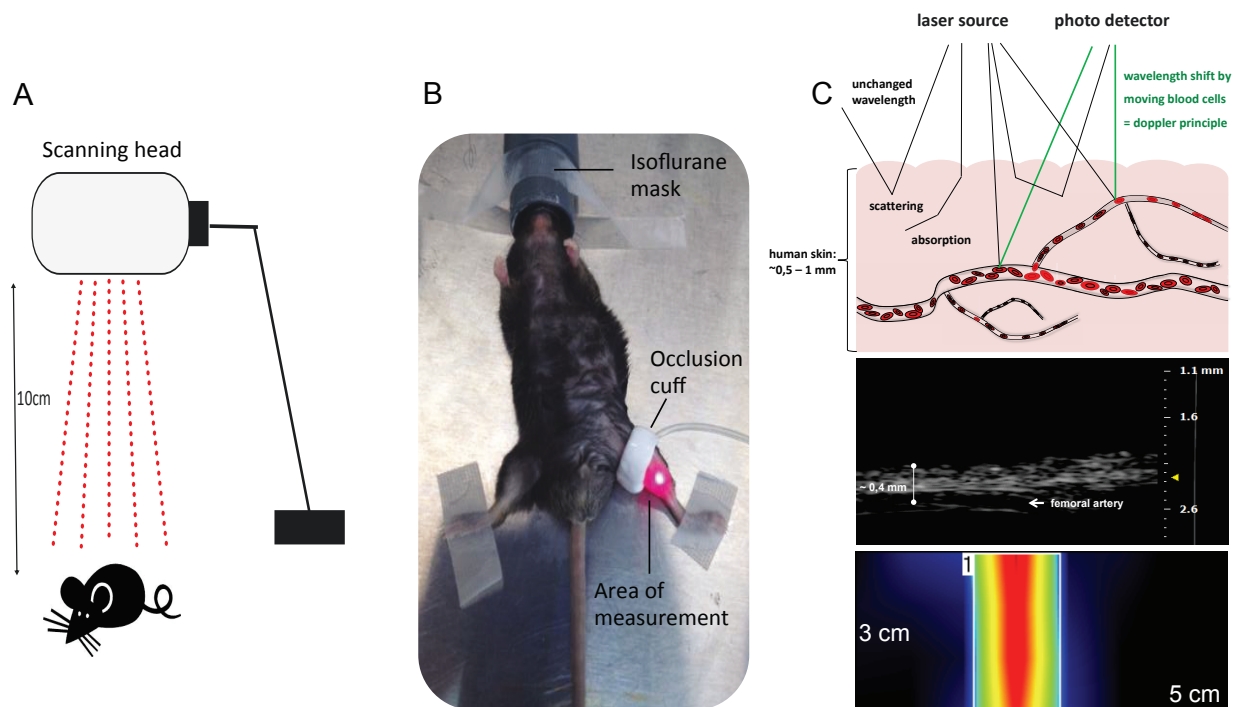


Fig. 5: Set up and measurement principles of Laser Doppler perfusion imaging (LDPI).

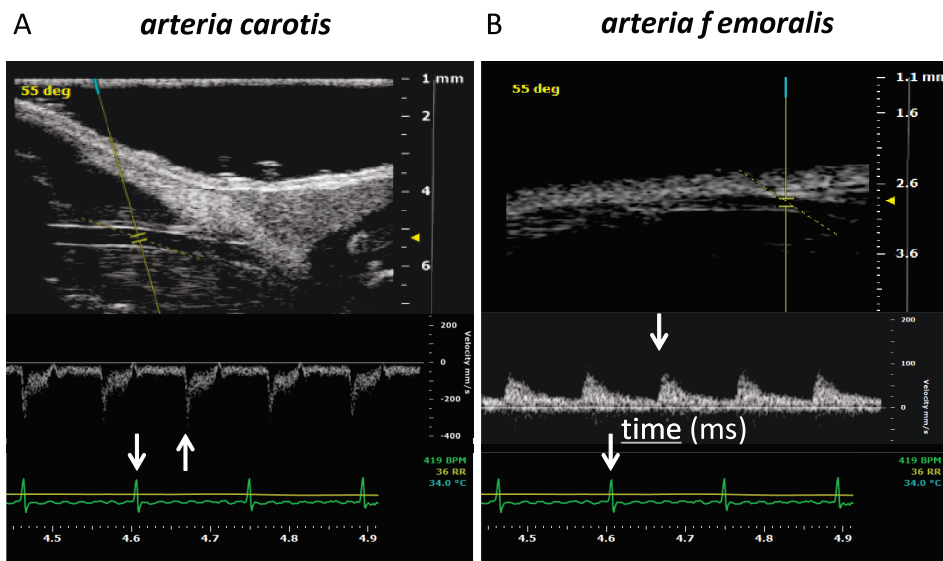
To determine reactive hyperemia prior to fixation the leg is pulled through a vessel occluder cuff. When laser light penetrates the tissue it undergoes a change in wavelength (Doppler shift) when hitting moving blood cells. Light returning to the instrument is registered by a photo detector inside and processed to extract information about perfusion and circulatory blood flow. The area for perfusion measurements is set to 5x3 cm. The laser is producing a colored image with red representing area of high and black area of low perfusion.

Ultrasound Measurements

A VEVO2100 high-resolution ultrasound device (VisualSonics, Toronto, Canada) with ultra-high frequency transducers (MS400: 18-38 MHz, MS700: 30-70 MHz) was used for visualization of conduit vessels in mice including *arteria femoralis* and *arteria carotis*. The technique allowed the assessment of vascular diameter (d) and flow velocity within the vessels (mm/s). In addition the heart rate (HR), respiration rate (RR) and body temperature (°C) of the mice was determined by the system. In preparation for measurements mice were anesthetized with isoflurane, fixed on the heated platform, and the upper hindlimb was cleared of hair with a depilation cream. Measurements were started after a 15 minutes (min.) equilibration period. The femoral artery was identified and visualized by its characteristic flow pattern using the color doppler mode, pulse-wave (PW)-Mode and image (B)-Mode. The position of the

probe was optimized to show clear vessel wall and lumen. The image and flow analyses were performed off-line using the Vevo2100 1.5 software (VisualSonics). Vessel diameter was evaluated by using the Brachial Analyzer 5 software (Medical Imaging Applications, Coralville, USA).

In addition to vascular diameter and flow velocity vascular pulsatility was determined as pulse wave velocity (PWV) (Fig. 6). PWV was calculated by following formula:



C time (ms) = interval: ECG R-wave - foot of Doppler wave

$$PWV \text{ (cm/ms)} = \frac{\Delta \text{ distance (cm)}_{\text{carotis-femoralis}}}{\Delta \text{ time (ms)}_{\text{carotis-femoralis}}}$$

Fig. 6: Measurement of pulse wave velocity (PWV).

For the calculation of PWV Doppler flow and ECG was detected in *arteria carotis* (A) and *arteria femoralis* (B). The transit time of the arterial pulse along the analyzed arterial segment measured at two distinct points is defined as the time interval between the R-wave of the ECG to the foot of the Doppler waveform (white arrows). C) The assessment of PWV involves measurement of two quantities: the distance between carotid and femoral artery divided by the transit time of the arterial pulse between both recording sites.

PWV is calculated from the measurement of blood flow velocity and the electrocardiogram (ECG) at two distinct points of the arterial vascular tree and determination of the distance between these two points. Here the left carotid artery and left femoral artery was used. The distance between the areas of measurement was determined as exact as possible using a ruler and exact marks on the transducer probe, on the skin and on the platform.

Assessment of PORH

To measure post-occlusive reactive hyperemia (PORH) as changes in MPU (by LDPI) and changes in vascular diameter (by ultrasound), occlusion and release of an air inflatable vascular occlude cuff (KentScientific, Connecticut, USA) was applied in mouse hindlimb (Fig. 7). Prior to fixation the leg is pulled through the cuff, so that the blood supply can be occluded by inflating the cuff to 200-300 mmHg proximal to the area of measurements. The hindlimb is pulled down to the length by applying gentle pressure and fixed by means of double adhesive tape to the foot of the bottom of the measuring platform. The experimental set-up is similar for LDPI and ultrasound measurements and consists of 7 min. baseline (stabilisation of perfusion), 5 min. ischemia (zero perfusion) and 8 min. of reperfusion (hyperemia and recovery of perfusion). PORH is analysed by calculating the % change ($\frac{\text{max. reperfusion} - \text{baseline}}{\text{baseline}} \times 100$), ratio ($\frac{\text{max. reperfusion}}{\text{baseline}}$), time to peak (postischemic reperfusion time to maximal perfusion) and postischemic area under curve (AUC). The dilation of the femoral artery is analysed by recording the diameter change every 15 sec. after occlusion release in relation to basal diameter expressed as flow mediated dilation (FMD).

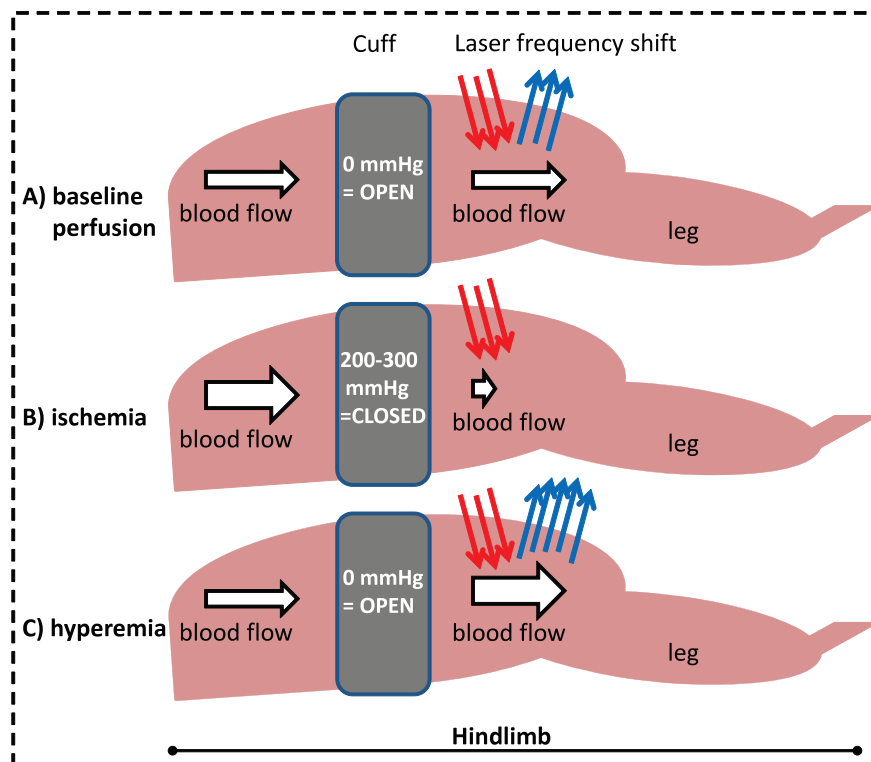


Fig. 7: Induction of reactive hyperemic blood flow in mouse hindlimb.

During baseline measurements (A) the cuff is open so blood flow is not interrupted. In the ischemic phase (B) the cuff is inflated to 200-300 mmHg so no perfusion can be detected at the distal measurement area, while after cuff release (C) hyperemic blood flow results in a strong signal increase. This setting is used for LDPI and FMD measurements

Surgical excision of the femoral artery

To determine the contribution of the femoral artery to the PORH signal measured by LDPI the artery was ligated exactly according to the protocol described by Limbourg et al. (Limbourg et al. 2009) and the mouse was measured one day after surgery. The surgery was performed by Dr. med. Dominik Schuler. Briefly the protocol includes a longitudinal 5 mm incision beginning at the inguinal crease along the femoral vessels visible through the skin, separation of the femoral nerve, artery and vein and proximal femoral ligation and excision of the femoral bifurcation with all branches.

Assessment of blood pressure

Mean arterial blood pressure in mice was measured invasively in the *aorta ascendens* using a 1.4F SPR-839 pressure catheter from Millar Instruments (Houston, USA) placed into the aorta through the right carotid artery. Stable pressure data were analyzed with the dedicated software (IOX, EMKA, Paris, France) to determine the developed pressure including peak systolic (PS) peak-diastolic (PD) pressure. For measurements the mice were anaesthetized with urethane adjusted to body weight at 1 mg/g.

Biochemical analysis**Western Blot**

Tab. 6: Antibodies for western-blot				
Gene symbol term		ID #	Dilution	
eNOS	endothelial nitric oxide synthase	610297	1000	BD
CAT	catalase	1877	2000	Abcam
GCLC	glutamate-cysteine ligase, catalytic subunit	80841	500	Abcam
GCLM	glutamate-cysteine ligase, modifier subunit	153967	500	Abcam
GPx	glutathione-peroxidase	22604	500	Abcam
GSR	glutathione-reductase	16801	1000	Abcam
GST	glutathione-S-transferase	108524	1000	Abcam
MLCK	myosin light chain kinase	M7905	1000	Sigma
MYPT1	protein phosphatase 1	SAB4501948	1000	Sigma
NQO1	NAD(P)H:quinone oxidoreductase 1	34137	1000	Abcam
P-MLCK	myosin light chain kinase	LS-C25729	1000	LSBio
P-MYPT1	protein phosphatase 1	Sc-33360	500	Santa Cruz
P-VASP	Vasodilator-stimulated phosphoprotein, P-Ser239	3114	1000	CellSignalling
PeNOS	endothelial nitric oxide synthase, P-Ser1177	C9C3	1000	CellSignaling
SOD1	superoxide dismutase 1, soluble	13498	5000	Abcam
VASP	Vasodilator-stimulated phosphoprotein	3112	1000	CellSignalling
α -TUB	alpha tubulin	4074	2000	Abcam
β -ACT	beta actin	8227	2000	Abcam

For Western blot analysis, tissues and cells were homogenised in RIPA- (radio immunoprecipitation assay) lysis buffer containing 1 % NP40, 0.5 % Deoxycholate and 0.1 % SDS in PBS, with successive 30 sec. of vortexing and sonification and 15 min. centrifugation at 14.000 rpm and 4°C. The concentration of total protein was

determined with the DC Protein Assay Kit from Bio-Rad (Munich, Germany). Briefly, 5 μ l of protein lysate was mixed with 25 μ l of provided reagent A and 200 μ l of reagent B, incubated for 15 min. at room temperature and the optical density was determined at 740 nm. A total of 10-15 μ g protein of tissue or 30 μ g of cell lysate was electrophoretically separated on 3-8 % or 10 % polyacrylamide gels at 160 V for one hour. The proteins were transferred to a nitrocellulose membrane at 30 V for one hour and probed with respective primary antibodies over night at 4°C and with secondary antibodies for one hour at room temperature. Gels and membranes were purchased from invitrogen, life technologies (Carlsbad, USA). Immunoreactive bands were detected using the Super Signal West Chemiluminescent System (Pierce, Bonn, Germany) following the manufactures protocol and the ImageQuant device and software. Used primary antibodies with respective dilutions prepared in 0.1 % Tween TBS buffer containing 5 % BSA are listed in tab. 6. As a positive control for western-blot analysis lysates from cultured human umbilical vein endothelial cells (HUVEC) and human hepatocellular carcinoma cells (HepG2) were used, both purchased from PromoCell (Heidelberg, Germany).

cGMP

To determine cGMP concentration the frozen tissue was homogenized in 1 ml ice-cold 5 % trichloroacetic acid (TCA) per 100 mg and centrifuged at 2000 g for 15 min. at 4°C. TCA in the supernatant fraction was extracted by addition of 3 ml diethyl ether per 1 ml TCA used and the samples were then lyophilized by 3-5 h vacuum centrifugation at 60 °C. The samples were reconstituted in 1 ml sample diluent per 1 ml TCA. All plasma and tissue samples were acetylated by addition of 15 μ l of the provided triethylamine/acetic anhydride (2:1) acetylation reagent to 300 μ l sample prior to measurement. cGMP was measured using an enzyme immunoassay kit (Arbor Assays, Michigan, USA) according to manufacturers descriptions. Briefly a cGMP- peroxidase conjugate is added to the standard and samples in the wells coated with an anti-IgG antibody. The binding reaction is initiated by the addition of a monoclonal antibody to cGMP. After an overnight incubation, the plate is washed and the chemiluminescent

substrate is added. The substrate reacts with the bound cGMP-peroxidase conjugate to produce light detected as luminescence. Concentrations in the samples are calculated from the standard curve.

GSH

To determine GSH concentrations the tissue was homogenized in 250 μ L/10 mg ice cold 0,01 M HCl, the sample was mixed *thoroughly*, sonificated for 30 sec. and centrifuged at 14000 rpm and 4°C for 10 min. The supernatant was mixed with an equal volume of ice cold 5% sulfo salicylic acid to yield a final concentration of 2.5 %, incubated on ice for five min. and centrifuged at 14000 rpm and 4°C for 10 min. to remove precipitated protein. The clear supernatant was used to measure GSH with the DetectX[®] Fluorescent Detection kit (Arbor Assays, Michigan, USA) according to manufactures descriptions. The kit utilizes a proprietary non-fluorescent molecule that covalently binds to the free thiol group on GSH to yield a highly fluorescent product. After mixing the sample and incubating at room temperature for 15 minutes, the GSH-generated signal is read at 510 nm in a fluorescent plate reader with excitation at 390 nm. Addition of a reaction mixture that converts all the GSSG into free GSH which then reacts during a second 15 min. incubation period yields the signal related to total GSH content.

Molecular biological analysis

Real Time PCR

A quantitative real-time reverse transcription (RT)–PCR technique was used to quantify messenger RNA (mRNA) expression of the Aryl hydrogen receptor (AhR) in the aorta. Commercial available TaqMan oligonucleotides labelled with a fluorescent dye purchased from Applied Biosystems (Foster City, USA) were used as primers to quantify mRNA expression. Tissue lysates were made by homogenisation in RLT-buffer (guanidine thiocyanate buffer) using the Tissue Ruptor homogenizer from Qiagen

(Hilden, Germany) and total RNA was isolated from the lysates with the RNeasy Mini Kit (Qiagen, Hilden, Germany) exactly according to manufacturers instructions. The concentration and quality of the isolated RNA was determined using the NanoDrop2000 (ThermoScientific, Waltham, USA) and 2100 Chip Bioanalyzer (Agilent, Santa Clara, USA) and a total of 500 ng RNA was reverse transcribed into cDNA with the QuantiTect Reverse Transcription Kit (Qiagen). Real-time RT-PCR was run on the ABI Prism 7900HT Sequence Detection System (Applied Biosystems, Foster City, USA). A total of 12.5 ng cDNA in a total volume of 25 μ l was used for one PCR reaction including Primers, H₂O and TaqMan® Universal PCR Master Mix (Applied Biosystems). Quantification was performed from the obtained C_t-values using the $\Delta\Delta$ C_t method. The relative quantities to the reference gene RplpO were determined for internal normalization, and fold-induction calculation was performed based on the vehicle treated control group.

Tab. 7: Primer for real-time PCR

Gene symbol	term	Assay ID #	
<i>Ahr</i>	aryl-hydrocarbon receptor	Mm00478932_m1	Applied Biosystems
<i>RplpO</i>	ribosomal protein, large, P0	Mm01974474_gH	Applied Biosystems

Microarray analysis

In order to perform transcriptional profiling in the aorta of the mice after (-)-epicatechin treatment, a Mouse GE 4x44K v2 Microarray Kit from Agilent Technologies (Santa Clara, USA) with 39,430 probes representing the mouse genome was used. Total RNA from five individual mice aorta samples per group was isolated, and quality was determined as previously described. The array including transcription of total RNA into labeled cDNA was run in the *Biologisch-Medizinisches Forschungszentrum* (BMFZ) institute of the Heinrich-Heine-University of Duesseldorf. Regulated targets with signal intensity higher than the threshold and with p-values ≤ 0.05 were selected for further

analysis. The results were sorted and interpreted by affiliation and functional classification of the targets using the Database for Annotation, Visualization and Integrated Discovery (DAVID) (open source, <http://david.abcc.ncifcrf.gov/>) and the Kyoto Encyclopedia of Genes and Genomes (KEGG) (open source, <http://www.genome.jp/kegg/>).

Analytical analysis

Measurement of nitrate and nitrite

Plasma and tissue nitrate and nitrite levels were measured with high-performance liquid chromatography (ENO20, Eicom, Dublin, Ireland). This method employs an autoinjection system (Eicom), ion chromatography with a chloride buffer carrier solution (Eicom) and on-line reduction of nitrate to nitrite and subsequent postcolumn derivatization with the Griess reagent (Hendgen-Cotta et al. 2008). Calculations of concentrations were performed with prepared standards from NaNO₂ and NaNO₃ using dedicated software (PowerChrom, eDAQ, Colorado Springs, USA). The detection limit for nitrite and nitrate was 10 nM (0.1 pmol) for either anion at an injection volume of 100 µl. The measurements were performed by Sivatharsini Thasian-Sivarajah, samples were prepared by myself as described. In preparation for the measurement the shock-frozen plasma samples were thawed on ice and ice-cold methanol was added in equal volume, the sample was mixed thoroughly and centrifuged for 10 min. at 14000 rpm and 4°C to precipitate proteins. After centrifugation 100 µl of the supernatant was subjected to analysis.

Measurement of (-)-epicatechin metabolites

The assessment of (-)-epicatechin metabolites in blood plasma of the mice was done by kindly help of Dr. A. Rodriguez-Mateos from the Molecular Nutrition Group, School of Chemistry, Food and Pharmacy at the University of Reading, England. To determine the concentrations the plasma samples were processed and measured by HPLC-

analysis using a system from Agilent Technologies (1100 series) as previously described by the group (Rodriguez-Mateos et al. 2013). Briefly, plasma (0.5 ml) samples were prepared by using enzymatic hydrolysis with β -glucuronidase and sulfatase (10.000 IU β -glucuronidase, 300 IU sulfatase; 40 min. at 37°C) to produce nonglucuronidated and nonsulfated metabolites for analysis. Samples were mixed with 1 ml 0.5 % acetic acid in water (vol:vol), and centrifuged at 17.000 g for 15 min. at 4 °C. The supernatant (10 μ l) was injected onto a column with 0.1 % (vol:vol) formic acid in HPLC water and 0.1 % (vol:vol) formic acid in acetonitrile as mobile phase. The detection and quantification of phenolic acids and their metabolites was performed by using authentic standards.

Statistical Analyses

When not stated otherwise values reported are means \pm SEM or medians with quartiles and whiskers in Tukey box plots. Comparisons between groups were made using either 2-sided student's t-test or ANOVA, followed by Bonferroni or Games-Howell posthoc test for multiple comparisons. Differences were deemed significant when $p < 0.05$. Statistical analyses were performed using GraphPad Prism 5.00 (AD instruments, El Paso, USA) or SPSS 18.0 statistics (IBM, Amonk, USA).

Results

1. Plan of the study and experimental setup

The aim of this study was to analyze the molecular mechanisms responsible for the (-)-epicatechin induced increase in vascular function in a mouse model.

The first step was to determine whether (-)-epicatechin is absorbed and metabolized in mice. The second step was to establish and validate methods for the in vivo measurement of vascular function in living mice by application of LDPI and high-resolution ultrasound, and to prove that dietary administration of (-)-epicatechin affects vascular function by a dose-response curve. Once established the experimental setup for this study includes the in vivo treatment of mice with oral (-)-epicatechin (see methods), subsequent analysis of vascular function and eNOS and redox-dependent molecular mechanisms in cardiovascular tissue (Fig. 8). Furthermore as a hypothesis generating approach this study analysed global changes in gene expression pattern in the vascular tissue by (-)-epicatechin using comparative Microarray analysis.

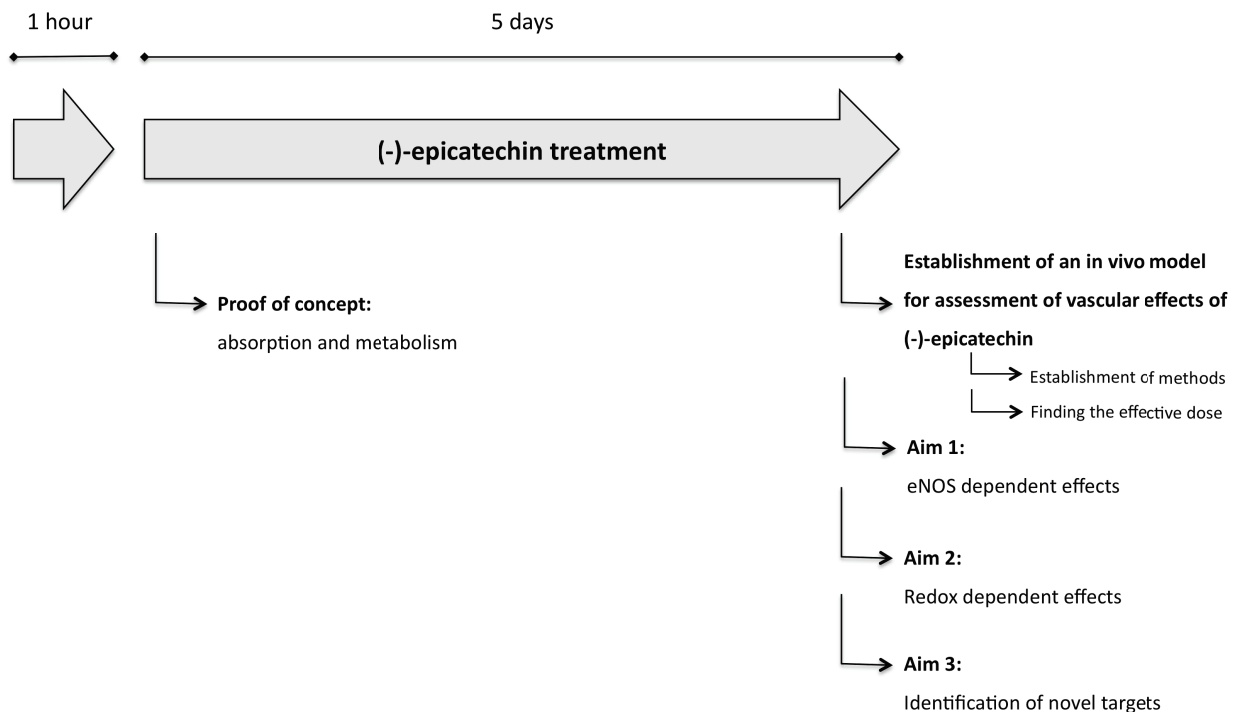


Fig. 8: Experimental plan for the analysis of oral (-)-epicatechin effects in mice in vivo

2. Proof of concept: (-)-Epicatechin is rapidly absorbed and metabolised in living mice

In order to determine the adsorption and metabolism pattern in mice, increasing dose of pure (-)-epicatechin were administrated by intraenteral gavage feeding and concentrations of (-)-epicatechin metabolites were measured in plasma after one hour by HPLC analysis (Fig. 9). The concentrations of flavanols in plasma of the mice increased by increasing the amount of administered (-)-epicatechin and reached a plateau at concentrations of 4 mg/kg. Moreover, up to 78 % of total metabolized (-)-epicatechin found in plasma is methylated. With increasing dose the amount of 3'-O-methylated epicatechin successively increased reaching up to 52 % of total metabolites.

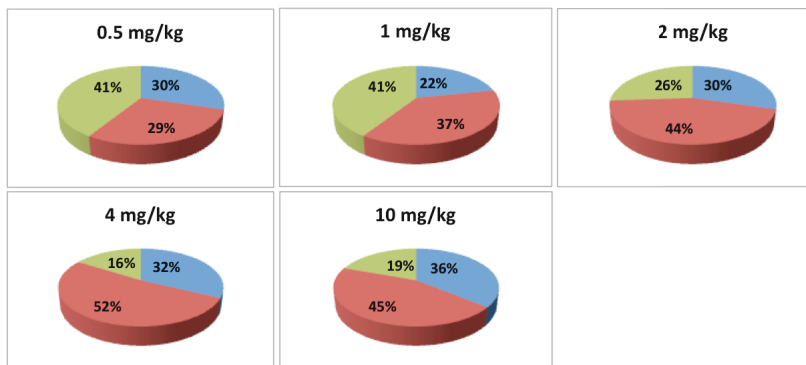
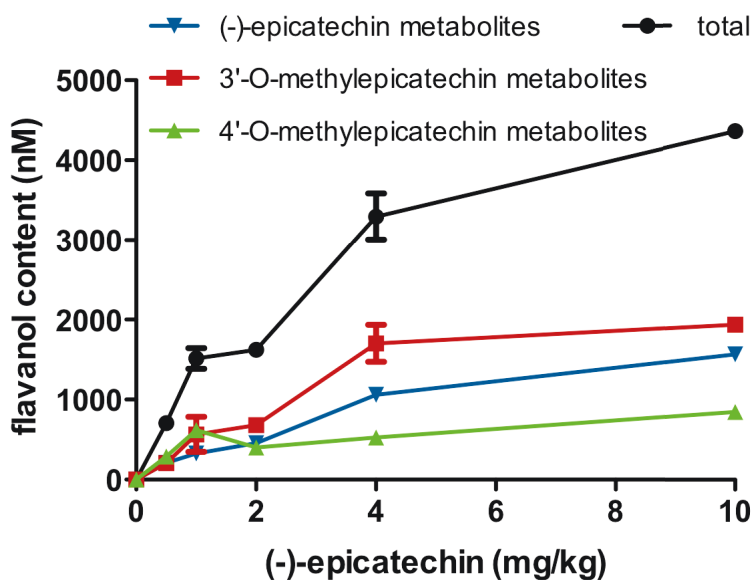


Fig. 9: (-)-Epicatechin is absorbed and metabolized in mice.

Plasma levels of non-methylated (blue), 3'-O-methylated (red) and 4'-O-methylated (green) derivatives of epicatechin were measured one hour after enteral gavage feeding of 0.5 – 10 mg/kg (-)-epicatechin. Concentrations in plasma of the mice were assessed by HPLC (HPLC of collected plasma was done by A. Rodriguez-Mateos). Six mice were treated / group. Plasma from two mice was used for each measurement.



In order to prove that dietary administration of (-)-epicatechin affects vascular function in mice a dose-response curve was generated with the same groups of mice using measurement of time to peak before and after intervention by scanning LDPI (Fig. 10).

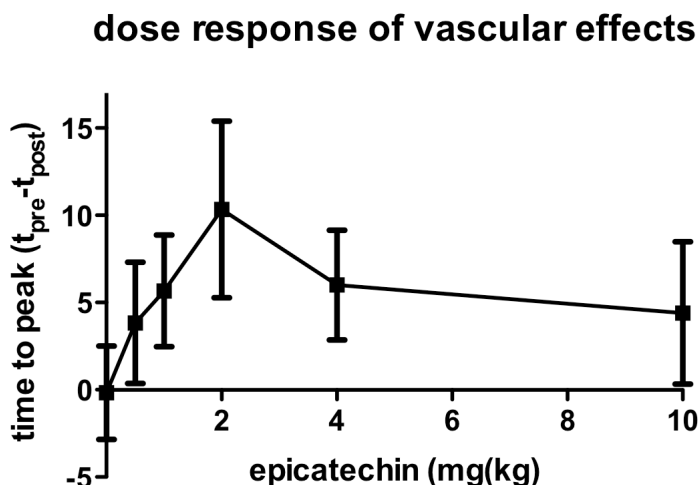


Fig. 10: (-)-Epicatechin has a dose-dependent effect on vascular function

A dose of 2 mg/kg (-)-epicatechin has the strongest effect on vascular reactivity measured as rapidity (time to peak: pre treatment – post treatment) of PORH by LDPI.

3. (-)-Epicatechin increases vascular reactivity in mice in vivo

3.1: Establishment of in vivo methods for assessment of vascular function: ultrasound and LDPI

As a first step to establish the assessment of vascular function in mice changes in the vessel diameter and tissue perfusion in response to well-characterized vasoactive molecules were assessed by ultrasound and LDPI. As a second step transient ischemia and reperfusion was induced to measure the physiological response to reactive hyperemic blood flow in the mouse hindlimb.

3.1.1: Vasoactive molecules modulate the vascular diameter and mean perfusion in the hindlimb.

Systemic i.p. injection of a 12 mg/kg NTG bolus rapidly increased vessel diameter and flow within the femoral artery as assessed by ultrasound (Fig 11A, panel I), and increased MPU as compared to baseline, reaching a maximum within approximately 100

Results

sec. (Fig. 11A, panel II), whereas the vehicle control had no effect. The maximal increase in MPU after administration of NTG was 128 % as compared to vehicle control (435 ± 23 MPU after NTG vs. 191 ± 36 MPU, $n=4$, Fig. 11A, panel III). Stimulation of purinergic receptors by i.v. bolus administration of 10^{-4} M adenosine significantly increased vessel diameter and peak flow velocity (Fig. 11B, panel I), as well as MPU within approximately 150 sec. (Fig. 11B, panel II), with a maximal increase of 41 % as compared to baseline values (316 ± 43 vs. 224 ± 34 MPU baseline) (Fig. 11B, panel III). Administration of 10^{-4} M s.c. epinephrine caused a rapid decrease in vessel diameter and flow (Fig. 11C, panel I), and a rapid 57 % drop in MPU (90 ± 18 MPU vs. 209 ± 59 , $n=4$, Fig. 11C, panel III), which lasted throughout the entire measurement interval (Fig. 11C, panel II). Intravenous injection of the endothelium-dependent vasodilator ACH (10^{-4} M) caused a significant increase in diameter and flow (Fig. 5D, panel I), and MPU (Fig. 11D, panel II and III), reaching a maximum of 32 % within 300 sec ($n=5$, 537 ± 35 MPU vs. 406 ± 48 MPU baseline). The LDPI signal remained unaffected after vehicle injection. During the treatments, there was no significant change in heart rate (HR), respiration rate (RR) and body temperature (Tab. 8). The systolic and diastolic blood pressure measured in the aorta was significantly decreased by vasodilators and increased by epinephrine (Tab. 8). In summary changes in blood flow in the femoral artery as a result of administration of well characterized vasodilators and vasoconstrictors directly correlate to changes in MPU, as assessed by LDPI.

Results

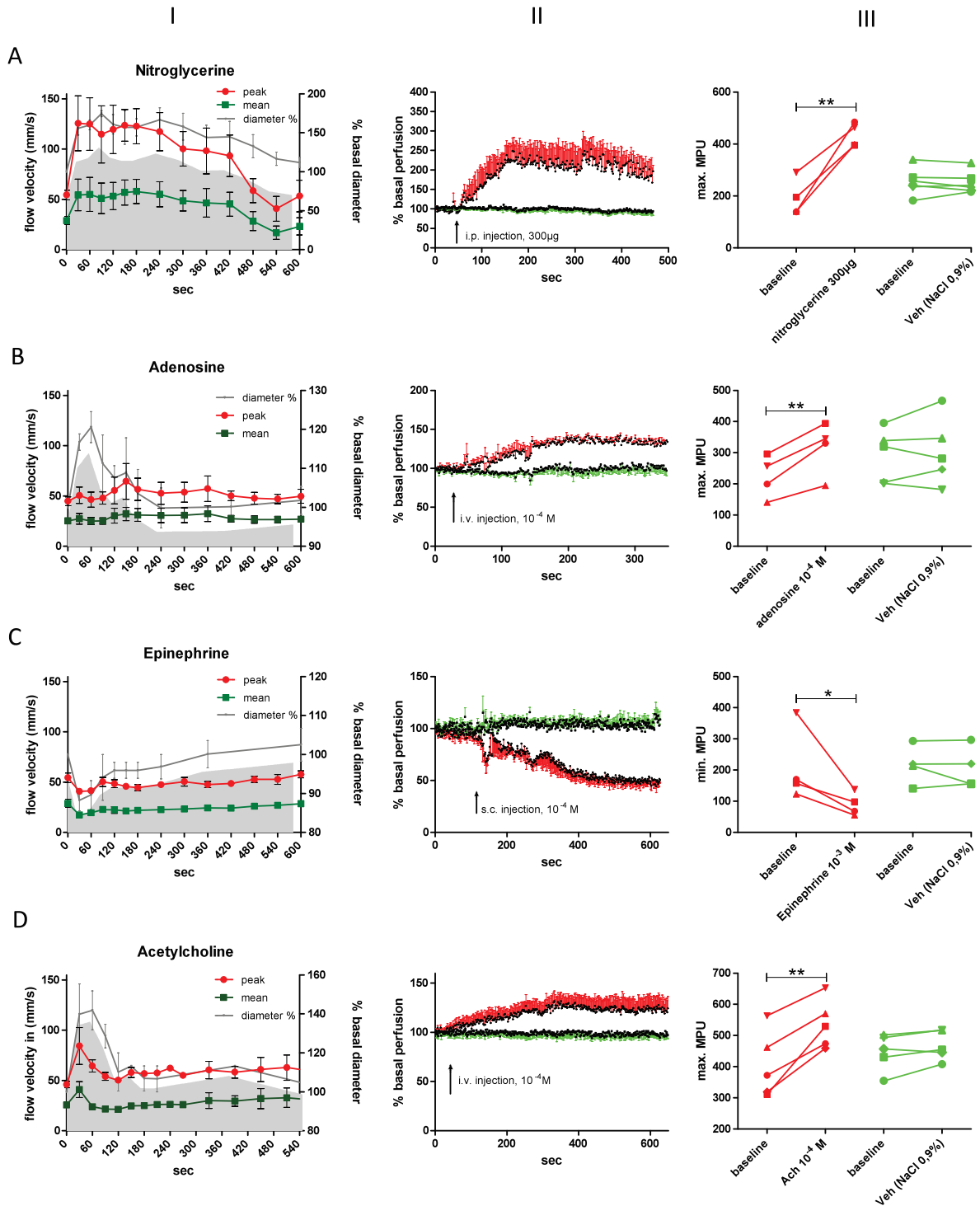


Fig. 11: Pharmacological modulation of vascular diameter and hindlimb perfusion.

Changes in femoral artery diameter and flow velocity by ultrasound (panel I) and changes in tissue perfusion by LDPI (panels II and III) were assessed in response to i.p. nitroglycerine (**A**, n=4), i.v. adenosine (**B**, n=4), s. c. epinephrine (**C**, n=4) and i.v. acetylcholine (**D**, n=5). Warm saline served as control and had no effect on the perfusion values. Symbols are means \pm SEM; * = $p < 0.05$, ** = $p < 0.01$ vs. baseline; Saline and pharmacological controls were run on the same mouse.

Results

Tab. 8: Physiological parameter (body temp., respiration, heart rate, blood pressure) during administration of nitroglycerin (NTG), acetylcholine (ACH), adenosine and epinephrine. Mean±SEM, paired t-test between baseline and treatment; * = P < 0.05, ** = P < 0.01, n=4 per group.

	body temp. (°C)	respiration rate (RR)	heart rate (HR)	Blood pressure (BP)	
				PS / PD (mmHg)	
				baseline	treatment
control	35.9 ± 0.4	124 ± 27	470 ± 59		
+ NTG	36.1 ± 0.3	130 ± 18	495 ± 38	97±10 / 59±10	80±10 / ** 56±9
+ ACH	35.9	123 ± 13	511 ± 58	101±3 / 72±3	92±8 / 63±5
+ Adenosine	35.9	125 ± 38	410 ± 69	94±10 / 62±11	88±10 / ** 54±13 *
+ Epinephrine	35.8 ± 0.7	139 ± 28	498 ± 55	95±7 / 66±5	108±7 / ** 73±4 *

3.1.2: Post-occlusive reactive hyperemia (PORH) in the hindlimb of the mouse

PORH was originated by using an inflatable cuff placed at the distal side of the hindlimb and induction of non-invasive transient ischemia (see methods). Release of the occlusion led to a rapid FMD of the femoral artery as demonstrated by an increase in femoral artery diameter (Fig. 12).

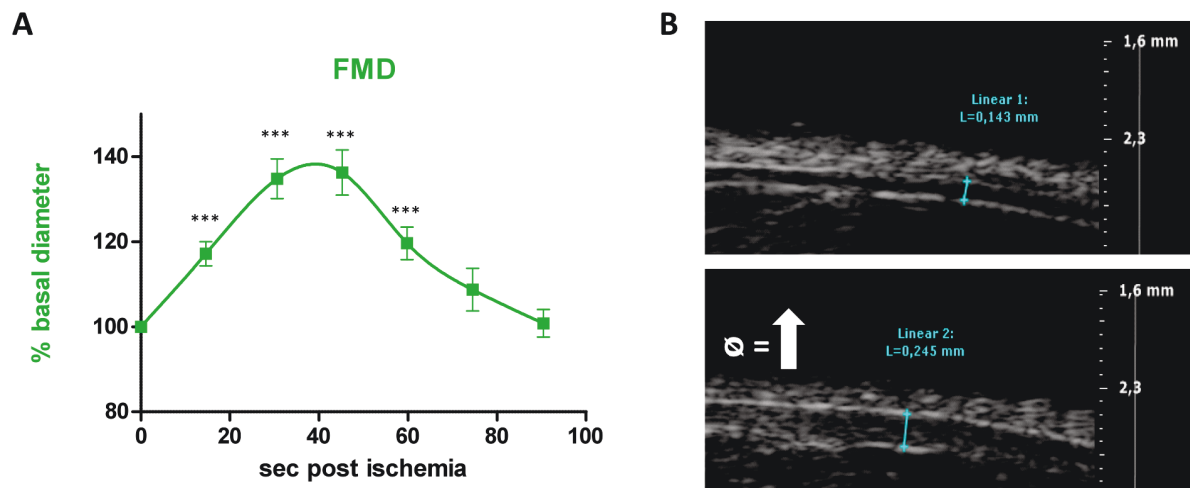


Fig. 12: Physiological modulation of diameter change in the femoral artery by PORH.

Significant changes in femoral artery diameter as FMD were assessed by high resolution ultrasound. The curve was derived from measurements in 10 different mice.

The maximal response was reached approx. 40 sec. after cuff release and dilated the artery by up to 35 % as compared to the basal diameter. The FMD response in mice lasted for approx. 90 sec. The maximum FMD due to PORH was comparable to the diameter change induced by administration of adenosine or acetylcholine (Fig. 11, panel I).

Changes in perfusion after PORH were also assessed by LDPI. The successful induction of ischemia by cuff inflation was confirmed as a drop of MPU < 30. Five minutes of occlusion time led to a rapid (< 1 min.) increase in MPU as compared to baseline values, which then returned to baseline after 5-6 min. (Fig. 13A). The peak of MPU after PORH (mean: 150 ± 15 %) was similar to the maximum NTG-induced MPU increase (149 ± 42 %), and significantly higher than the ACH (38 ± 12 %) and adenosine (43 ± 8 %) induced response. The parameters used to quantify PORH are described in fig. 13A (also see methods for details). Fig. 13B depicts exemplary perfusion images during baseline, ischemia and hyperemia measurements.

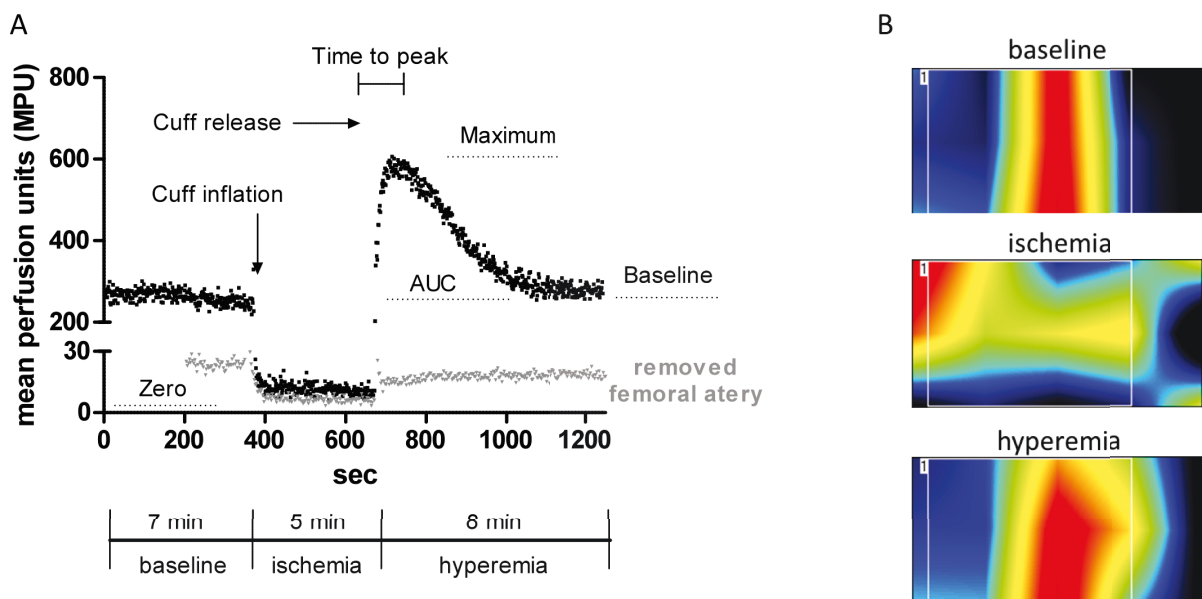


Fig. 13: Physiological modulation of hindlimb perfusion by PORH.

Representative curve (black line, **A**) and images (**B**) showing changes in tissue perfusion during baseline, ischemia and reactive hyperemia with the analysed parameters: baseline, zero perfusion, maximum, time to peak, amplitude (max-basal perfusion), perfusion reserve (amplitude/basal perfusion*100), ratio (max/basal perfusion) and AUC (area under curve). The grey line represent zero perfusion obtained after surgical excision of the femoral artery. Representative measurement from three different mice.

Importantly, after surgical excision of the femoral artery, MPU was as low as zero perfusion after inducing transient ischemia in control animals, and the PORH response was absent (Fig. 13A grey curve).

Comparison of both methods revealed that the time course of the first phase of reperfusion was similar in both measurements as the peak of maximum dilation of the femoral artery corresponded to a maximum increase in MPU (Fig. 14A). However the PORH assessed by LDPI lasted longer than the FMD response of the femoral artery. Also the slope and maximum response of PORH was similar detected as increase in femoral artery diameter and tissue perfusion (Fig. 14A and 14B).

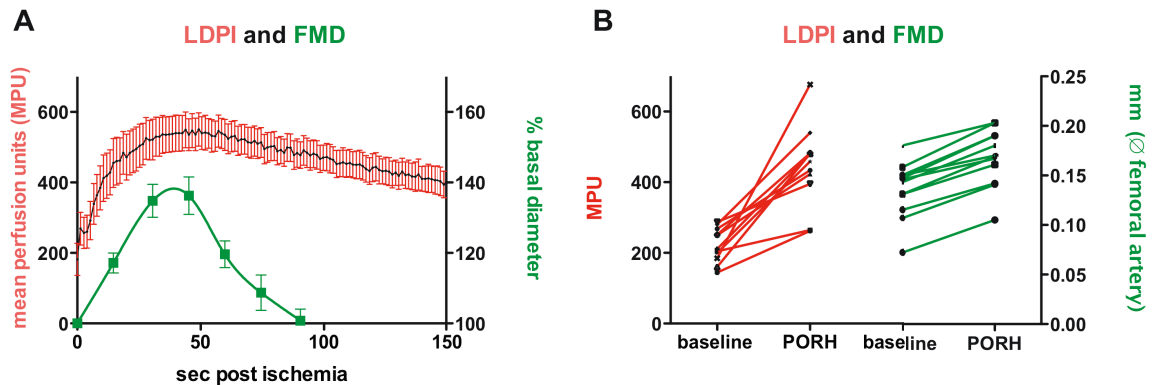


Fig. 14: Course and slope of PORH assessed as FMD and changes in MPU.

A) Original courses of changes in femoral artery diameter (green) and MPU (red) during PORH after release of transient occlusion. **B)** Maximum changes in femoral artery diameter (green) and MPU (red) in PORH from intra-individual measurement in the same mouse.

3.1.3: Validation of PORH in mouse hindlimb assessed by LDPI

To test the dependency of the PORH response on duration of ischemia as assessed by LDPI, the hindlimb perfusion was occluded for one, three and five minutes (Fig. 15A-D). By increasing the occlusion time, an increase in maximal MPU, and time-to-peak was measured, while the AUC (C) was only significantly increased after five minutes of ischemia (Fig. 15A-D; * $p < 0.05$, $n = 5$).

Results

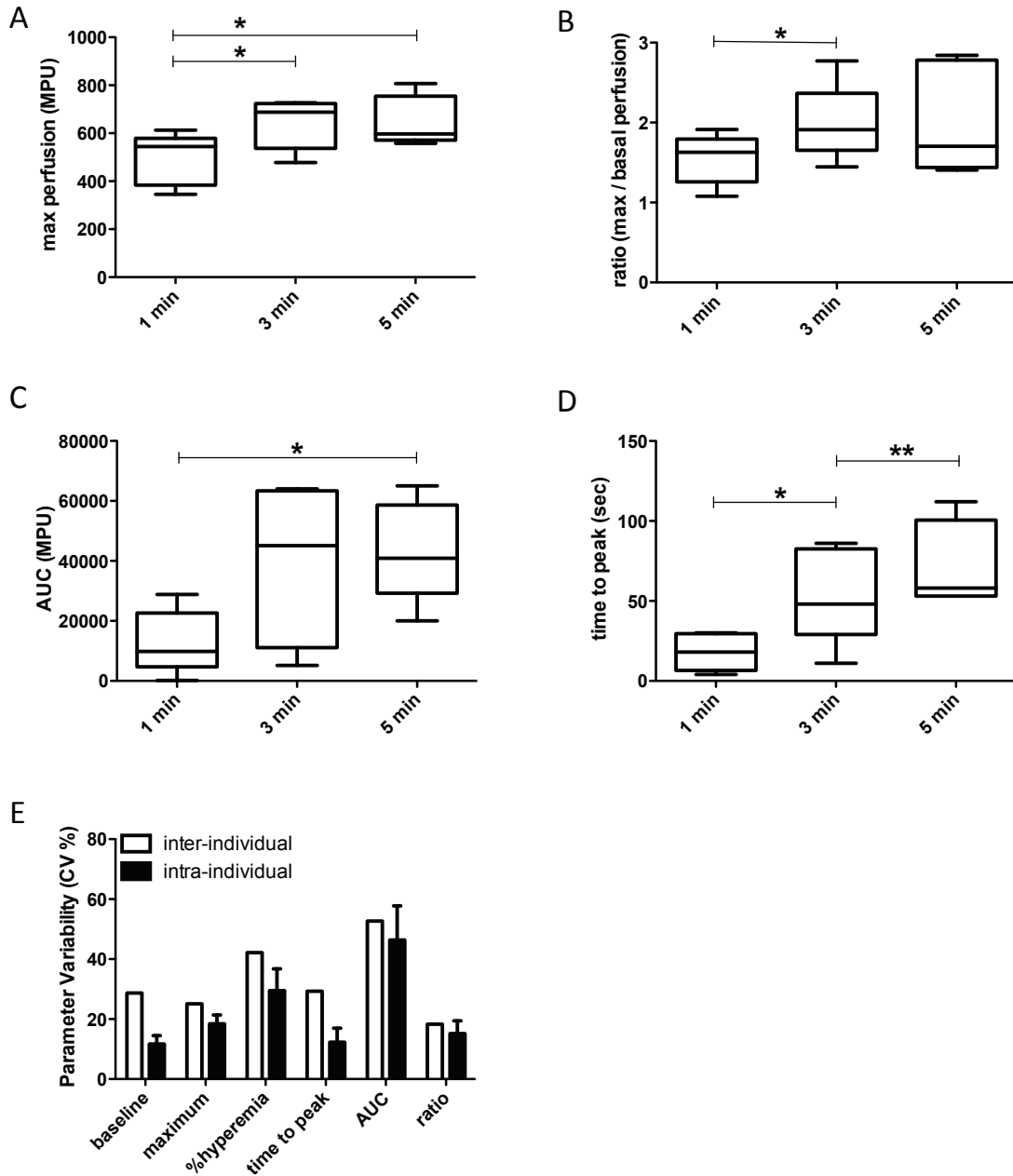


Fig. 15: Validation of the PORH response as assessed by LDPI

A,B,C,D) The degree of maximal hyperemic blood flow depends on the duration of occlusion. * = $P < 0.05$.

E) Coefficient of variation for all parameters of PORH after 5 min occlusion. For intraindividual reproducibility four repeated measurements were performed on the same mouse in four different individuals ($n=4$) and for inter-individual variability by comparing the coefficient of variation (CV) of $\geq n=10$ mice.

To further validate the method, repeated measurements of PORH were performed in individual mice. Intra-individual variability was assessed by four repeated measurements

Results

of the same mouse (black bars, n=4) and inter-individual variability (white bars) by comparing the coefficient of variation of the different parameters assessed in different mice (Fig. 15E, n= ≥10). The smallest variation was found for time to peak and ratio, while AUC measurements showed the highest variability.

3.1.4: Endogenous vasodilators modulate the PORH response

NOS inhibition assessed by administration of L-NNA (1.6 mg/ml = 270 mg/kg/d) significantly decreased the rapidity of the PORH response with a greater time to peak determined both in different groups and in intra-individual measurements (Fig. 16A-B).

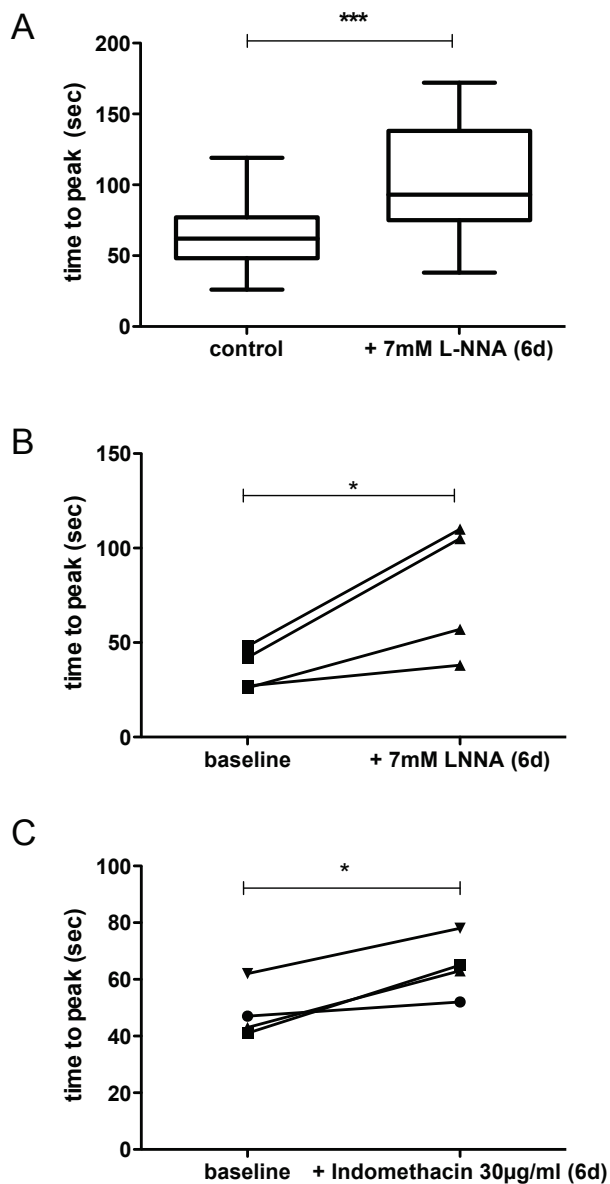


Fig. 16: The hyperemic response is NOS and COX dependent.

A, B) Effects of chronic inhibition of NO synthase (NOS) by L-NG-Nitroarginine (L-NNA). Six day chronic inhibition of NOS with L-NNA in drinking water (7 mM, ad libitum) significantly prolonged time to peak perfusion in **(A)** inter-individual (median: 62 vs. 93 sec., n=20) and **(B)** intra-individual measurements. **C)** Effects of chronic COX (cyclooxygenase) inhibition with 30 µg/ml indomethacin.

Results

A decrease in prostaglandin production was achieved by administration of the cyclooxygenase inhibitor indomethacin (30 µg/ml = 5 mg/kg/d) in drinking water for six days (Fig. 16C), which resulted in an increase in time-to-peak (48±5 vs. 64±5 sec.). While rapidity of the response was NOS and COX dependent, other parameters of PORH remained unchanged (Tab. 9). Further the PORH response in mice with a genetic deletion of eNOS (eNOS^{-/-}) was not changed compared to wild type mice (Tab. 9).

Tab. 9: NOS dependence of PORH by LDPI. Parameter of perfusion measurements (baseline, maximum, % hyperemia, time to peak, AUC, ratio) after L-NNA and Indomethacin treatment. Paired t-test between control and treatment * = P < 0.05. ** = P < 0.01. Intra-individual: n=5; inter-individual: n=20 per group.

		baseline (MPU)	maximum (MPU)	% hyperemia	time to peak (s)	AUC (MPU)	ratio
Wildtype	mean	317.9	562.6	106.5	63.8	34314.8	2
	SD	184.3	255.3	68.44	20.0	24437.2	0.74
	SEM	43.1	59.7	16	4.8	6051.4	0.2
Wildtype + LNNA	mean	263.3	481.7	88.5	101.3 ***	19510.9 *	1.9
	SD	53.7	69.5	40.9	39.3	8701.4	0.4
	SEM	11.7	15.2	8.9	8.8	1993.2	0.09
eNOS^{-/-}	mean	230.6	442.1	95.3	70.6	25547	2
	SD	77.8	140.1	32.1	23.9	22401	0.3
	SEM	17.4	32.1	7.2	7.2	5422.3	0.08
Intra-Individual measures							
baseline	mean	206.5	409.9	100.8	35.8	71319.8	1.9
	SD	48.1	124	45	11	52713	0.4
	SEM	21.5	55.4	20.1	5.5	26356.5	0.2
+ LNNA	mean	222.6	542.3	146.8	77.5 *	281125	2.6 *
	SD	31.3	59.7	35.9	35.6	113296	0.3
	SEM	14	26.7	16.1	17.8	56648	0.1
baseline	mean	236.3	601.9	155.5	48.3	63377	2.6
	SD	31.8	101.7	32.5	9.5	5420.5	0.3
	SEM	15.9	50.9	16.2	4.8	3832.8	0.2
+Indomethacin	mean	260.2	601.8	126.2	64.5 *	31747.5	2.3
	SD	119	335.9	49.8	10.7	30221.4	0.5
	SEM	59.5	168	24.9	5.3	21369.8	0.2

3.1.5: PORH response decreases with age in mice.

As a proof of concept PORH has been additionally determined in old wildtype mice (Fig. 17). The rapidity of hyperemic reperfusion was altered with a prolonged time to peak

(A) and a faster perfusion drop to baseline values in older mice (B). Furthermore 12 months and 24 months old mice had a significantly diminished PORH response assessed as % perfusion increase (C) and AUC (D) as compared to younger mice.

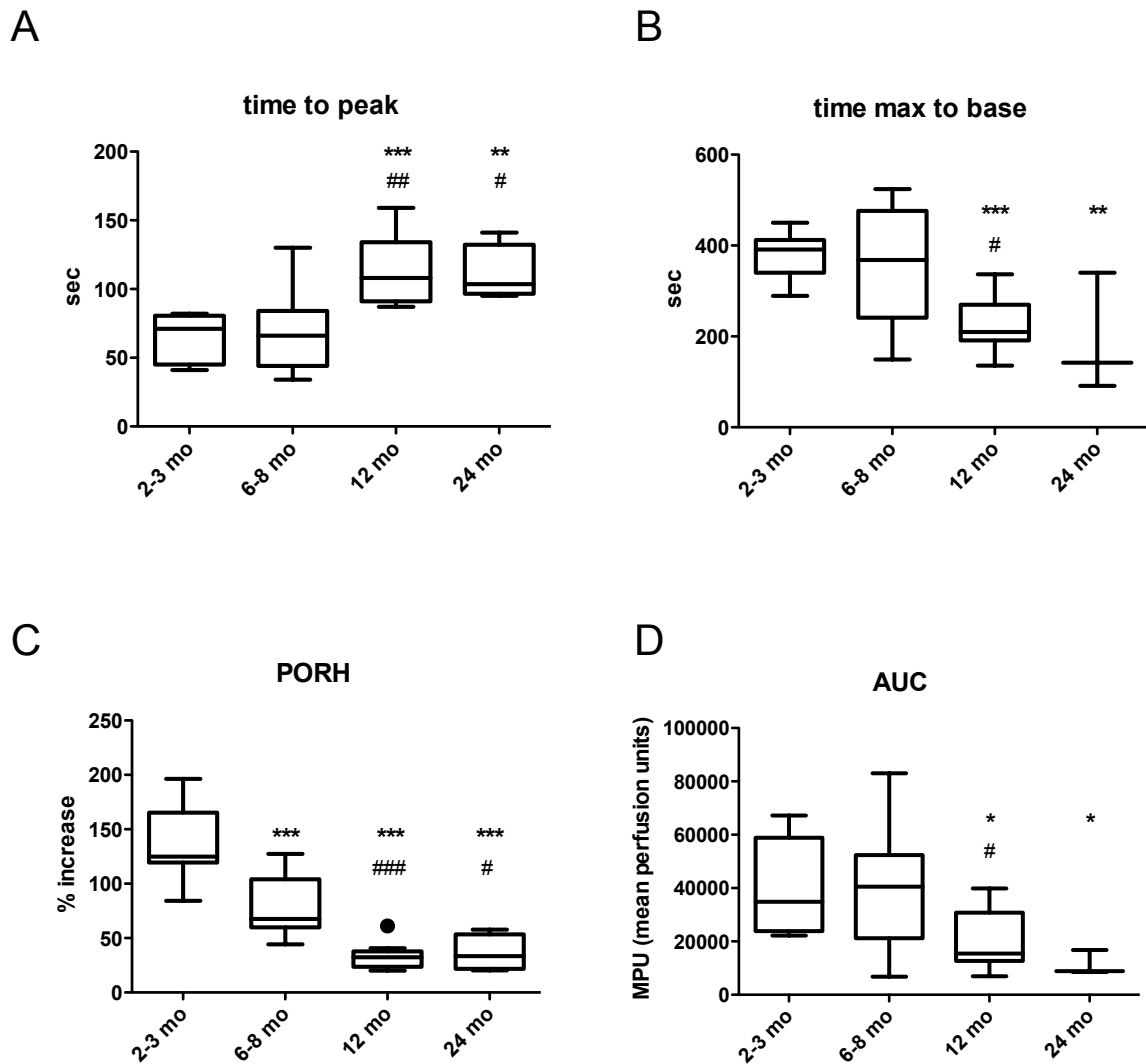


Fig. 17: The degree of PORH decreases with age.

Significant differences were detected in the rapidity of reperfusion in the first phase (A) and in the second phase of hyperemia (B). C) The degree of PORH after ischemia is significantly lower in adult and aging mice (6, 12, 24 months) vs. young mice (2-3 months). Maximum reperfusion is compared to baseline values. D) Overall perfusion in the reperfusion phase is decreased in 12 and 24 mo. old mice measured as area under curve (AUC). * = P < 0.05 vs. 2-3 mo., # = P < 0.05 vs. 6-8 mo. n=11 per group, n=4 in 24 mo. old.

Taken together these data show that the measurement of perfusion in the mouse hindlimb by LDPI is sensitive to pharmacological and flow-dependent changes in vessel diameter and is valid for evaluating intra-individual changes for significant in vivo investigations with limited numbers of animals. Because of small variation, dependence on NOS/COX and physiological relevance the time to peak parameter was used for analysis of vascular (-)-epicatechin effects.

3.2: Oral (-)-epicatechin increases vascular function in living mice

Measurements of FMD by high-resolution ultrasound and PORH by LDPI were applied in order to determine whether oral (-)-epicatechin treatment improved vascular response in living mice.

3.2.1: (-)-Epicatechin increases vascular function in an eNOS-dependent fashion

Dietary treatment of mice with 2 mg/kg (-)-epicatechin corresponded to a significant 1.5 fold increase in FMD of the femoral artery compared to control treatment as assessed by high resolution ultrasound (Fig. 18A). Maximal dilation of the femoral artery is reached 45 seconds after releasing the occluding cuff as shown in panel I (53.3 ± 6.7 % 2 mg/kg (-)-epicatechin (green) vs. 36.2 ± 5.3 % vehicle (black)) and panel II (59.8 ± 3.6 % vs. 37.2 ± 4.8 %). These effects corresponded to a significant increase in the rapidity of PORH, as determined by measuring the time-to-maximum response (Fig. 18B). Importantly these beneficial effects of (-)-epicatechin on vascular function were fully blunted by administration of the specific NOS inhibitor L-NNA as well as in eNOS^{-/-} mice (Fig 18). Increasing the dose to 10 mg/kg fully blunted the response indicating a very small window of effective dose.

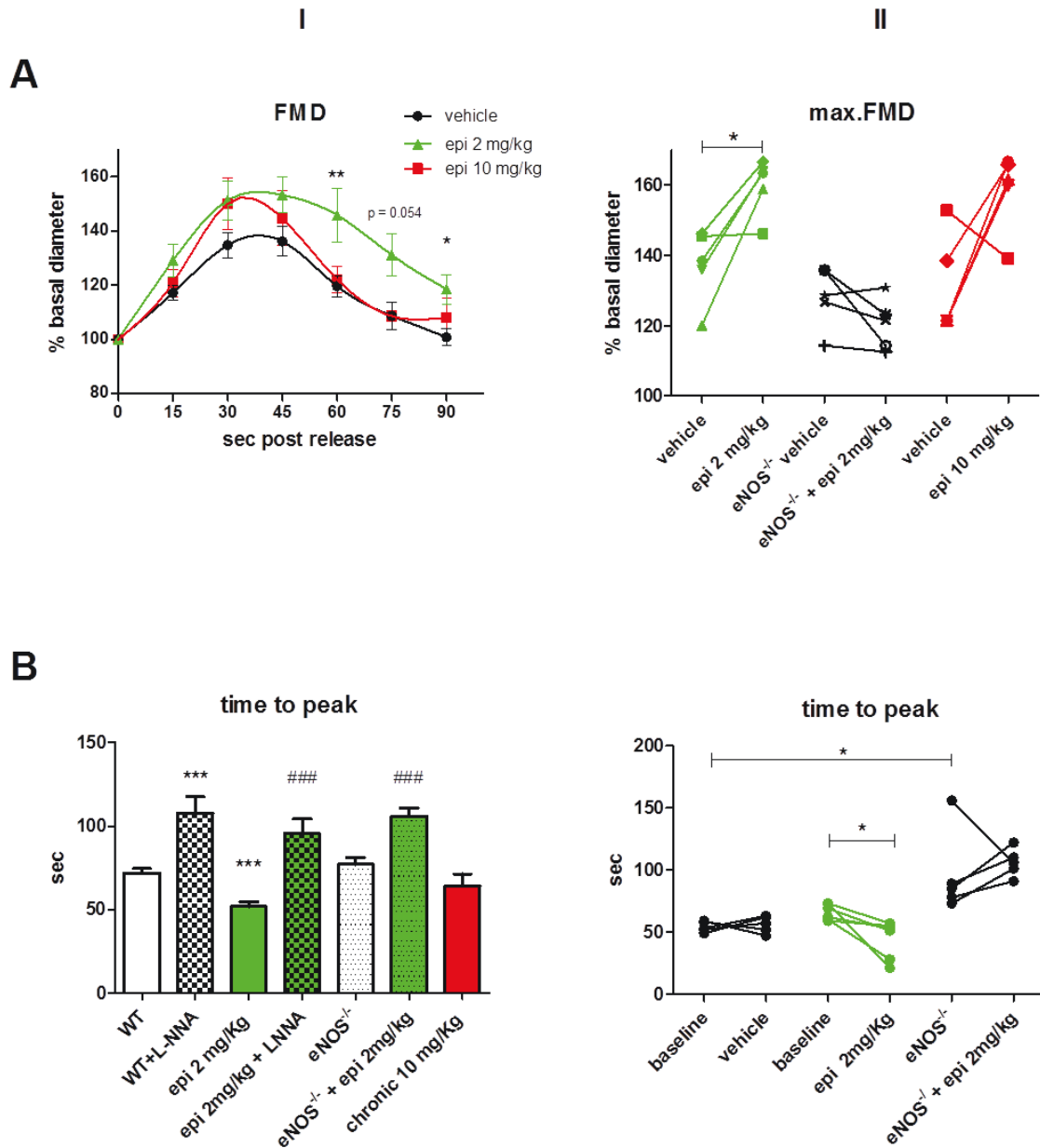


Fig. 18: (-)-Epicatechin increases FMD and accelerates PORH in vivo in an eNOS dependent fashion.

(A) Vascular function assessed as FMD of the femoral artery after five min. ischemia by ultrasound. Time course of FMD (panel I) and maximal intraindividual increase in FMD (panel II), n=5. (B) Interindividual (panel I) and Intraindividual (panel II) effects of (-)-epicatechin treatment on hyperemic blood flow measured as time to maximal increase (time to peak) after five min. ischemia by LDPI, n ≤ 10. * = p ≤ 0.05, t-test between the groups. For inter-individual measurements one control group is shown, because no differences were detected in the vehicle treatments.

In addition to the vascular response to PORH, administration of 2 mg/kg (-)-epicatechin in drinking water significantly decreased pulse-wave velocity (PWV), assessed by high-

resolution ultrasound (Fig. 19), while the higher dose had no effect. This parameter is NOS dependent as demonstrated by NOS-inhibition. Thus because a dose of 2 mg/kg but not 10 mg/kg improved vascular function in mice, the lower dose was further used in this study to investigate the molecular mechanisms of (-)-epicatechin induced vascular response in vivo.

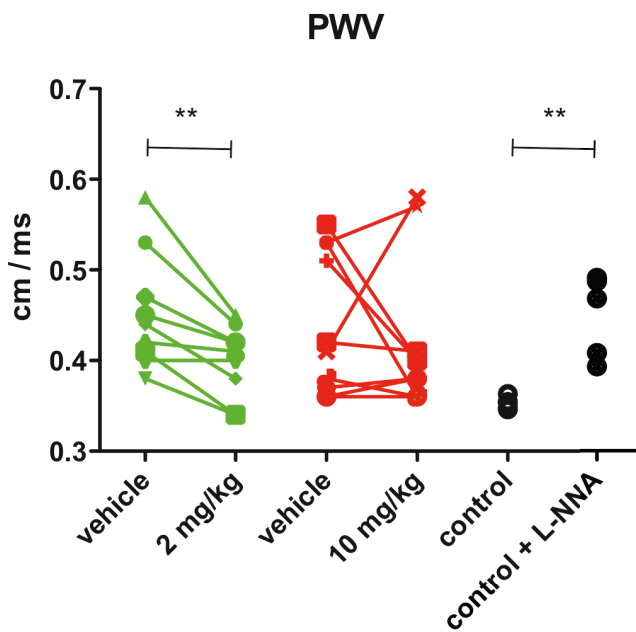


Fig. 19: (-)-Epicatechin increases vascular pulsatility in mice.

(-)-Epicatechin was administrated in drinking water for 5 days at the indicated dosis of 2 mg/kg and 10 mg/kg. Effect of (-)-epicatechin on vascular pulsatility was as assessed as PWV (*pulse wave velocity*) using high-resolution ultrasound. ** = $p \leq 0.005$, t-test between the groups

To determine whether increased vascular functionality is paralleled by regulation of blood pressure, which is a physiological parameter strongly associated with NO-bioavailability (Wood et al. 2013) and which was regulated by vasoactive agents, the arterial pressure was measured in mice after (-)-epicatechin treatment. No differences in pressure were found after a five day treatment with 2 mg/kg (-)-epicatechin (Tab.10). However, simultaneous administration of L-NNA significantly increased systolic and diastolic arterial pressure demonstrating NOS dependence of this parameter.

Results

Tab. 10: Blood pressure is not changed by (-)-epicatechin. Systolic (PS) and diastolic (PD) pressure was measured in aorta of mice treated with 2 mg/kg (-)-epicatechin for five days by a pressure-catheter. Contribution of NOS was analysed by additional LNNA administration for six days, n=5. * = $p \leq 0.05$, ** = $p \leq 0.05$, t-test between the groups.

		Vehicle	Epi + 2 mg/kg	Epi + 2 mg/kg + LNNA
PS (mmHg)	mean	97.06	98.01	119.9 **
	SD	5.89	7.45	9.07
	SEM	2.63	3.33	4.54
PD (mmHg)	mean	67.84	69.34	84.19 *
	SD	5.75	7.56	5.28
	SEM	2.57	3.38	2.64

3.2.2: (-)-Epicatechin increases vascular function in a Nrf2-dependent fashion

NO-bioavailability is dependent on both NO production and NO consumption by ROS. The transcription factor Nrf2 is a key master switch controlling the expression of enzymes involved in the regulation of the cellular redox state. Thus Nrf2^{-/-} mice have a decreased capacity of maintaining the redox state in tissues. To investigate whether (-)-epicatechin regulates vascular homeostasis and therefore vessel functionality via Nrf2, vascular function was measured after administration of 2 mg/kg (-)-epicatechin.

The vascular effects of (-)-epicatechin are diminished in Nrf2^{-/-} mice, as compared to wildtype mice. When comparing the actual time course and degree of FMD no differences were detected with dietary (-)-epicatechin treatment compared to the vehicle control (Fig. 20A). Although the maximal dilative response is increased in intra-individual measures (Fig. 20B), this effect is not significant as previously shown for wildtype mice. As demonstrated by application of the specific NOS inhibitor L-NNA the (-)-epicatechin effect is completely abolished when NOS is blocked (Fig. 20B). Moreover PWV as a measure of vascular stiffness is not affected by five-day (-)-epicatechin treatment (Fig. 20C), while (-)-epicatechin even decreased PWV one hour after feeding. Again NOS inhibition abolished this (-)-epicatechin effect.

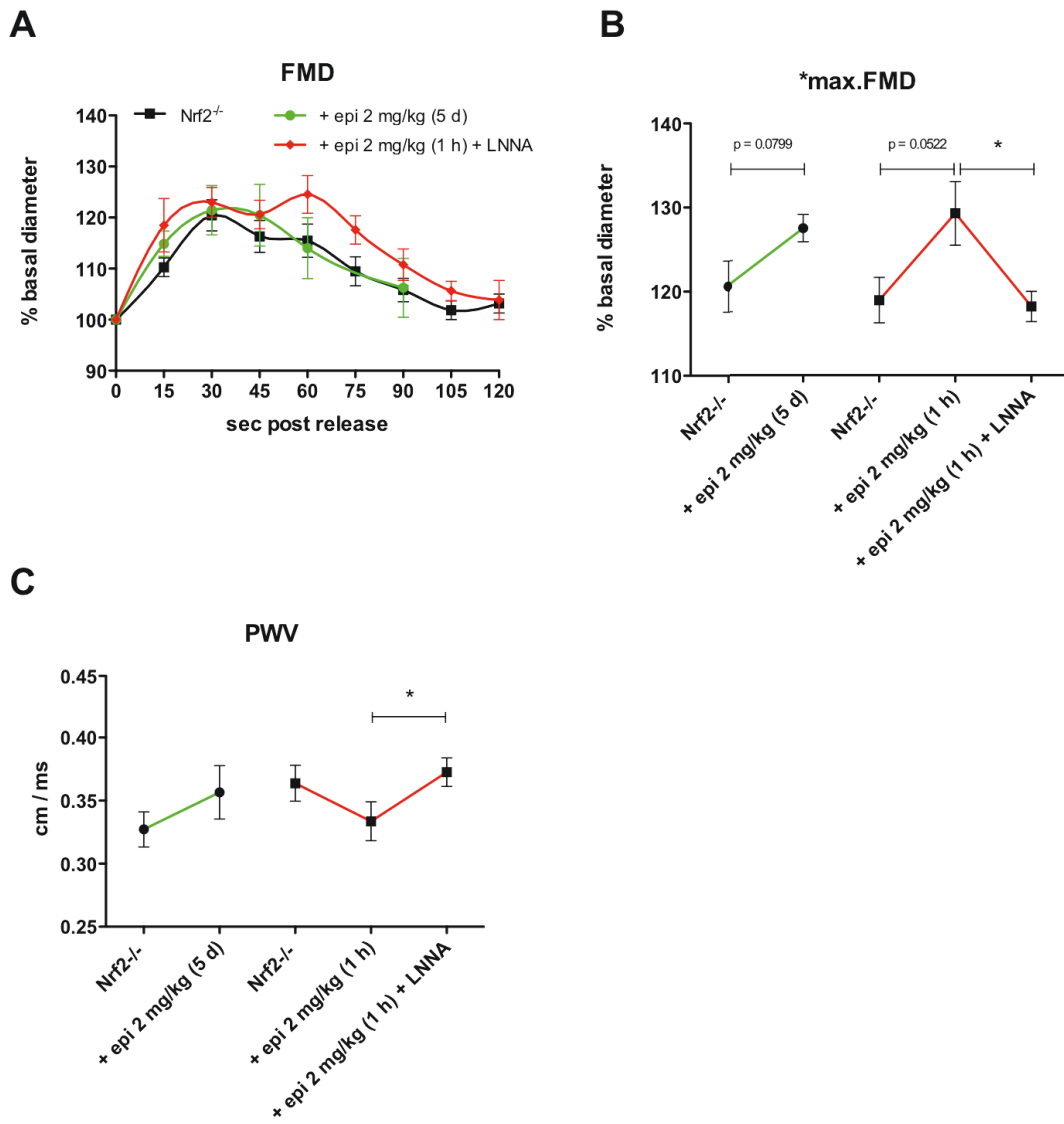


Fig. 20: (-)-Epicatechin does not improve FMD in Nrf2^{-/-} mice in vivo.

A-B) Long-term 2 mg/kg (-)-epicatechin treatment does not increase FMD of the femoral artery in Nrf2^{-/-} mice assessed after five min. ischemia. **C)** Vascular function is not affected by (-)-epicatechin in Nrf2^{-/-} mice measured as PWV. n=5 in each group.

In contrast to these findings in Nrf2^{-/-} mice 2 mg/kg (-)-epicatechin significantly increased FMD and decreased PWV in wildtype mice as shown previously. Moreover both long-term and acute dietary feeding with 2 mg/kg (-)-epicatechin did not change the PORH response in Nrf2^{-/-} mice assessed by LDPI (Fig. 21) as shown for inter-individual (panel I) and intra-individual (panel II) measurements. As previously demonstrated (-)-

Results

epicatechin significantly decreased time to peak and increased the perfusion reserve in wildtype mice.

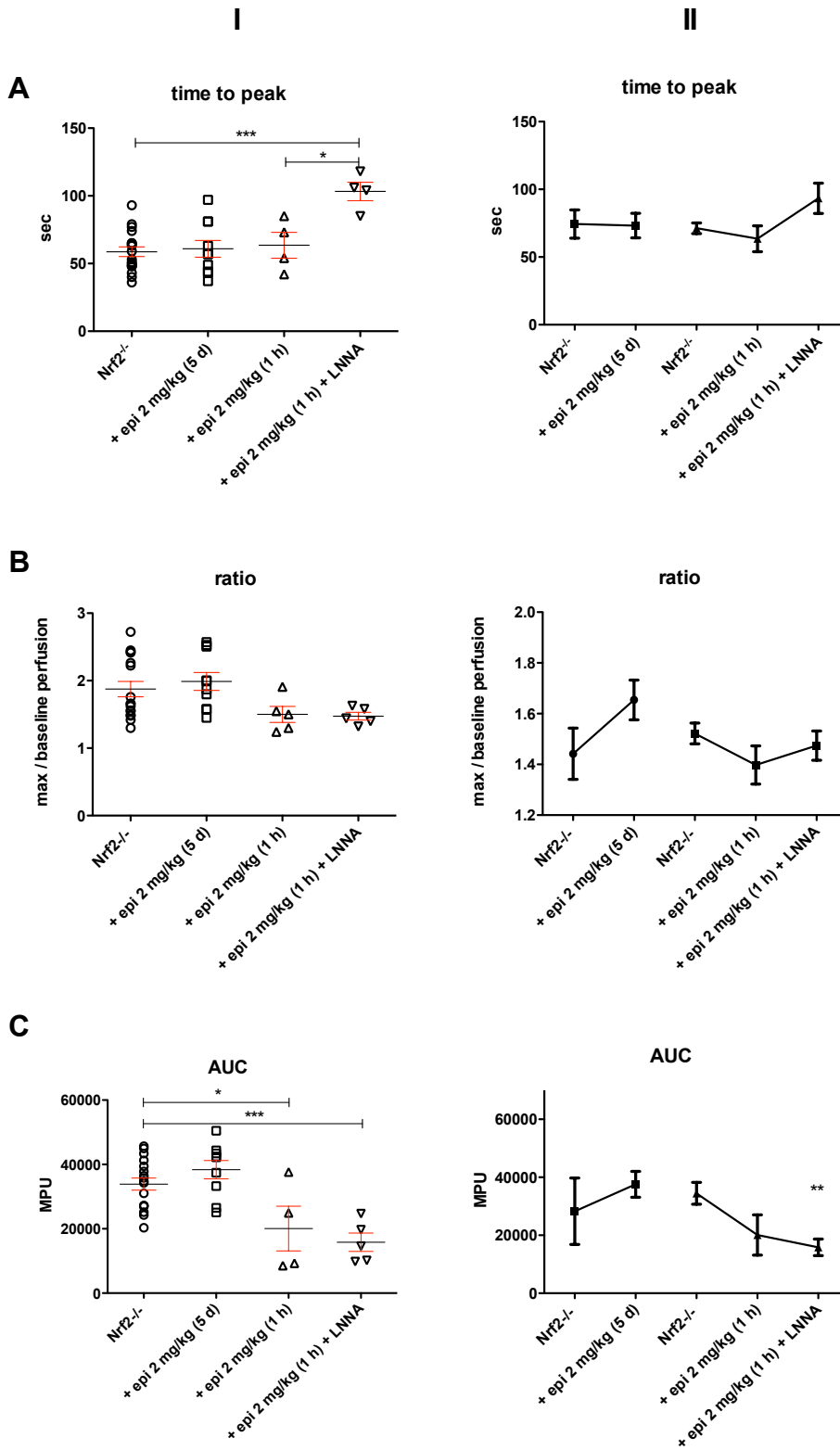


Fig. 21: (-)-Epicatechin does not improve PORH in Nrf2^{-/-} mice in vivo

The reperfusion blood flow after five min. ischemia was measured after 2 mg/kg (-)-epicatechin treatment in inter-individual (panel I) and intra-individual (panel II, n=5) measurements. Parameter of hyperemic blood flow were analysed as time to maximal reperfusion (time to peak; A), the perfusion reserve measured as max /baseline perfusion (ratio; B) and overall perfusion in the reperfusion phase measured as area under curve (AUC; C).

Taken together these findings demonstrate that (-)-epicatechin treatment for five days improves vascular function in wildtype mice but not in eNOS^{-/-}, after NOS-inhibition or in Nrf2^{-/-} mice. However (-)-epicatechin still improves vascular function when response is measured one hour after enteral feeding in Nrf2^{-/-} mice.

These studies demonstrate that 1) (-)-epicatechin increases vascular function in a NOS-dependent fashion as show by simultaneous NOS inhibition and measurements in eNOS^{-/-} mice 2) the effects of (-)-epicatechin administration in water for five days are blunted in Nrf2^{-/-} mice.

4: Molecular mechanisms (I) – (-)-Epicatechin activates eNOS mediated NO-signaling

4.1: (-)-Epicatechin activates eNOS in the vasculature in vivo by increasing phosphorylation

One main goal of this work it was to verify that oral administration of (-)-epicatechin affects expression and/or activity of eNOS in the vasculature and herewith improves vascular function. Phosphorylation is known to activate eNOS and increase eNOS-derived NO production.

(-)-Epicatechin treatment significantly increased the phosphorylation of eNOS at the activation Ser1177 residue in aorta as compared to control treatment already one hour after intraenteral administration (Fig. 22A, panel I). This increased ratio of phosphorylated and unphosphorylated eNOS was also detected with longer treatment for five days (panel II). In addition oral administration of 2 mg/kg for five days did not affect protein levels of eNOS in the aorta of the mice, as assessed by western blot analysis.

Results

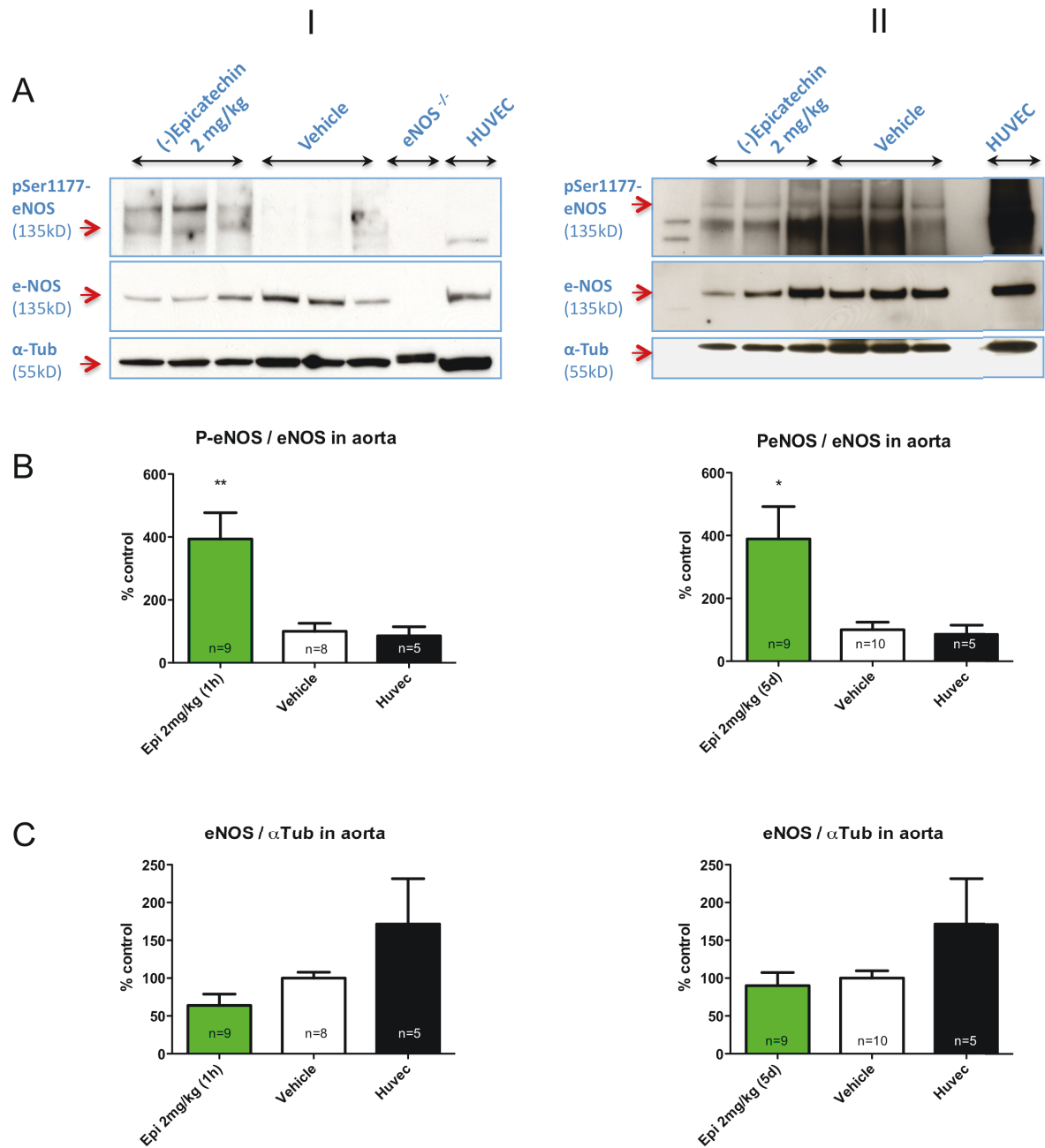


Fig. 22: (-)-Epicatechin increases eNOS phosphorylation in the aorta.

Western blot analysis of eNOS phosphorylation and expression in the mouse aorta after acute (panel I) and long-term (panel II) 2 mg/kg (-)-epicatechin treatment. Densitometric analysis of bands from at least 2 gels was performed by normalization of the pSer1177-eNOS signal to eNOS expression (B, C) or the eNOS signal to alpha tubulin expression and shown as % of the control.

Besides an increased phosphorylation of eNOS by (-)-epicatechin in large conduit arteries as demonstrated in the aorta, this study shows increased eNOS phosphorylation also in highly vascularized tissues like the lung of the mice (Fig. 23).

Results

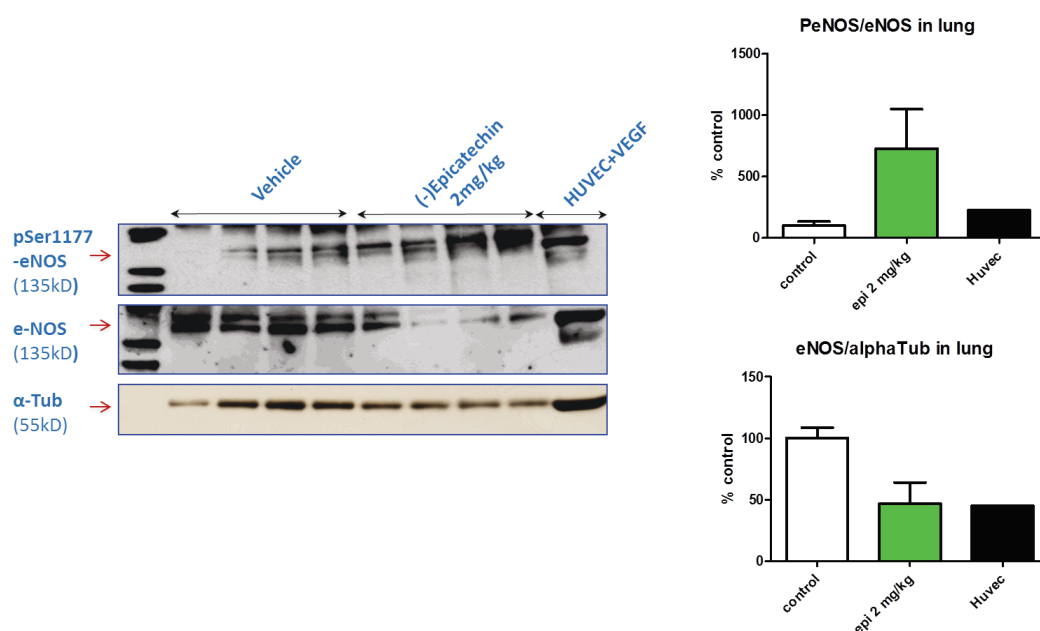


Fig. 23: (-)-Epicatechin increases eNOS phosphorylation in the lung.

Western blot analysis of eNOS phosphorylation and expression in the mouse lung long-term 2mg/kg (-)-epicatechin treatment. Densitometric analysis of bands (n=4) was performed by normalization of the pSer1177-eNOS signal to eNOS expression or the eNOS signal to alpha tubulin expression and shown as % of the control.

4.2: Increased eNOS activity leads to an increase in vascular NO-bioactivity

4.2.1: The increase in vascular NO-bioactivity is eNOS dependent

Further this study verified whether (-)-epicatechin induced activation of eNOS leads to an increase in vascular NO-bioactivity and thus vascular function in mice. To determine the effects of (-)-epicatechin treatment on NOS dependent NO activity in the vessel wall cGMP-level were measured in aortic lysates. Cyclic GMP is the most important NO-dependent secondary messenger in smooth muscle cells and therefore in the vasculature (Kapakos et al. 2010, Morgado et al. 2012).

It was found that (-)-epicatechin significantly increased cGMP levels more than 2 fold as compared to control treatment (Fig. 24A). Moreover this epicatechin-induced increase in cGMP was abolished by administration of the specific NOS inhibitor L-NNA (Fig. 25A). Mice lacking eNOS (eNOS^{-/-}) have completely blunted cGMP levels as compared to

Results

wildtype mice. Importantly, epicatechin treatment does not increase the cGMP levels in aorta of $eNOS^{-/-}$ mice as compared to vehicle-treated $eNOS^{-/-}$ mice (Fig. 24A). To test whether increased levels of cGMP modulate downstream vascular signaling the activity of PKG was measured via assessment of vasodilator-stimulated phosphoprotein (VASP) phosphorylation by Western-blot-analysis (Fig. 24B). In vivo (-)-epicatechin treatment resulted in a significant augmentation of VASP phosphorylation and therefore increased PKG activity in aorta of the mice.

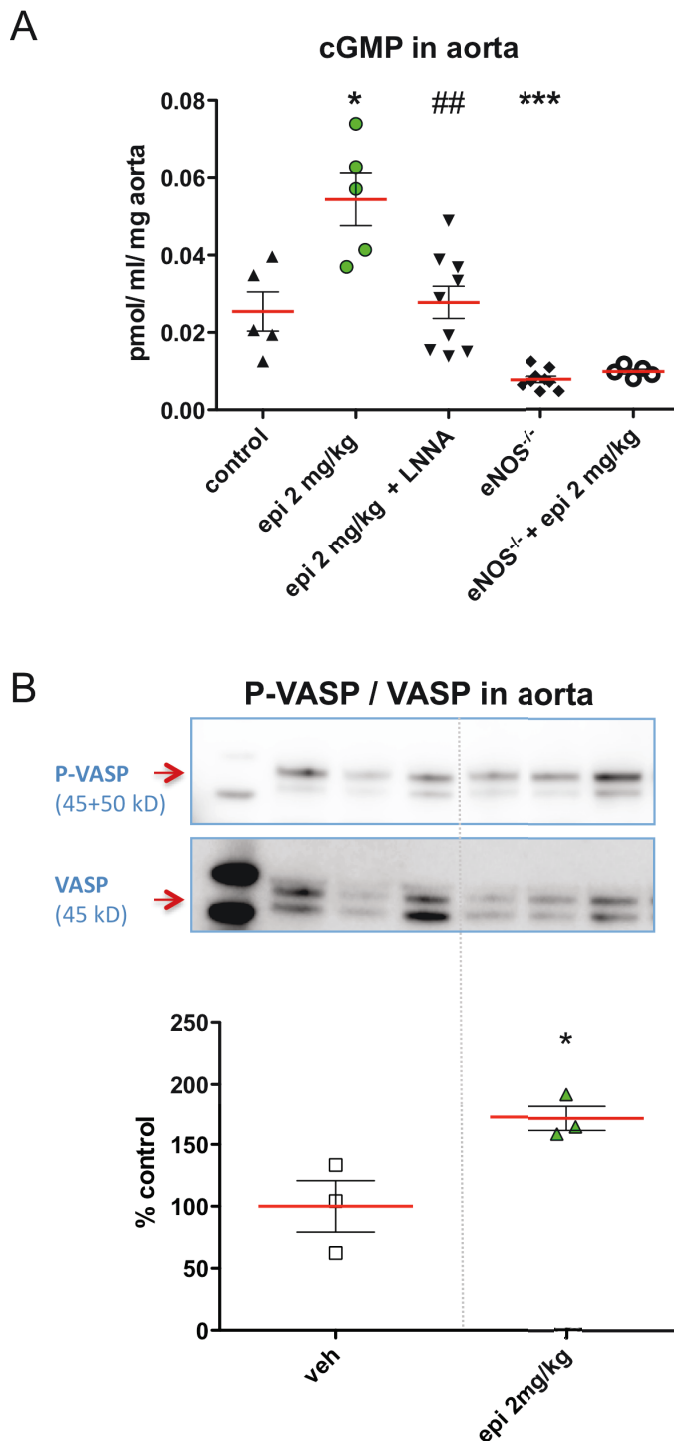


Fig. 24: (-)-Epicatechin activates the NO-stimulated cGMP – PKG pathway in aorta in a NOS dependent fashion.

(-)-Epicatechin was administrated in drinking water for five days at 2 mg/kg to wildtype and eNOS knockout mice. (A) cGMP level in aorta of mice following treatment with (-)-epicatechin. eNOS-dependence of vascular cGMP production and (-)-epicatechin mediated increase is shown by additionally administrated NOS-inhibitor LNNA and measurements in eNOS knockout mice. (B) Examination of VASP phosphorylation in the aorta as a biochemical marker for the activity of the cGMP-dependent protein kinase (PKG). * = $p \leq 0.05$ vs. control, # = $p \leq 0.05$ vs. epi 2 mg/kg, t-test between the groups.

4.2.2: The increase in vascular NO-bioactivity in Nrf2 dependent

(-)-Epicatechin increased NO-bioactivity in the vessel wall in an eNOS dependent fashion as shown in wildtype mice.

In order to verify whether Nrf2 participates in the NO-mediated effects of (-)-epicatechin, cGMP in the aorta (Fig. 25) was measured in mice lacking Nrf2 expression. In contrast to the effects of (-)-epicatechin on vascular NO-bioavailability in wildtype mice, long-term 2 mg/kg (-)-epicatechin administration did not increase GMP level in vascular tissue of Nrf2^{-/-} mice.

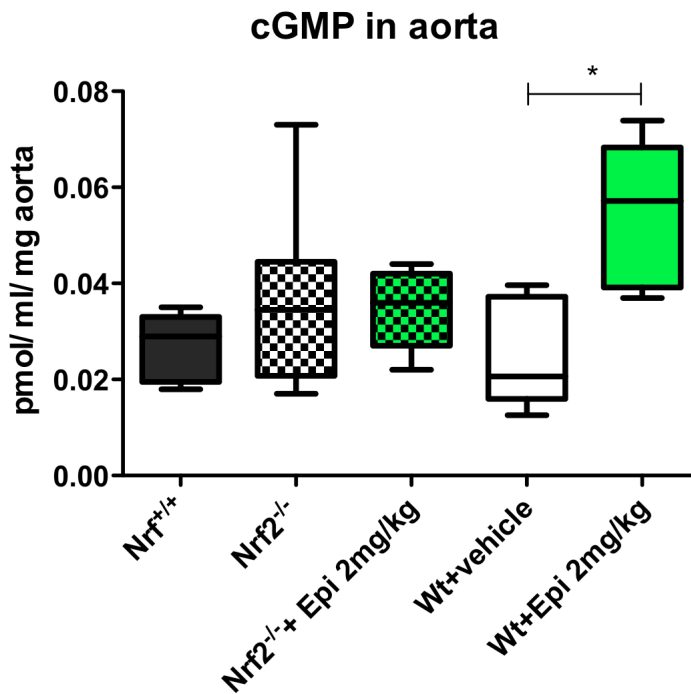


Fig. 25: Effect of (-)-epicatechin on NO-bioavailability in Nrf2^{-/-} mice. cGMP level in aorta of wildtype (Wt), wildtype littermates (Nrf2^{+/+}) and Nrf2 knockout mice (Nrf2^{-/-}) after long-term 2 mg/kg (-)-epicatechin treatment, n=5. * = p ≤ 0.05. Groups are shown separately to exclude the effects different mice groups and time points of (-)-epicatechin treatment and tissue harvesting.

These findings demonstrate that an intact antioxidant response in addition to eNOS is necessary to increase NO-bioavailability in the vasculature in vivo when dietary (-)-epicatechin is administered over a longer period.

Taken together the results of this study demonstrated increased eNOS phosphorylation, increased eNOS and Nrf2 dependent level of cGMP and activation of NO-dependent

downstream signaling in the vasculature of mice by dietary (-)-epicatechin feeding. This was accompanied by increased eNOS and Nrf2 dependent vascular function.

4.3: Effect of (-)-epicatechin on systemic NO-bioavailability.

To determine whether increased systemic NO-bioavailability by (-)-epicatechin accompanies increased vascular reactivity cGMP was measured in plasma of wildtype mice (Fig. 26), which was previously reported to reflect NO activity (Levett et al. 2011).

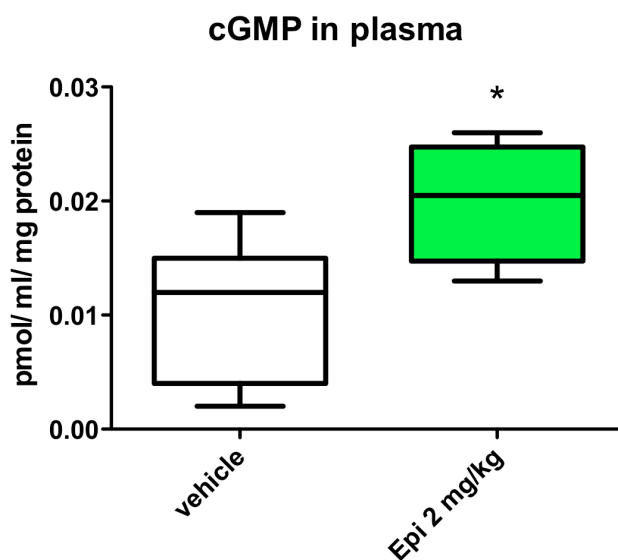


Fig. 26: Effect of (-)-epicatechin on systemic NO-bioavailability.

(A) cGMP level were measured in mice plasma were measured after (-)-epicatechin treatment. In addition nitrite (NO_2^-) (B) and nitrate (NO_3^-) (C) concentrations were assessed in plasma. Contribution of NOS was analysed by L-NNA administration for five days, n=5. * = $p \leq 0.05$, t-test between the groups.

Plasma cGMP levels in mice fed with (-)-epicatechin were significantly increased 2 fold as compared to control treatment (Fig. 26). Normalized to the protein amount cGMP-level in the aorta were up to 45 fold higher compared to plasma. As an additional readout NO_2^- and NO_3^- plasma concentrations were determined and the $\text{NO}_2^-/\text{NO}_3^-$ ratio was calculated after (-)-epicatechin treatment in wildtype and $\text{Nrf2}^{-/-}$ mice (Tab. 11). Administration of 2 mg/kg (-)-epicatechin did not increase plasma NO_2^- and NO_3^- concentration neither in wildtype nor $\text{Nrf2}^{-/-}$ mice, while NOS-inhibition with L-NNA resulted in up to 78% decrease in NO_2^- and NO_3^- level. Compared to wildtypes, mice lacking Nrf2 had significantly decreased NO_3^- concentrations in plasma and therefore a higher $\text{NO}_2^-/\text{NO}_3^-$ ratio.

Results

Tab. 11: Level and ratio of nitrite (NO_2^-) and nitrate (NO_3^-) in plasma of Nrf2 knockout ($\text{Nrf2}^{-/-}$) and wildtype (Wt) mice after 2 mg/kg (-)-epicatechin treatment. Mean \pm SEM, paired t-test Wt vs. Wt+LNNA; *** = $P < 0.001$, $\text{Nrf2}^{-/-}$ vehicle vs. Wt vehicle; ## = $P < 0.005$.

	Nrf2^{-/-} + vehicle (n=9)	Nrf2^{-/-} + Epi 2 mg/kg (n=9)	Wt + vehicle (n=5)	Wt + Epi 2 mg/kg (n=5)	Wt + LNNA (n=4)
NO₂⁻ (μM)	0.40 ± 0.01	0.33 ± 0.06	0.28 ± 0.07	0.39 ± 0.14	0.12 ± 0.06
NO₃⁻ (μM)	35.07 ± 4.23##	34.54 ± 5.85	57.03 ± 5.42	46.72 ± 7.94	12.38 ± 1.49***
	1.2x10 ⁻² ±	1x10 ⁻² ±	5.1x10 ⁻³ ±	7.9x10 ⁻³ ±	8.9x10 ⁻³ ±
NO₂⁻ / NO₃⁻	1.4x10 ⁻³ ##	1.6x10 ⁻³	9.9x10 ⁻⁴	2.4x10 ⁻³	4x10 ⁻³

Taken together (-)-epicatechin treatment resulted in a significant increase in circulating plasma cGMP, a marker for systemic NO-bioavailability, but did not affect NO_2^- and NO_3^- concentrations. The increase in $\text{NO}_2^-/\text{NO}_3^-$ ratio after (-)-epicatechin treatment in wildtype mice was not significant.

5. Molecular mechanisms (II) – effects of (-)-epicatechin on tissue redox state (GSH)

5.1: (-)-Epicatechin increases redox state in tissues of the cardiovascular system

It is likely that (-)-epicatechin, as a compound with electrophilic properties, affects redox state in vivo. Antioxidant properties of flavanols have been previously demonstrated ex vivo (Galleano et al. 2010, Martin et al. 2010). To determine whether changed systemic and vascular antioxidant state parallels the observed vascular effect, concentrations of the major antioxidant factor GSH were assessed in cardiovascular tissue of the mice (Fig. 27).

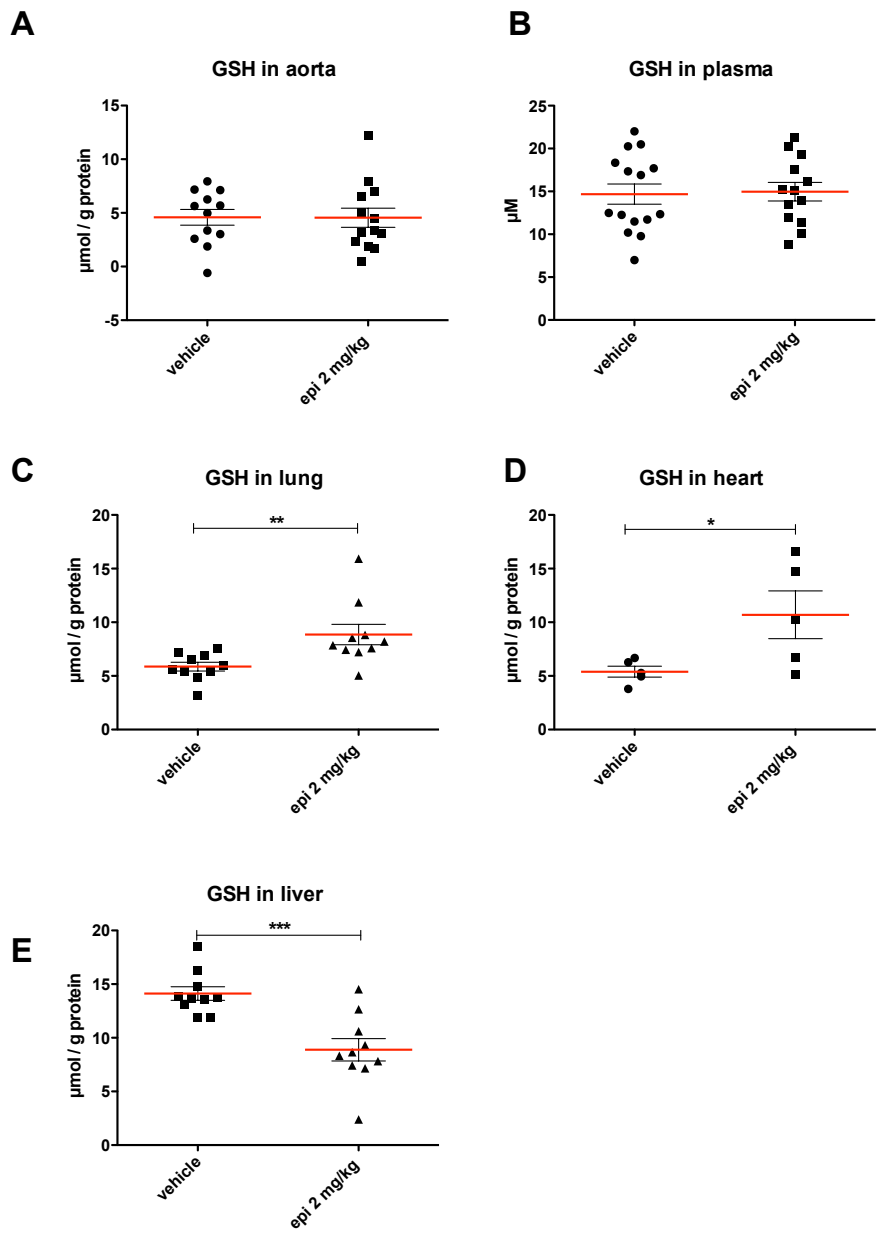


Fig. 27: (-)-Epicatechin increases redox state in cardiovascular tissues.

GSH was determined in the tissue after 2 mg/kg (-)-epicatechin treatment. In aorta (A) and plasma (B) no changes were determined while (-)-epicatechin increased levels in lung (C) and heart (D). In liver (E) a reverse reaction with decreased GSH has been observed * = $p \leq 0.05$, t-test between the groups.

While GSH level in the aorta (A) and in plasma (B) remained unchanged after dietary administration, in lung (C) and heart (D) 2 mg/kg (-)-epicatechin significantly increased tissue GSH concentration up to 2-fold. However dietary (-)-epicatechin treatment in mice increases the antioxidant defense in other cardiovascular tissues. Interestingly in contrast to aorta, plasma, heart and lung significantly diminished concentrations of GSH were determined in the liver of the mice (E).

5.2: The increase in redox state in tissues of the cardiovascular system is Nrf2 dependent

The lack of Nrf2 expression in vivo not only changes the effects of (-)-epicatechin on NO-bioactivity, but also results in a dysregulation of the basal tissue redox-state, measured as a significant decrease of GSH in aorta (A, panel I) and liver (B, panel I) of Nrf2^{-/-} mice (Fig. 28).

In wildtype mice dietary (-)-epicatechin did not change GSH content in aorta but significantly reduced GSH level in the liver. To determine whether (-)-epicatechin regulates GSH level via Nrf2 the effects were also determined in Nrf2^{-/-} mice (Fig. 28).

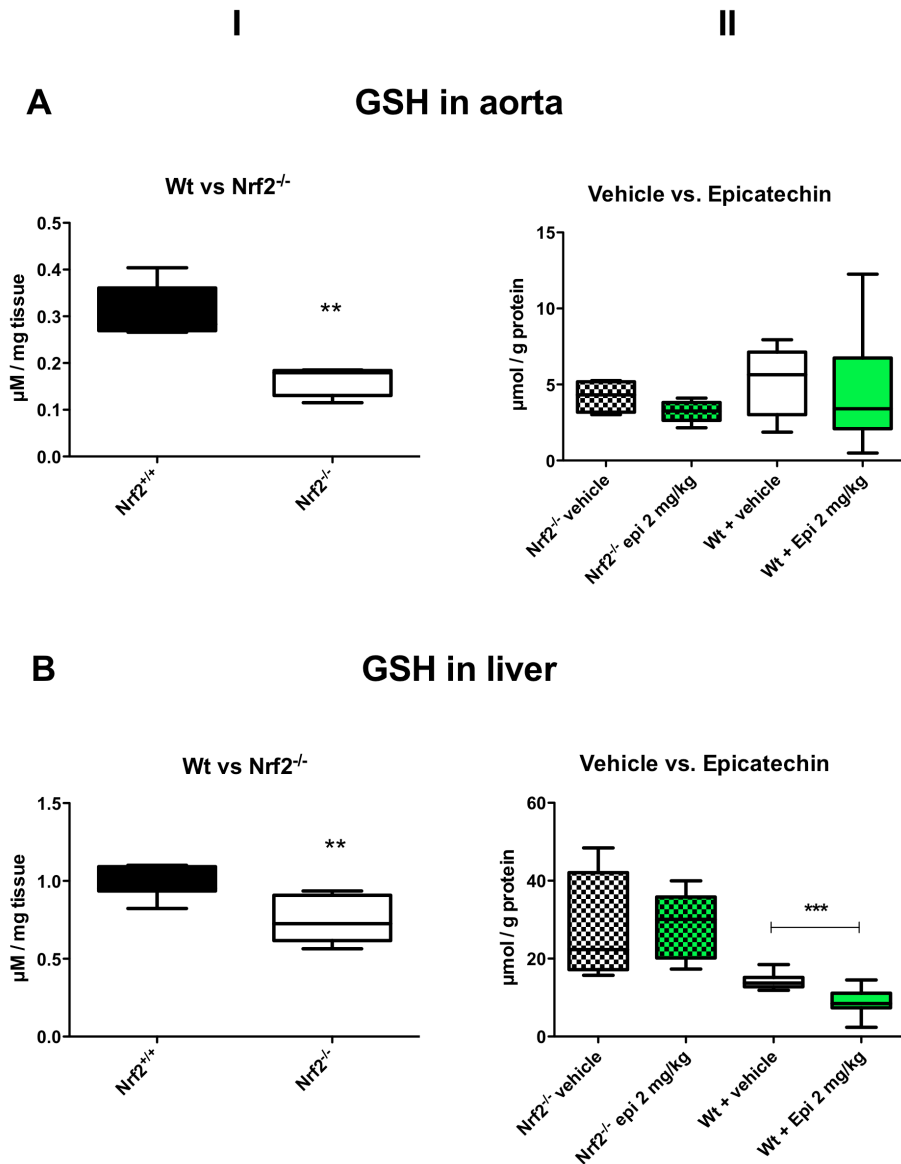


Fig. 28: Effect of (-) epicatechin on redox state in Nrf2^{-/-} mice. GSH-level in aorta (A) and liver (B) of Nrf2^{-/-} mice were compared to wildtype (Wt) littermates (panel I) or after vehicle treatment to (-)-epicatechin treated Wt and Nrf2^{-/-} mice (panel II), n=5 per group. Separate groups are shown to exclude effects of different mice groups and time points of treatment and tissue harvesting.

Different to wildtype mice (-)-epicatechin supplementation decreased GSH level (-23 %) in aorta of Nrf2 knockout mice (A, panel II) whereas in liver no change was found with (-)-epicatechin (B, panel II) in Nrf2^{-/-}, which is a reverse reaction to the findings in wildtype mice.

5.3: (-)-Epicatechin regulates the expression of antioxidant genes in cardiovascular tissues

Synthesis of GSH is a main regulatory response to increased oxidative and electrophilic stress in cells and tissues (Sies 1999). This work demonstrates that dietary (-)-epicatechin affects the expression of enzymes involved in the synthesis and metabolism of GSH as assessed in aorta (Fig. 29), heart, lung and liver (Fig. 30) of the mice by Western-blot analysis.

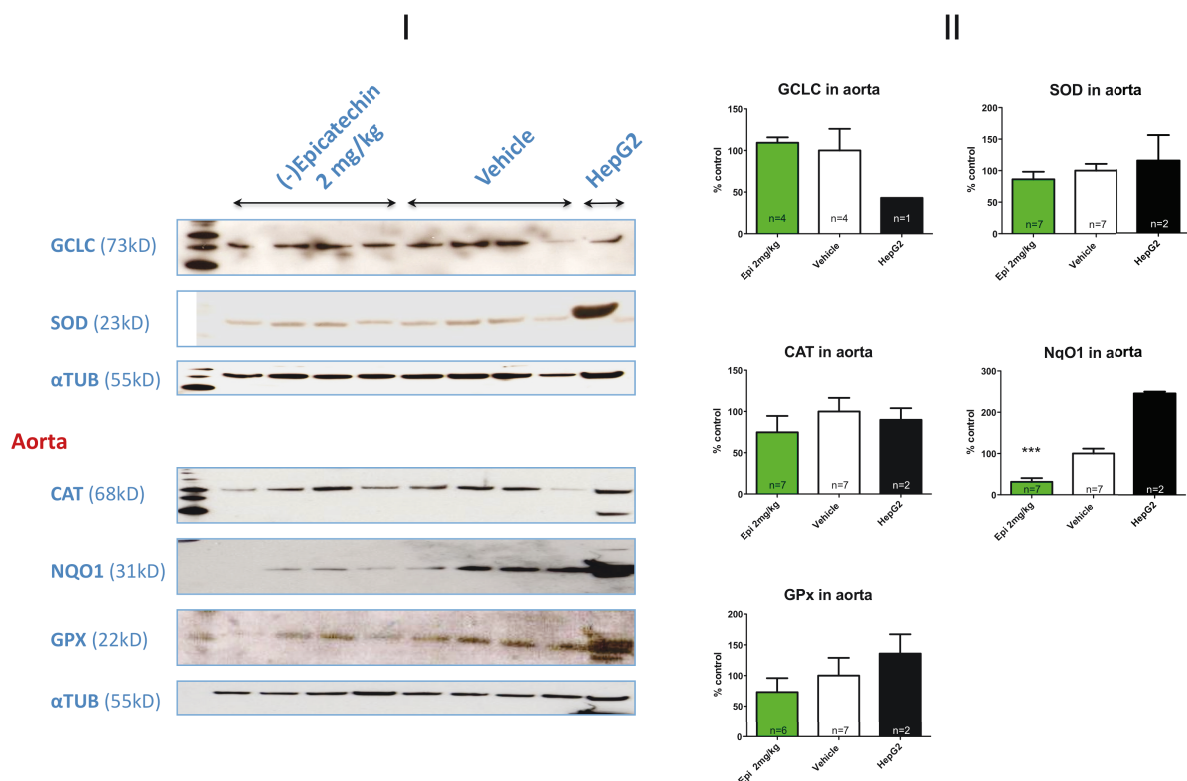


Fig. 29: Protein expression of antioxidative genes in aorta after (-)-epicatechin treatment. Bands (panel I) were analysed by densitometric normalization of the target signal to α-Tub expression and compared to control treatment (panel II). GCLC = Glutamate—cysteine ligase catalytic subunit, SOD = Superoxide dismutase, CAT = Catalase, NQO1 = NAD(P)H:quinone oxidoreductase, GPX = Glutathione peroxidase, α-TUB = Tubulin.

Results

In the aorta GCL protein expression remained unchanged. Also expression of SOD, CAT (catalase) and GPX (GSH peroxidase) was not affected by 2 mg/kg (-)-epicatechin treatment, while protein expression of NQO1 was markedly reduced. Distinct to the findings in vascular tissue, enzymes of the redox-state are regulated in other organs of the cardiovascular system. In the heart level of GCL, an essential enzyme of GSH-synthesis were elevated by (-)-epicatechin together with the GSH-metabolising factors GPX and GSR (Fig. 30A). In the lung GCL and GPX were not regulated but the level of GST was increased (Fig. 30B). In the liver of the mice (-)-epicatechin treatment resulted in a reduced expression of GCL and GST while GPX level remained unchanged (Fig. 30C).

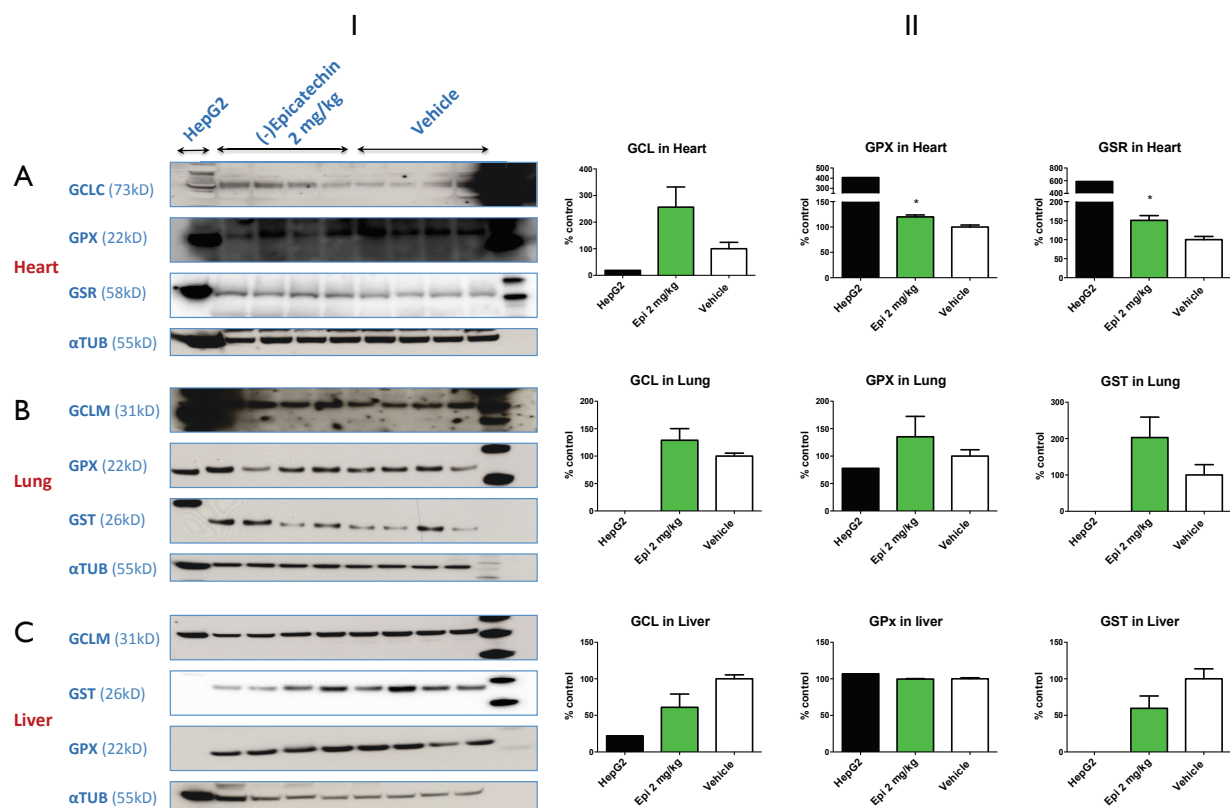


Fig. 30: Protein expression of genes involved in GSH metabolism in heart, lung and liver after (-)-epicatechin treatment.

Expression of protein in heart (A), lung (B) and liver (C) of the mice after long-term 2 mg/kg (-)-epicatechin treatment. Bands (panel I) were analysed by densitometric normalization of the target signal to α -Tub expression and compared to control treatment (panel II). GCLC = Glutamate—cysteine ligase catalytic subunit, GCLM = Glutamate—cysteine ligase modifier subunit, GPX = Glutathione peroxidase, GSR = Glutathione reductase, GST = glutathione S-transferase, α -TUB = Tubulin.

Taken together dietary (-)-epicatechin affected the redox-state of tissues of the cardiovascular system (lung and heart) in mice in vivo demonstrated by increased level of GSH and regulation of GSH metabolizing enzymes. These regulatory responses are Nrf2 dependent, because the GSH regulation pattern is altered in Nrf2^{-/-} mice.

6. Identification of novel targets of (-)-epicatechin in vascular tissue by microarray analysis

6.1: Transcriptional profiling of genes in an (-)-epicatechin dose-response model

To investigate the effect of long-term in vivo (-)-epicatechin treatment on gene transcription profiles in aorta of mice, genomic mRNA expression was characterized by comparative microarray analysis. The transcriptional profile of (-)-epicatechin treated mice was generated using the Agilent Murine Genome GE 4x44K v2 Microarray Kit and was logically analysed for set of genes regulated. Three categories of comparisons were performed: 2 mg/kg vs. vehicle, 10 mg/kg vs. vehicle and 10 mg/kg vs. 2 mg/kg (Fig. 31). With approximately 39,430 probes representing the mouse genome, targets were detected with signal intensity higher than the threshold and were selected for further analysis. Up-regulated and down-regulated genes were analysed with p-values ≤ 0.05 .

Results

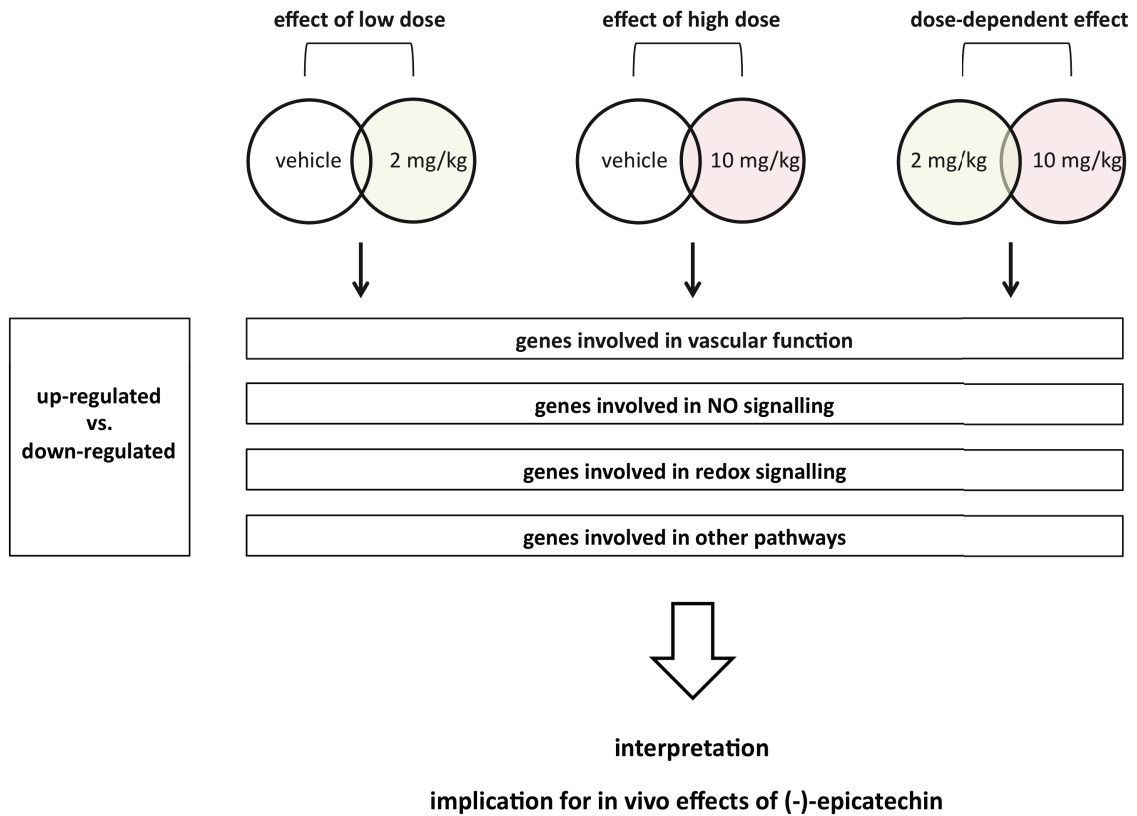


Fig. 31: Strategy of comparative micro-array analysis to identify gene clusters regulated by (-)-epicatechin in vivo.

In a pool of 7115 probe sets, 4208 probes were identified as differentially expressed in the groups treated with (-)-epicatechin (Fig. 32). Specifically, 1507 probes were differentially expressed in 2 mg/kg (665 up-regulated, 842 down-regulated) and 2701 in 10 mg/kg treated mice (1114 up-regulated, 1587 down-regulated). Focusing on the dose-response effect of (-)-epicatechin, 1274 probes were identified to have dose-response behaviour only when comparing 10 mg/kg and 2 mg/kg treated mice (487 up-regulated, 787 down-regulated).

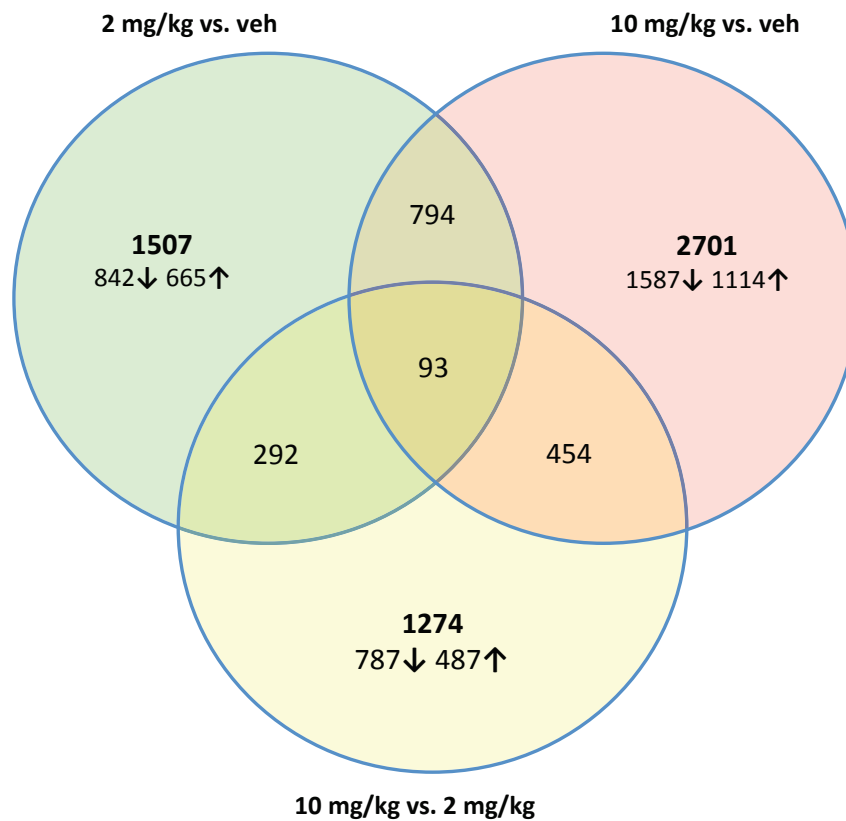


Fig. 32: Transcriptional profiling of targets dose-dependently regulated by (-)-epicatechin in mice in vivo.

The Venn diagram shows probe sets regulated by low-dose only (2 mg/kg vs. veh, green circle), high-dose only (10 mg/kg vs. veh, red circle) and dependent on increasing dose (10 mg/kg vs. 2 mg/kg, yellow circle). Up- or down-regulation is shown by upward and downward arrows.

Tab. 12 depicts the 20 most up-regulated and down-regulated genes in all investigated groups. For 2 mg/kg a yet uncharacterised gene (predicted gene 129) is most up-regulated (47-fold) and the Aryl hydrocarbon receptor nuclear translocator protein (ARNT), an essential partner of the xenobiotic ligand Aryl hydrocarbon receptor (AhR) is most down-regulated (31-fold). For 10 mg/kg a homeobox representative is most up-regulated (7-fold) and collagen is most down-regulated (7-fold).

Results

Tab. 12. Top 20 most regulated genes in the aorta by 2 mg/kg and 10 mg/kg (-)-epicatechin determined by microarray analysis.

Condition	↑ by (-)-epicatechin		↓ by (-)-epicatechin	
	term	fold change	term	fold change
2 mg/kg	predicted gene 129	46,50	aryl hydrocarbon receptor nuclear translocator-like	-30,82
	D site albumin promoter binding protein	14,86	a disintegrin-like and metallopeptidase (reprolysin type)	-8,76
	period circadian clock 2	7,32	betaine-homocysteine methyltransferase	-6,64
	hepatic leukemia factor	5,10	solute carrier family 25, member 34	-5,76
	reproductive homeobox 3A	4,58	nuclear factor, interleukin 3, regulated	-5,30
	methylenetetrahydrofolate dehydrogenase (NADP+ dependent)	4,37	dehydrogenase/reductase (SDR family) member 9	-4,77
	thyrotroph embryonic factor	3,98	spondin 2, extracellular matrix protein	-4,39
	period circadian clock 1	3,68	thrombospondin 4	-4,07
	titin-cap	3,59	Rho GTPase activating protein 20	-3,71
	solute carrier family 25, member 41	3,12	thyroid stimulating hormone receptor	-3,70
	von Willebrand factor C domain containing 2	2,86	histidine ammonia lyase	-3,65
	synaptotagmin XII	2,80	keratin 20	-3,59
	tetraspanin 4	2,79	epiphygan	-3,47
	cystin 1	2,73	prepronociceptin	-3,47
	phosphoinositide-3-kinase interacting protein 1	2,73	cannabinoid receptor 1 (brain)	-3,33
	cryptochrome 1 (photolyase-like)	2,70	chromogranin A	-3,17
	ATPase, Ca++ transporting, plasma membrane 2	2,67	hemicentin 1	-3,05
	NK-3 transcription factor, locus 1	2,64	vitamin D receptor	-3,03
	ankyrin repeat domain 45	2,59	polycystic kidney disease 1 like 2	-2,90
	N-deacetylase/N-sulfotransferase (heparan glucosaminyl) 3	2,59	formyl peptide receptor, related sequence 3	-2,89
10 mg/kg	reproductive homeobox 3A	7,19	collagen, type II, alpha 1	-6,94
	D site albumin promoter binding protein	7,18	taste receptor, type 2, member 118	-5,64
	ATP-dependent RNA helicase	6,16	actinin alpha 2	-4,64
	SH3/ankyrin domain gene 2	3,94	nuclear factor, interleukin 3, regulated	-4,60
	RAB GTPase activating protein 1	3,88	cholinergic receptor, muscarinic 2, cardiac	-4,56
	T-box transcription factor 22	3,82	aryl hydrocarbon receptor nuclear translocator-like	-4,35
	Period circadian clock 2	3,79	dopamine receptor D4	-3,96
	Period circadian clock 3	3,69	otoraplin	-3,37
	CD300 antigen like family member F	3,68	tetraspanin 32	-3,32
	MAS-related GPR, member G	3,64	chloride intracellular channel 6	-3,09
	killer cell lectin-like receptor, subfamily A, member 1	3,63	interleukin 19	-3,07
	olfactory receptor 1500	3,48	APC membrane recruitment 2	-2,96
	galactose-3-O-sulfotransferase 3	3,38	UDP glucuronosyltransferase 1 family, polypeptide A6B	-2,94
	sodium channel, voltage-gated, type III, beta	3,38	formyl peptide receptor, related sequence 6	-2,90
	NK-3 transcription factor, locus 1 (Drosophila)	3,31	growth differentiation factor 6	-2,88
	developing brain homeobox 1	3,28	myogenic factor 6	-2,87
	ankyrin repeat domain 45	2,91	thyroid stimulating hormone receptor	-2,82
	solute carrier family 25, member 41	2,87	dual specificity phosphatase 5	-2,77
	fragile X mental retardation 1 neighbor	2,82	muscle, skeletal, receptor tyrosine kinase	-2,69
	hepatic leukemia factor	2,77	extracellular proteinase inhibitor	-2,69

Interestingly treatment with the higher (-)-epicatechin dose did not result in similar or stronger regulated genes, but had a smaller impact or even affected other targets.


6.2: Functional analysis of genes constitutively induced or suppressed by (-)-epicatechin


To categorize the cluster and functions of genes induced or suppressed by (-)-epicatechin, constitutively up-regulated and down-regulated probe sets of 2 mg/kg and 10 mg/kg groups were submitted separately to the Database

Results

for annotation, visualization and Integrated discovery v6.7 (DAVID). For the analysis of the largest and most relevant groups it was distinguished between annotation clustering of genes based on gene function and clustering of genes based on the pathway involved. In vivo (-)-epicatechin treatment regulated similar gene clusters independently of the dose used (Tab. 13 and Tab. 14). Annotation clustering revealed the highest enrichment of phosphoproteins in all groups representing 37 % (235 genes) of up-regulated and 44 % (348 genes) of down-regulated targets with 2 mg/kg (Tab. 13).

Tab. 13. Annotation Clustering of Genes constitutively induced or suppressed by 2 mg/kg (-)-epicatechin using DAVID Analysis. The DAVIDs modified fisher exact p-value equal or smaller than 0.05 is considered strongly enriched in the annotation categories. Top regulated gene clusters are listed in order of decreasing count. In addition cluster are shown, which are regulated by one dose only or up-or down-regulated only.

 by 2 mg/kg		
term	count	%
phosphoprotein	235	37,1
nucleus	161	25,4
splice variant	159	25,1
alternative splicing	158	25
ion binding	137	21,6
metal ion binding	135	21,3
cation binding	135	21,3
cytoplasm	126	19,9
regulation of transcription	104	16,4
metal-binding	99	15,6
transition metal ion binding	92	14,5
nucleotide binding	87	13,7
transcription	82	13
.....		
calmodulin binding	9	1,4
.....		
Insulin signaling pathway	9	1,4

 by 2 mg/kg		
term	count	%
phosphoprotein	348	43,6
alternative splicing	213	26,7
splice variant	213	26,7
nucleus	206	25,8
cation binding	177	22,2
ion binding	177	22,2
metal ion binding	175	21,9
cytoplasm	164	20,5
acetylation	162	20,3
metal-binding	128	16
transition metal ion binding	124	15,5
nucleotide binding	112	14
regulation of transcription	105	13,1
.....		
calcium	38	4,8
.....		
blood vessel development	22	2,8
vasculature development	22	2,8
.....		
blood vessel morphogenesis	17	2,1

A similar pattern with 36 % (412 genes) and 39 % (621 genes) respectively was found with 10 mg/kg (Tab. 14). Furthermore genes located in the nucleus and genes involved in splicing, ion binding, and regulation of transcription are highly enriched in all groups representing more than 10 % of all targets.

Results

Tab. 14. Annotation Clustering of Genes constitutively induced or suppressed by 10 mg/kg (-)-epicatechin using DAVID Analysis. The DAVIDs modified fisher exact p-value equal or smaller than 0.05 is considered strongly enriched in the annotation categories. Top regulated gene clusters are listed in order of decreasing count. In addition cluster are shown, which are regulated by one dose only or up- or down-regulated only.

↑ by 10 mg/kg			↓ by 10 mg/kg		
term	count	%	term	count	%
phosphoprotein	412	35,8	phosphoprotein	621	38,7
alternative splicing	304	26,4	alternative splicing	384	23,9
splice variant	304	26,4	splice variant	383	23,8
nucleus	267	23,2	nucleus	369	23
ion binding	234	20,3	ion binding	312	19,4
cation binding	231	20,1	cation binding	311	19,4
metal ion binding	229	19,9	acetylation	309	19,2
cytoplasm	186	16,1	metal ion binding	309	19,2
metal-binding	166	14,4	cytoplasm	271	16,9
regulation of transcription	160	13,9	transition metal ion binding	224	13,9
transition metal ion binding	154	13,4	nucleotide binding	200	12,5
plasma membrane	146	12,7	zinc ion binding	193	12
nucleotide binding	137	11,9	regulation of transcription	187	11,6
.....				
calcium	45	3,9	vasculature development	28	1,7
.....				
Calcium signaling pathway	14	1,2	blood vessel development	27	1,7
.....				
regulation of calcium ion transport	5	0,4		
			blood vessel morphogenesis	22	1,4
				
			WNT Signaling Pathway	7	0,4
				
			myogenesis	5	0,3

These results show that despite a broad range of targets, in vivo (-)-epicatechin treatment predominantly up- and down-regulates specific clusters in the aorta independent of the dose used. Nonetheless some gene clusters are down-regulated only (e.g. blood vessel and vasculature development, blood vessel morphogenesis) or regulated by one dose only (e.g. insulin signaling (2 mg/kg), calmodulin-binding (2 mg/kg), myogenesis (10 mg/kg), WNT signaling (10 mg/kg)) indicating dose-dependent effects of (-)-epicatechin treatment on regulation of gene expression in vascular tissue.

6.3: Analysis of pathways constitutively regulated by low and high dose (-)-epicatechin

To further classify the microarray results in a more functional way, pathway analysis was performed with the DAVID tool by clustering differentially expressed gene lists from 2 mg/kg and 10 mg/kg treatment (Tab. 15). Interestingly analysis of both probe sets 2 mg/kg and 10 mg/kg revealed highest enrichment of similar gene clusters including pathways in cancer (43 and 51 genes), mitogen-activated protein kinase (MAPK) signaling pathway (27 and 46 genes), regulation of actin cytoskeleton (21 and 37 genes) and endocytosis (20 and 38 genes). However these signaling cascades are not self-evident to explain the protective antioxidative and cardiovascular properties of flavanols. Therefore the analysis was specified by focus on gene clusters and signaling cascades potentially involved in regulation of the redox state and vascular function.

Tab. 15. Functional Clustering of Genes Constitutively regulated by 2 mg/kg and 10 mg/kg (-)-epicatechin using DAVID Analysis and KEGG pathway Analysis. The DAVIDs modified fisher exact p-value equal or smaller than 0.05 is considered strongly enriched in the functional categories. Top regulated gene clusters are listed in order of decreasing count. In addition pathways are shown, which are correlated with cardiovascular function and antioxidant response.

pathway clustering with 2 mg/kg			pathway clustering with 10 mg/kg		
term	count	%	term	count	%
Pathways in cancer	43	2,8	Pathways in cancer	51	1,9
MAPK signaling pathway	27	1,8	MAPK signaling pathway	46	1,7
Regulation of actin cytoskeleton	21	1,4	Endocytosis	38	1,4
Endocytosis	20	1,3	Regulation of actin cytoskeleton	37	1,4
.....				
Calcium signaling pathway	17	1,1	Calcium signaling pathway	28	1
.....				
Insulin signaling pathway	15	1	Insulin signaling pathway	24	0,9
.....				
Phosphatidylinositol signaling system	9	0,6	Vascular smooth muscle contraction	18	0,7
.....				
Vascular smooth muscle contraction	9	0,6	VEGF signaling pathway	13	0,5
.....				
Drug metabolism	7	0,5	Phosphatidylinositol signaling system	11	0,4
.....				
VEGF signaling pathway	6	0,4	Metabolism of xenobiotics	7	0,3
.....				
Metabolism of xenobiotics	4	0,3	Drug metabolism	6	0,2
.....				
Glutathione metabolism	3	0,2	Glutathione metabolism	4	0,1
.....				
			Cardiac muscle contraction	4	0,1

Several genes involved in pathways such as Ca⁺⁺-signaling, insulin signaling, phosphatidylinositol signaling, vascular smooth muscle contraction, vascular endothelial growth factor (VEGF) signaling, drug metabolism, xenobiotic metabolism and GSH

metabolism are regulated by (-)-epicatechin in the vascular tissue (Tab. 15). These pathways can mediate beneficial effects of (-)-epicatechin on vascular health either by regulation of the stress response (detoxification from drugs and xenobiotics, antioxidant Nrf2 dependent response, regulation of the redox-state by GSH) or by improving vascular reactivity (NO- and Ca⁺⁺-dependent regulation of vascular smooth muscle relaxation/contraction) (Fig. 33).

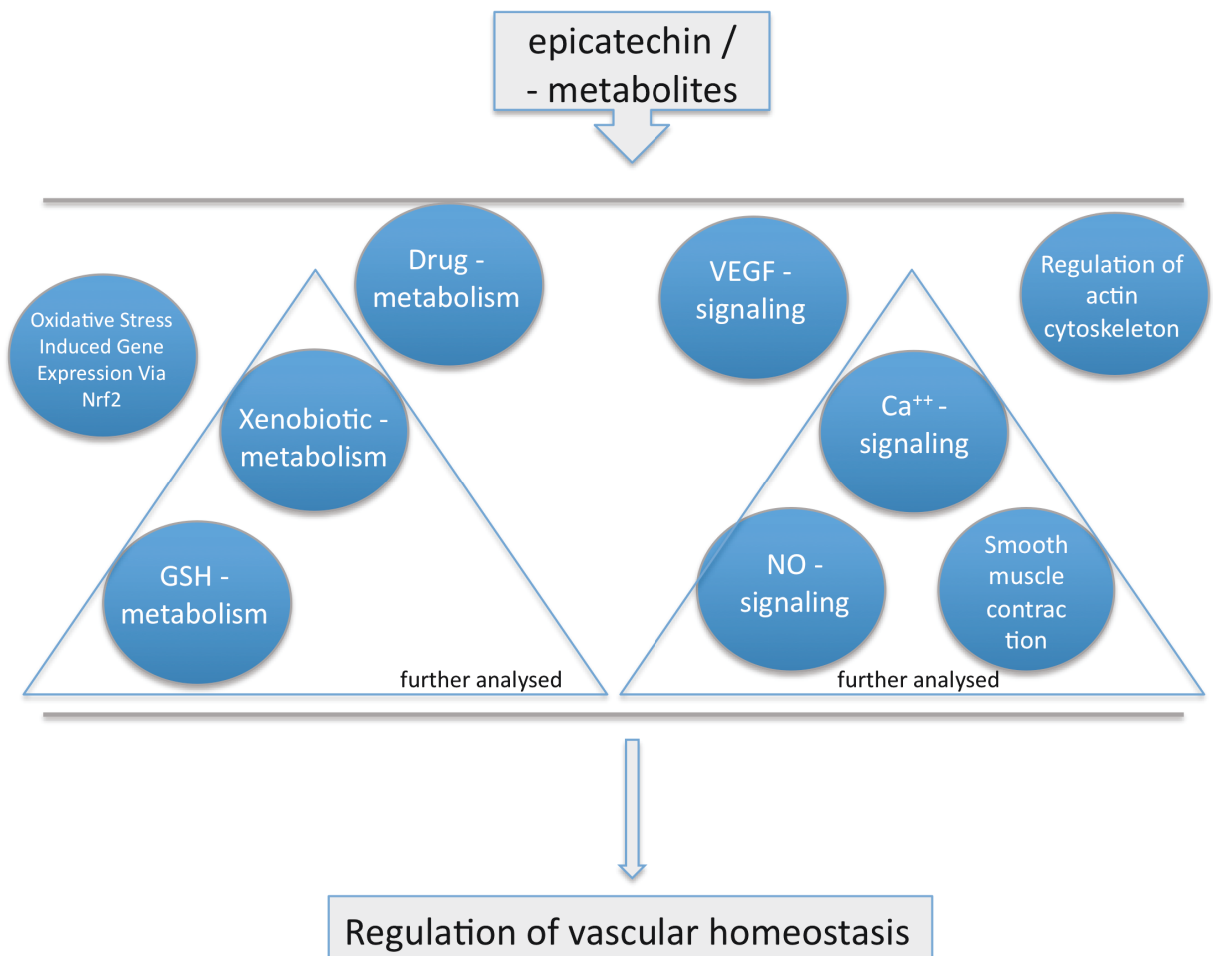


Fig. 33: (-)-Epicatechin regulated pathways contributing to maintenance of vascular health by regulation of stress response and vascular functionality.

Selected pathways were further analysed in this study (triangle).

6.4: Novel potential targets of (-)-epicatechin – AhR and Xenobiotic metabolism

As described, *Arnt* is the most down-regulated gene by low-dose (-)-epicatechin in vascular tissue (Tab. 12). Moreover mRNA level of Aryl hydrocarbon receptor (*Ahr*), a xenobiotic ligand and essential complex-forming binding partner of ARNT, are markedly decreased in the aorta after 2 mg/kg and 10 mg/kg (-)-epicatechin treatment as assessed by real-time PCR analysis (Fig. 34).

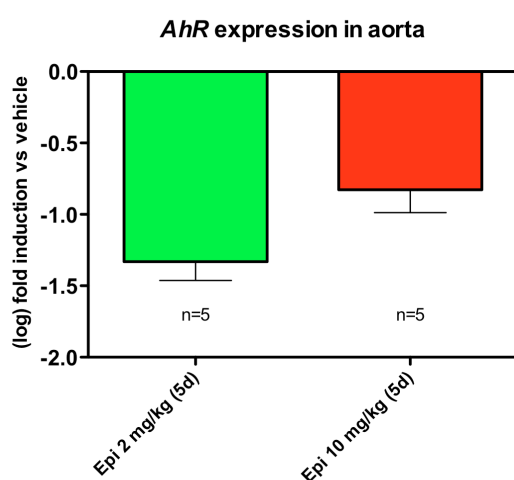


Fig. 34: mRNA expression of AhR in the aorta after 2 mg/kg and 10 mg/kg (-)-epicatechin treatment.

In addition further genes involved in drug and xenobiotic metabolism including several cytochrome and monooxygenase isoforms, cytochrome oxidoreductase, uridine synthetase and kinase and aldehyde dehydrogenase were regulated by (-)-epicatechin in the aorta (Tab. 16).

Results

Tab. 16. Summary of genes involved in Glutathione , Xenobiotic and Drug metabolism that are up- (green arrow) or down-regulated (red arrow) by 2 mg/kg and 10 mg/kg (-)-epicatechin in the aorta. Genes were included which are strongly enriched in the pathways according to DAVIDs modified fisher exact p-value equal or smaller than 0.05.

term	(-)-epicatechin	
	2 mg/kg	10 mg/kg
Glutathione - metabolism		
gamma-glutamyltransferase 5		↓
glutathione peroxidase 2	↑	↑
glutathione S-transferase, theta 2	↑	
glutathione S-transferase, pi 2; pi 1		↑
glutathione reductase		↑
spermidine synthase	↑	
Xenobiotic and Drug metabolism		
activating transcription factor 4	↓	↓
aldehyde dehydrogenase 3		↓
aryl hydrocarbon receptor nuclear translocator protein (<i>Arnt</i>)	↓	↓
Cytochrome P450 family 1	↓	↓
Cytochrome P450 family 2	↓	↑
Cytochrome P450 family 3		↑
Inosine triphosphatase		↓
mitogen-activated protein kinase 1		↓
monooxygenase 2	↑	
monooxygenase 4	↑	
monooxygenase 5	↑	
nuclear factor, erythroid derived 2, like 2 (<i>Nrf2</i>)		↓
P450 (cytochrome) oxidoreductase	↑	
thiopurine methyltransferase		↓
UDP glycosyltransferase 1		↓
uridine-monophosphate synthetase	↓	↓
uridine-cytidine kinase	↓	

Furthermore a direct effect of (-)-epicatechin on the in vivo regulation of the vascular redox state can be estimated from the regulation of genes involved in glutathione metabolism (Tab. 15 and Fig. 33). Compared to control dietary treatment (-)-epicatechin up-regulates transcription of GSH-s-transferase, GSH-peroxidase and GSH-reductase in the vasculature of mice in vivo (Tab. 16).

6.5: Novel potential targets of (-)-epicatechin – Ca⁺⁺-signaling in vascular smooth muscle cells

Among others VEGF-, NO- and in particular Ca⁺⁺ and vascular smooth muscle signalling were regulated in aorta by dietary (-)-epicatechin treatment (Tab. 15 and Fig. 33).

Calcium is essential for muscle cell function. In the vasculature relaxation/contraction of smooth muscle cells mediates the dilation/constriction of the vessel by regulation of intracellular Ca⁺⁺ concentrations ([Ca⁺⁺]_i). This work demonstrates that Ca⁺⁺-signaling is strongly regulated by (-)-epicatechin in the aorta of the mice. Tab. 17 summarizes genes involved in Ca⁺⁺-and vascular smooth muscle signalling that are up- or down-regulated by 2 mg/kg and 10 mg/kg (-)-epicatechin. In general both doses show similar regulation pattern but some genes are only regulated by low-dose (e.g. Ca⁺⁺-dependent adenylate cyclase, myosin regulatory light chain interacting protein) or high-dose (-)-epicatechin (e.g. CaM, endothelin receptor, prostaglandin receptor, myosin kinase (MLCK), myosin phosphatase catalytic subunit). Interestingly the voltage dependent Ca⁺⁺ channel (down by 2 mg/kg and up by 10 mg/kg) and inositol trisphosphate receptor (IP₃R, up by 2 mg/kg and down by 10 mg/kg) are differentially regulated by low and high dose (-)-epicatechin. Both targets are directly involved in the regulation of [Ca⁺⁺]_i level.

Vascular smooth muscle signaling including regulation of [Ca⁺⁺]_i is one of the most prominent candidate mechanisms mediating vascular functionality. The regulation of [Ca⁺⁺]_i is already targeted at the membrane receptor mediated side where Ca⁺⁺-Channel (up by 10 mg/kg) and endothelin receptor (down by 10 mg/kg) are affected by (-)-epicatechin treatment. Within smooth muscle cells Ca⁺⁺-signaling is directly regulated at distinct site involving the channels, CaM (up by 10 mg/kg) and IP₃R (up by 2 mg/kg) and indirectly by the actions of several kinases. Among these kinase mediated phosphorylation signaling is regulated involving protein kinase A and C (PKA, PKC; down by 2 mg/kg and 10 mg/kg).

Results

Tab. 17. Summary of genes involved in Ca⁺⁺-signaling and vascular smooth muscle contraction that are up- (green arrow) or down-regulated (red arrow) by 2 mg/kg and 10 mg/kg (-)-epicatechin in the aorta. We included genes which are strongly enriched in the Ca⁺⁺-signaling and vascular smooth muscle contraction pathway according to DAVIDs modified fisher exact p-value equal or smaller than 0.05. Because both pathways strongly interact to regulate vascular function, redundant genes are only shown in one table.

Ca ⁺⁺ -signaling			Vascular smooth muscle contraction		
term	(-)-epicatechin		term	(-)-epicatechin	
	2 mg/kg	10 mg/kg		2 mg/kg	10 mg/kg
adenylate cyclase, Ca ⁺⁺ -dependent	↑		adenosine A2b receptor	↓	↓
ATPase, Ca ⁺⁺ transporting	↑	↑	endothelin receptor type A		↓
calcium channel, voltage-dependent	↓	↑	guanine nucleotide binding protein	↓	↓
calmodulin		↑	mitogen activated protein kinase 1		↓
cholinergic receptor, muscarinic 2, cardiac		↓	myosin 1H	↑	↑
glutamate receptor, ionotropic	↓	↓	myosin 1C	↑	
histamine receptor H1		↓	myosin, light polypeptide kinase		↑
inositol 1,4,5-triphosphate receptor 3	↑	↓	myosin phosphatase 1, catalytic subunit		↓
myosin, light polypeptide kinase		↑	myosin phosphatase 1, regulatory (inhibitor) subunit	↑	↑
phospholipase C, delta 1		↑	myosin phosphatase Rho interacting protein	↓	↓
phospholipase C, delta 3	↓		myosin regulatory light chain interacting protein	↑	
phospholipase C, gamma 1	↑	↑	phospholipase A2	↓	↓
phosphorylase kinase	↑	↑	prostaglandin F receptor		↓
platelet derived growth factor receptor, alpha polypeptide	↓	↓	protein kinase C	↓	↓
platelet derived growth factor receptor, beta polypeptide		↑	protein phosphatase 3, catalytic subunit		↓
platelet-activating factor receptor	↓	↓	receptor (calcitonin) activity modifying protein 2	↑	
protein kinase A	↓	↓	Rho guanine nucleotide exchange factor (GEF) 1		↑
purinergic receptor P2X, ligand-gated ion channel	↑	↑	sphingosine kinase 2	↓	
			VEGF receptor 2		↑

These kinases have direct or indirect impact on the activity of MLCK and myosin phosphatase (MYPT), which directly regulate the phosphorylation state and herewith the function of the contractile myosin apparatus in vascular smooth muscle cells. According to our micro-array findings in the aorta myosin kinase is up-regulated and myosin phosphatase is down-regulated by 10 mg/kg (-)-epicatechin (Tab. 17). In addition the myosin phosphatase inhibitory subunit is up-regulated while the obligatory myosin phosphatase Rho interacting protein is down-regulated by (-)-epicatechin. Furthermore other regulatory, catalytic or inhibitory factors of actin-myosin interaction are targeted by long-term (-)-epicatechin treatment in the aorta in vivo. To determine an effect on protein level expression and phosphorylation of MLCK and MYPT in the aorta was assessed after administration of 2 mg/kg and 10 mg/kg long-term treatment (Fig. 35).

Results

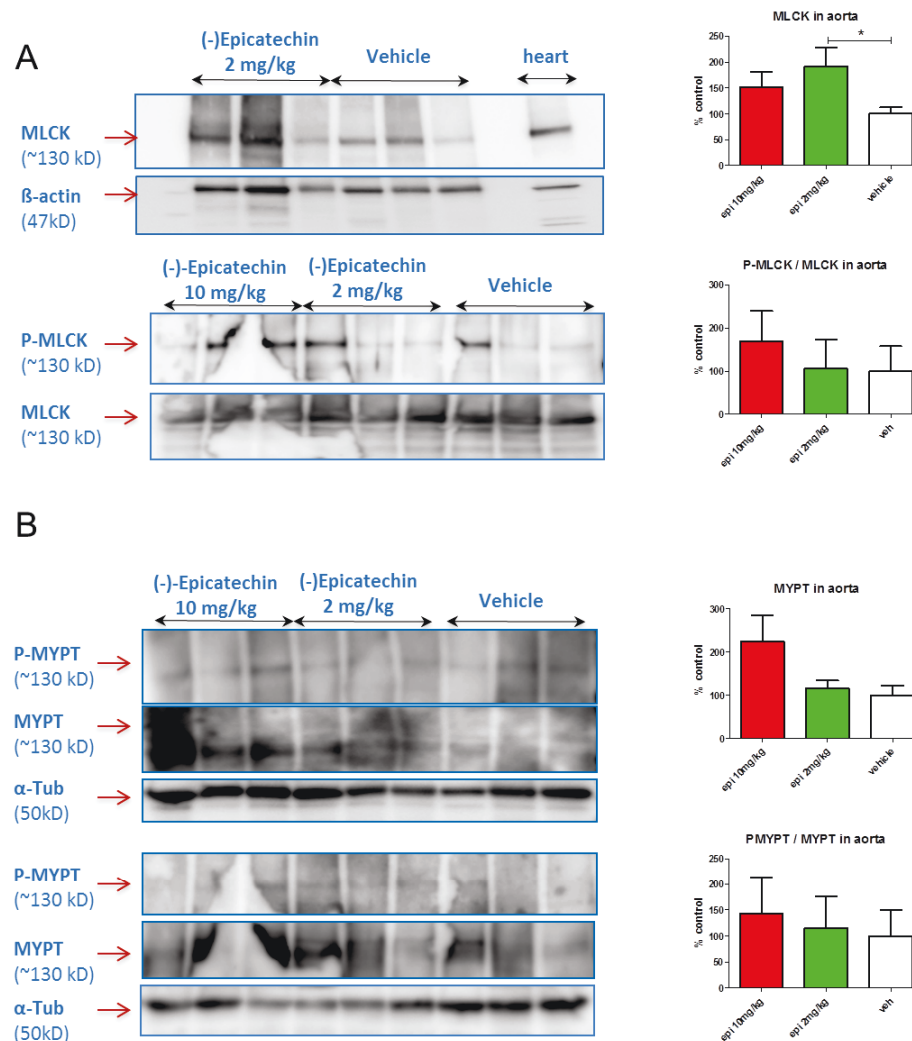


Fig. 35: Regulation of MLCK and MYPT in the aorta.

Representative Western blot analysis of (A) MLCK (myosin light chain kinase) and (B) MYPT (myosin phosphatase) phosphorylation and expression in the mouse aorta after long-term 2 mg/kg (-)-epicatechin treatment. Quantitative densitometry from three independent gels with n=8 samples was analysed by normalisation to α-Tub in relation to control.

The results show a significant increase in MLCK (Fig. 35A) but not MYPT (Fig. 35B) expression in the aorta of the mice after (-)-epicatechin treatment. The transient phosphorylation state of these enzymes is not changed as assessed at time point of tissue harvesting.

Taken together this study provides evidence that oral (-)-epicatechin treatment in vivo massively changes global gene expression pattern in the aorta of mice. Phosphoproteins involved in gene transcription were identified as the main regulated gene cluster.

Among many other pathways (-)-epicatechin regulates vascular smooth muscle signalling by affecting membrane receptors, kinases, and factors of Ca^{++} -signaling and myosin phosphorylation state. Together with eNOS-mediated NO-signaling these pathways underpin the demonstrated beneficial effects of in vivo (-)-epicatechin on vasculature.

7. Summary of main findings

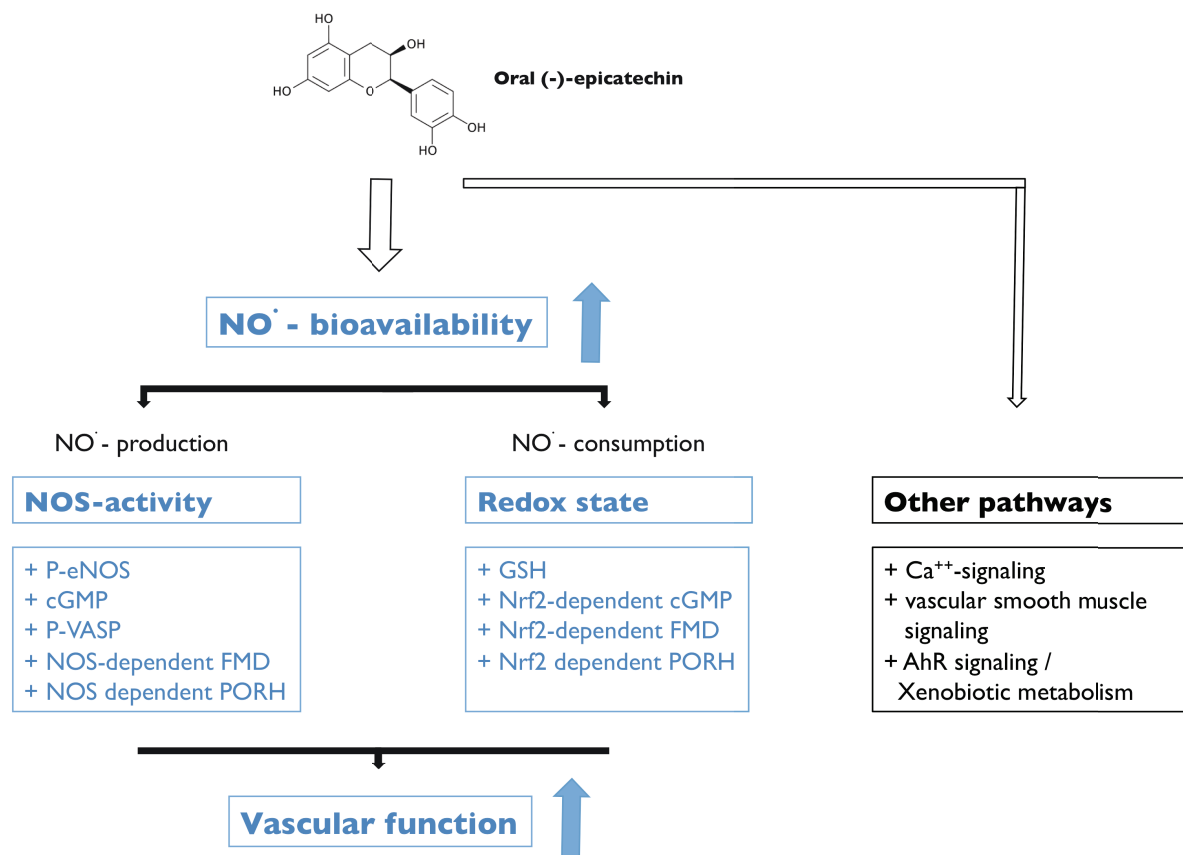


Fig. 36: Summary of the main results of this study.

It was found that oral (-)-epicatechin increases vascular function in vivo by increasing NO-bioavailability through regulation of eNOS-activity and redox-state via Nrf2. Furthermore other pathways are targets of (-)-epicatechin in vascular tissue as assessed by microarray analysis.

Discussion

The present work investigated the mechanisms underlying the beneficial effects of dietary (-)-epicatechin in the cardiovascular system in vivo. It was driven by the hypothesis that flavanols increase vascular function through increase of NO-bioavailability by increasing both – NO synthesis and antioxidant defense. The main findings of this study are:

- 1) (-)-Epicatechin increases vascular function in an eNOS and Nrf2 dependent fashion
- 2) (-)-Epicatechin activates the NO- cGMP pathway and downstream signaling in the vessel wall in dependence of eNOS and Nrf2
- 3) (-)-Epicatechin regulates the redox state of tissues belonging to the cardiovascular system
- 4) (-)-Epicatechin modulates expression of > 4000 targets in vascular tissue thus contributing to long term changes in the vasculature in vivo. Novel pathways significant for vascular action of (-)-epicatechin are: Ca⁺⁺-signaling, vascular smooth muscle signaling, AhR-signaling and Xenobiotic metabolism

Why assessing the effects of (-)-epicatechin in vivo in mice ?

The analysis of molecular mechanisms underpinning vasodilatory effects in tissue is an extraordinary advantage of animal in vivo studies, and a main limitation of human studies. In this study mice models were chosen to analyze the molecular mechanisms underlying the effects of (-)-epicatechin on vascular function. In human studies it was also possible to verify a correlation between administration of cocoa flavanols or pure (-)-epicatechin and increased FMD, and increase in nitroso-species in plasma. While these parameters are in some conditions dependent on eNOS activity (i.e. can be inhibited by administration of NOS inhibitors) a biochemical link between administration of cocoa flavanols and/or (-)- epicatechin and NO-bioavailability was not demonstrated so far. In addition the mechanisms of (-)-epicatechin cannot be studied in vitro in cultured cells, because the concentrations of (-)-epicatechin in the plasma compartment are very low as compared to the concentration of its metabolites

as also shown here. A further advantage of the use of mice was the possibility to test the role of specific targets (i.e. eNOS and Nrf2) by applying both pharmacological inhibition and genetic depletion in parallel, to overcome eventual unspecific or compensatory effects, which are typical for the first or the second approach. Pure (-)-epicatechin was administered at a dose previously demonstrated to increase endothelium-dependent vascular function in human in acute (Schroeter et al. 2006) and long-term administration (Heiss et al. 2007) (Engler et al. 2004). This approach allowed to analyse the effects of vascular function and at the same time the underlying mechanisms in cardiovascular tissue.

Is eNOS required for the beneficial vascular effects of (-)-epicatechin in vivo?

Data presented in this work clearly demonstrate that dietary administration of 2 mg/kg (-)-epicatechin improves vascular function in mice, as assessed by increased FMD/PORH and decreased PWV (Fig. 18 and 19). Importantly eNOS expression and activity are required for these effects because both pharmacological inhibition and genetic deletion of eNOS in eNOS^{-/-} mice completely block the (-)-epicatechin effects. Previously it was shown that exposure of pre-constricted rat aortic and femoral rings from hypertensive rats to (-)-epicatechin resulted in an increased endothelium-dependent relaxation (Gomez-Guzman et al. 2012, Galleano et al. 2013). Importantly, when NOS was chronically inhibited rats developed hypertension and (-)-epicatechin was not longer able to restore defects in endothelium-dependent ex vivo aortic ring vasorelaxation in those animals (Gomez-Guzman et al. 2011). The only study demonstrating the in vivo effects of (-)-epicatechin describes an effective dilation of the femoral artery in living rats after direct arterial injection of (-)-epicatechin into hindlimb circulation (Ottaviani et al. 2011). However the effects of absorption and metabolism were not taken into consideration.

The vascular effects of (-)-epicatechin very likely include a regulation of NO-dependent vasodilation. Compared to wildtype mice, eNOS^{-/-} mice have a decreased, but not significantly blunted vascular function. Similar results were observed before by analyzing coronary circulation in the same mouse strain: it was shown that eNOS^{-/-} mice compensate for the deficiency for instance by endothelium derived release of other vasoactive factors e.g. prostaglandins (Godecke et al. 1998).

In addition to an increase in acute vascular response to occlusion this work for the first time shows that (-)-epicatechin treatment affects vascular stiffness in mice measured as reduced PWV. An increased PWV is widely accepted as a measure for endothelial dysfunction and also for structural changes of the vascular bed for instance in chronic cardiovascular pathological disorders (Mattace-Raso F 2010). Moreover also acute changes in PWV have been reported within few hours as shown for exercise and exposure to smoke (Mc Clean et al. 2007, Doonan et al. 2011, Figueroa et al. 2011, Unosson et al. 2013) and with acute inhibition of NOS (Davies et al. 2003). In the present study inhibition of NOS also increased PWV in mice.

In conclusion this is the first work demonstrating an improved vascular reactivity and a direct contribution of eNOS to the (-)-epicatechin effects in an animal in vivo model. Other investigations in rodents are limited to ex vivo aortic ring explantation, a method uncoupling the flavanol effects from systemic response of other organ and cell systems, metabolism and distribution by blood. It is important to notice, that young, healthy BL/6 mice were used in this study, which amongst others are known to have a pronounced ability for vascular regeneration (Helisch et al. 2006). Therefore the beneficial effect of nutritional flavanol supplementation on endothelium-dependent vascular function might be even stronger in aged mice, mice models of cardiovascular disease or other strains, when a functional eNOS is presupposed and should be subject of further investigation.

Is maintenance of NO-bioavailability and redox state essential for the effects of (-)-epicatechin ?

As shown here dietary (-)-epicatechin increases phosphorylation on the Ser-1177 residue (Fig. 22 and 23), which leads to increased eNOS activity by decreasing the dependency on Ca^{++} activation (Balligand et al. 2009). This is an important regulatory mechanism to increase NO production in vascular tissue and is a significant mechanism in health and disease (Kolluru et al. 2010). Several studies in the last decade showed an impact of flavanol compounds on eNOS in cultured endothelial cells. In HUVEC (-)-epicatechin had no effect on eNOS mRNA level (Brossette et al. 2011) but increased eNOS phosphorylation at the activation site and decreased phosphorylation at the inhibitory site reported in coronary artery endothelial cells (CAEC) (Auger et al. 2010, Ramirez-Sanchez et al. 2010, Ramirez-Sanchez et al. 2011). Findings of this study showing an activation of eNOS in healthy vascular tissue in vivo are supported by investigations in rat models of hypertension (Gomez-Guzman et al. 2012) and obesity (Agouni et al. 2009) reporting increased eNOS phosphorylation by (-)-epicatechin and (-)-epicatechin containing red wine polyphenols (RWPs) in the aorta. These in vivo and ex vivo experiments conducted with (-)-epicatechin further show that increased phosphorylation of eNOS is paralleled by increased phosphorylation of protein kinase B (Akt).

To the best of my knowledge this is the first study showing a rapid (1 h) and sustained (after 5 d) activation of eNOS in healthy vascular tissue in vivo. This effect correlates with the acute effects of (-)-epicatechin on vasodilation and NO-bioavailability observed in human (Schroeter et al. 2006) and also shown as dose-response curve in this mouse model. How flavanols are able to modify the post-translational phosphorylation state of eNOS is not clear. In vitro findings with cultured endothelial cells propose that (-)-epicatechin induces eNOS phosphorylation by activation of the $\text{PI}_3\text{K}/\text{Akt}$ pathway, the CaM dependent kinase pathway ($\text{Ca}^{++}/\text{CaM}/\text{CaMKII}$) and eNOS decoupling from caveola. Many mechanistic possibilities are discussed in this context: 1) the presence of a cell membrane “putative flavanol receptor”, 2) allosteric sites, 3)

receptor-independent signaling and 4) binding to intracellular molecules. Whether or not indeed a “putative flavanol receptor” is involved or whether the entry into endothelial cells and binding to intracellular molecules dominates is a challenging object of future *in vitro* and *in vivo* investigations.

Importantly increased eNOS activity by increased eNOS phosphorylation corresponded to an increase in vascular NO-bioavailability *in vivo* shown as an elevation of cGMP in the aorta. The production and rise of cGMP by (-)-epicatechin are fully eNOS dependent since NOS inhibition completely blocked cGMP production and (-)-epicatechin had no effect in eNOS^{-/-} mice (Fig. 24). Cyclic GMP is the most important NO-dependent secondary messenger in the vasculature. *In vitro* the ability of (-)-epicatechin to modulate this signaling is reported as increased NO and cGMP level in HUVEC and HCAEC in the absence but not in the presence of a NOS-inhibitor. *In vivo* dietary treatment with (-)-epicatechin-rich RWPs increased vascular NO and cGMP level (Benito et al. 2002, Agouni et al. 2009) and also resulted in a NOS-dependent cGMP increase in rat aortic rings directly incubated with RWPs (Andriambeloson et al. 1997). Importantly this study in mice demonstrates that increased cGMP level stimulate cGMP-dependent downstream signaling in the vasculature shown as increased phosphorylation of VASP in the aorta (Fig. 24). VASP phosphorylation is an established readout for cGMP signaling in vascular tissue (Oppermann et al. 2011, Ying et al. 2012), as it is highly selective for cGMP dependent kinases (i.e. PKG) (Smolenski et al. 1998). Therefore findings presented in this work for the first time provide evidence that the complete vascular eNOS/NO/cGMP/PKG pathway is eNOS-dependently activated by oral administration of (-)-epicatechin. Activation of this pathway has been already shown by administration of RWPs but was never demonstrated for (-)-epicatechin.

The dietary intake of cocoa flavanols in human is associated with an increase in systemic NO-bioavailability measured in blood plasma (Schroeter et al. 2006, Heiss et al. 2007, Loke et al. 2008). The present study demonstrates significantly increased cGMP level in plasma of the mice with (-)-epicatechin treatment (Fig. 26), which is

accepted as a readout for NO activity (Levett et al. 2011), whereas the plasma concentrations of NO_2^- and NO_3^- remained unchanged as also reported in hypertensive rats (Litterio et al. 2012). As also shown here up to 70–90 % of circulating plasma NOx in humans and other mammals are dependent on eNOS expression and are derived from NOS activity (Kleinbongard et al. 2003). The formation of NO_2^- and NO_3^- in the body can directly result from catabolism of the daily diet rich in NO_3^- or from oxidative enzymatic transformation (Tannenbaum 1979). However, the ratio of NO_2^- to NO_3^- , and not the absolute concentrations are related to changes in the redox state. Taken together (-)-epicatechin increases systemic eNOS/NO activity (Levett et al. 2011) as demonstrated by increases in cGMP levels in aorta and plasma, but does not affect the levels of circulating nitrite and nitrate, while the ratio of NO_2^- to NO_3^- is not significantly increased.

A physiological parameter known to be strongly associated with NO-bioavailability is the systemic blood pressure (Wood et al. 2013). In the present study oral treatment of mice with (-)-epicatechin did not affect arterial blood pressure whereas simultaneous NOS-inhibition resulted in a significant pressure increase (Tab. 10). Cocoa flavanols can modulate physiological blood pressure in human in dependence of duration and dose of oral administration (Ried et al. 2012). Oral supplementation with cocoa flavanols has been shown to reduce blood pressure in pathophysiological state such as hypertension and coronary artery disease (Grassi et al. 2005, Heiss et al. 2010, Hooper et al. 2012). However, the effects on blood pressure in healthy individuals are not clear (Engler et al. 2004, Vlachopoulos et al. 2005, Balzer et al. 2008) and need further investigation. In rats oral (-)-epicatechin treatment reduced blood pressure in different models of hypertension (Litterio et al. 2012, Galleano et al. 2013) while other studies report unchanged blood pressure with (-)-epicatechin in healthy and hypertensive rats (Gomez-Guzman et al. 2011, Gomez-Guzman et al. 2012). Therefore cocoa flavanols in general and (-)-epicatechin in particular have a stronger effect on blood pressure in pathophysiological state compared to physiological conditions.

To summarize the data show that (-)-epicatechin 1) increases vascular reactivity in an eNOS dependent fashion measured as FMD, PWV and PORH, 2) activates eNOS in the aorta measured as increased phosphorylation at the activation site 3) activates NO-signaling in the vasculature in an eNOS dependent fashion measured as increased cGMP level and VASP phosphorylation. Taken together this work provides novel evidence that oral (-)-epicatechin improves vascular health by activation of eNOS-dependent NO-bioactivity in vascular tissue in vivo.

Is Nrf2 required for the beneficial vascular effects of (-)-epicatechin in vivo?

Metabolic screening in this work demonstrates that (-)-epicatechin regulates the redox state in cardiovascular tissue in vivo reported as increased level of GSH in the lung and heart of the mice. This effect was paralleled by increased expression of enzymes involved in GSH synthesis and GSH metabolism (Fig. 30). Interestingly an opposite regulation with decreased GSH concentrations and decreased protein expression was observed in the liver of the mice. GSH is the most abundant and important cellular antioxidant, controlling the redox state (Sies 1999). GCL, the enzyme catalyzing the rate-limiting step of GSH de novo synthesis is one of the transcriptional targets of Nrf2 (Kaspar et al. 2009, Baird et al. 2011). Even though there are compensatory mechanisms for the Nrf2-pathway e.g. by Nrf1 (Ohtsuji et al. 2008), the deletion of Nrf2 results in decreased level of GSH in the tissue as also shown for aorta and liver of Nrf2^{-/-} mice in this study. The synthesis and metabolism of GSH is a main regulatory response to increased oxidative stress in cells and tissues and has even been demonstrated to affect vascular functionality (Prasad et al. 1999, Levy et al. 2012). GSH exerts its antioxidant activity by directly scavenging ROS and free radicals or in enzymatic reactions where it acts as a cofactor to detoxify harmful agents e.g. H₂O₂ (Sies 1999).

Since investigations on the beneficial effects of cocoa flavanols concentrate on endothelial and vascular function and therefore NO-bioactivity, still not much is known about the in vivo antioxidant effects of these compounds. Because of their chemical structure flavanols have the potential to exert redox active properties as predominantly demonstrated through thermodynamic and kinetic analysis (Galleano et al. 2010) and in solution (Rice-Evans et al. 1996). Some authors (Ruijters et al. 2013) attribute to flavanols in general and (-)-epicatechin in particular direct antioxidant effects. However the concentrations needed for such effects are 100-1000 fold higher as compared to circulating (-)-epicatechin concentrations. Activation of the GSH metabolism depends on the cell type: while (-)-epicatechin increased GSH level and activated GSH metabolizing enzymes in hepatic and neuronal cells (Martin et al. 2010, Martin et al. 2013), unchanged GSH-level and enzymatic activities were reported in a colon-derived cell line (Rodriguez-Ramiro et al. 2011).

This study reports an in vivo regulation of the redox state in tissues of the cardiovascular system by oral (-)-epicatechin. These findings are supported by similar approaches in rats showing increased GSH level and enzyme activity in the heart after administration of flavanol-rich grape extract (Seymour et al. 2013) but unchanged regulation of plasma GSH after administration of (-)-epicatechin (Litterio et al. 2012). However, the GSH pool, and herewith the NO pool, along the vascular tree is also determined by the blood and blood cells permanently streaming through the lumen. Regulation of GSH level in red blood cells (Lee et al. 2004) and also white cells (Zhu et al. 2008) is dependent on the presence of Nrf2 as demonstrated in Nrf2^{-/-} mice. Moreover, in cardiovascular and metabolic disorders with vascular dysfunction GSH level are decreased in red blood cells as shown for hypertension (Kumar et al. 2010) and type2 diabetes (Rizvi et al. 2001) in human and for bacterial infection with increased oxidative stress in mice (Guleria et al. 2002). Importantly, ex vivo incubation with (-)-epicatechin increased GSH-level in red blood cells from healthy people and patients in a dose-dependent bell-shaped fashion. In vivo oral flavanol-rich green tea extract increased red blood cell GSH in infected mice and oral administration of

flavanols from grapes increased the GSH/GSSG ratio in human red blood cells (Weseler et al. 2011). The physiological relevance of GSH in blood cells is further supported by positive correlation of decreased GSH in mononuclear cells with decreased FMD (Fratta Pasini et al. 2012) and in red blood cells with the pathogenesis of slow coronary flow in human (Enli et al. 2008). As demonstrated in this study, (-)-epicatechin increased GSH level in the heart of mice *in vivo*. Previously it has been shown that GSH is able to increase coronary vasodilation and flow in isolated rat heart by a NO and sGC dependent mechanism (Cheung et al. 1997, Levy et al. 2012) and that cardiac dysfunction in hypertension is associated with decreased GSH in the rat heart (Seymour et al. 2013). Thus this work provides further evidence for the accumulating data of flavanol-mediated regulation of the physiological relevant tissue redox state *in vivo*. It is obvious that the type of tissue and even the cellular type has strong impact on the described effects. On the one hand this is certainly due to different flavanol distribution, metabolism and action under different physiological and biological conditions, on the other hand the redox state itself, its regulation and sources of oxidative stress vary when comparing different cellular types and tissues (Sies 1999, Sugamura et al. 2011). Although it is often communicated that cocoa flavanol-mediated antioxidant effects are also an underlying principle in human (Keen et al. 2005, Corti et al. 2009) and may increase plasma antioxidant capacity and decrease plasma oxidation products (Rein et al. 2000, Wang et al. 2000), convenient evidence from controlled interventional trails remains elusive (Heiss et al. 2007, Heiss et al. 2010, Scheid et al. 2010, Ellinger et al. 2011, Hollman et al. 2011).

This work provides strong evidence that the (-)-epicatechin effects on vascular function are absent if GSH levels are decreased and antioxidant regulation is less effective, as shown in *Nrf2*^{-/-} mice. In contrast to wildtype mice oral administration of (-)-epicatechin to *Nrf2*^{-/-} mice did not improve vascular function (Fig. 20 and Fig. 21), did not increase NO-bioactivity in the vasculature (Fig. 25) and did not regulate tissue redox state (Fig. 28). These are unreported novel findings, which describe the contribution of *Nrf2* to the vascular (-)-epicatechin effects *in vivo*. In other context *Nrf2*

is essential for (-)-epicatechin mediated prevention of stroke damage in mice (Shah et al. 2010, Leonardo et al. 2013) and is associated with a reduction of cardiac dysfunction by flavanol-rich grape extract in hypertensive rats (Seymour et al. 2013). In vitro findings confirm that (-)-epicatechin is able to activate Nrf2 signaling as demonstrated in cultured neuronal cells (Shah et al. 2010, Leonardo et al. 2013), while this effect is lacking (Ruijters et al. 2013) or not reported in endothelial cells. Thus although flavanols possess an electrophilic chemical structure and although there is evidence for an activation of Nrf2 in non vascular cells this is the first work to demonstrate that Nrf2 is required to increase vascular reactivity and plays an important role in the in vivo effects of oral administration of (-)-epicatechin in vascular tissue. Since cGMP levels are not increased when Nrf2 is lacking, the activation of eNOS by (-)-epicatechin is obviously not sufficient to restore the defects in Nrf2^{-/-} mice. Because regulation of the redox state is dependent on Nrf2, the involved mechanism may include an increased NO degradation due to increased oxidative stress. These effects have been demonstrated for longer term treatment, while (-)-epicatechin was still able to increase vascular function after one hour. This indicates, that the rapid activation of eNOS by (-)-epicatechin in the vessel wall acutely increases vascular function, whereas longer term treatment additionally includes (-)-epicatechin effects via regulation of the redox state by Nrf2.

In summary, so far there was no evidence for regulation of the antioxidant state and a role of Nrf2 in the cardiovascular system in vivo. This work for the first time demonstrates that maintenance of the redox state and GSH level is required for the beneficial effects of (-)-epicatechin on vascular function in the living animal. Orally administered (-)-epicatechin regulates the NO-bioactivity, redox state and antioxidant gene expression in wildtype mice, while these effects are absent when Nrf2 is deleted. As this regulation is different in aorta, heart/lung and the liver, it is likely that an altered distribution and metabolism or activation of different signaling cascades in different tissues underlies the antioxidant properties of (-)-epicatechin in vivo. However, the hypothesis generating approach of metabolic screening for the tissue

Discussion

redox-state can not picture the complete signaling-cascades and herewith the (patho)physiological mechanisms of the (-)-epicatechin effect. Still, the improvement of vascular function by increased NO-bioactivity might not only be determined by increased eNOS dependent NO production but also by stabilization of the NO-pool. Thus regulation of GSH and enzymes belonging to antioxidant defense (=Nrf2 targets) may be necessary for the (-)-epicatechin induced effects.

What other mechanisms are involved in the vascular effects of (-)-epicatechin ?

Endothelial NOS-dependent NO-signaling and Nrf2-dependent antioxidant response are mechanisms by which oral (-)-epicatechin mediates its beneficial cardiovascular effects. However, a modulation of daily diet, especially under longer-term conditions, also results in global changes, e.g. in the regulation of gene transcription (Liang et al. 2001, Stephanie J. Muga 2004, Swain et al. 2007). Surprisingly, this has never been investigated for the effects of dietary flavanols in the vasculature in vivo, although the identification of novel targets and signaling cascades would permit a better and more comprehensive understanding of the in vivo effects of flavanols on cardiovascular health. Transcriptional profiling in this work demonstrates that oral (-)-epicatechin treatment has a dose-dependent, global impact on the transcriptional profile in vascular tissue in vivo. Interventional studies with flavanols predominantly focus on one or few potential targets only and no other study performed comparative transcriptome analysis in vascular tissue, nor in other organs, after in vivo treatment. Examples of global gene expression analysis involving dietary/nutritional intervention in mice are numerous and include effects of iron in intestinal tissue (Swain et al. 2007), linoleic acid in colon (Stephanie J. Muga 2004) or leptin in liver (Liang et al. 2001). An indication for similar potential of flavanols is provided from the effects of flavanol-rich green tea on lung cancer gene profile in mice (Lu et al. 2006) and epigallocatechin-3-gallate (EGCG) on global gene expression profile in human prostate cancer cells (Wang et al. 2002) and neuronal cells (Weinreb et al. 2003).

Transcriptional profiling of genes in an (-)-epicatechin dose-response model

Oral administration of (-)-epicatechin regulates 4208 targets from which 1507 are affected by 2 mg/kg and 2701 by 10 mg/kg. First, these findings demonstrate that oral feeding with (-)-epicatechin in vivo results in strong changes of the vascular gene expression profile. Second, a dose-dependent response strongly determines the number and identity of genes regulated. Therefore results of this study suggest important implications for nutritional studies with (-)-epicatechin in vivo. Several mechanisms such as NO-bioactivity, antioxidant properties, and others are currently in the focus to explain the beneficial action of cocoa flavanols on cardiovascular health

(Heiss et al. 2010) and it is reasonable that possible targets and signaling cascades are analyzed separately to explain these effects. However results of this work provide evidence that other targets out of the main focus are regulated and may play an essential role. In addition the dose used in in vivo nutritional studies is important because transcriptional profiling in vascular tissues identified many targets, which are regulated by low or high dose (-)-epicatechin only.

To further categorize the targets it was distinguished between annotation clustering of genes based on gene affiliation and functional clustering of genes based on the pathway involved. The strongest enrichment of (-)-epicatechin regulated targets was found in the phosphoprotein cluster, followed by genes located in the nucleus, involved in regulation of transcription, splicing and ion binding (Tab. 13 and 14). Sublist-analysis revealed that most of these phosphoproteins are located in the nucleus and are involved in regulation of gene transcription. Phosphorylation plays a major role in cellular signaling and is a key reversible modification that can regulate enzymatic activity, subcellular localization, complex formation and degradation of proteins (Delom et al. 2006). Therefore global activation/suppression of genes regulating transcription and other essential cellular processes accounts for the mechanisms discussed for cocoa flavanols on vasculature. However, affiliation clustering of genes limits the possibility of a functional and more stringent interpretation of the results. To connect the novel findings with known vascular in vivo effects pathway clustering of (-)-epicatechin regulated genes was done with focus on signaling cascades potentially involved in regulation of the redox state and vascular function.

Novel (-)-epicatechin targets: vascular smooth muscle signalling and protection from toxic and oxidative stress

Besides others (-)-epicatechin regulates gene clusters of cellular xenobiotic and antioxidant defense in the aorta in vivo (Tab. 15). Among all targets *Arnt* is the most down-regulated gene by low-dose (-)-epicatechin (Tab. 12). The ARNT protein forms a complex with AhR, which is also down-regulated by (-)-epicatechin at mRNA level (Fig.

34). Regulation of these factors by (-)-epicatechin is a significant mechanism because the ARNT/AhR complex plays a major role in the adaptive response of biological systems to xenobiotic (e.g. drugs, dioxins) stress by binding eligible ligands. However, the detoxification process itself produces reactive and harmful intermediate compounds, which have to be further processed and detoxified by the Nrf2-dependent pathway (Wakabayashi et al. 2010). Importantly cocoa flavonoids can also act as exogenous ligands for the ARNT/AhR complex as demonstrated in vitro as a competitive antagonist role and an inhibition of ARNT/AhR-mediated signal transduction (Mukai et al. 2010, Han et al. 2012), and in vivo in liver of mice and rats as disrupted formation of the ARNT/AhR complex by inhibited binding between AhR and its toxic ligands (Fukuda et al. 2007, Mukai et al. 2008). Therefore there is accumulating evidence that the intake of flavanoids suppresses the toxicological effects of xenobiotic agents in the body by inhibition of ARNT/AhR signaling. Even though a transcriptional down-regulation of *Arnt* and *Ahr* in aorta by (-)-epicatechin as demonstrated in this study disagrees with recent findings with grape extract in the hearts of rats (Seymour et al. 2013), this mechanism would permit a suppression of ligand mediated toxicological effects in the vascular system which is similar to ARNT/AhR inhibition. Importantly the AhR-signaling includes a negative feedback regulation in which an inactive ARNT/AhR complex inhibits the transcription of *Ahr* (Denison et al. 2011). Therefore a disrupted formation of the ARNT/AhR complex by (-)-epicatechin, as previously demonstrated for other class of flavonoids, can explain a down-regulation of these factors at mRNA level. These novel findings in vascular tissue in vivo have significant implications for pathophysiological conditions because toxic AhR ligands mediate cardiovascular disease development and progression in mammals and vertebrates which is correlated with an activation of ARNT-AhR signaling (Korashy et al. 2006).

The AhR system strongly interacts with the antioxidant Nrf2 signaling pathway (Wakabayashi et al. 2010), which also can be activated by flavanol compounds (Shah et al. 2010, Scapagnini et al. 2011, Seymour et al. 2013). As a main protective antioxidant response to regulate cellular and tissue redox state, enzymes involved in GSH-

metabolism are transcriptionally activated (Janssen-Heininger et al. 2013). Transcriptional profiling in mouse aorta demonstrates that genes clustered in the phase II GSH-metabolism pathway (GSH-S-transferase, GSH-peroxidase, GSH-reductase) are up-regulated by (-)-epicatechin treatment in vascular tissue in vivo (Tab. 16). While this pattern could not be proven in aorta on protein level (Fig. 29) an increase in GSH metabolizing enzymes was also detected in the heart and highly vascularized lung of the mice (Fig. 30). As previously discussed an activation of GSH metabolizing enzymes and an elevation of GSH by (-)-epicatechin has been predominately reported in cultured cells of non-vascular origin in vitro (Martin et al. 2010, Martin et al. 2013) whereas these effects are not proven for vascular tissue in vivo.

A focus of the functional clustering approach was to identify candidate pathways that explain the increase of vascular function by (-)-epicatechin. Among others this work determined gene clusters of calcium-signaling and vascular smooth muscle signaling to be regulated by (-)-epicatechin in vascular tissue in vivo. Both pathways essentially contribute to the vasoactive properties of the vascular wall by regulation of $[Ca^{++}]_i$ through NO-cGMP signaling (Nausch et al. 2008, Morgado et al. 2012). Since (-)-epicatechin eNOS-dependently increases cGMP level and PKG activity in vascular tissue in vivo (Fig. 24) a regulation of $[Ca^{++}]_i$ and myosin phosphorylation is a self-evident mechanism for the effect on vascular function. In fact pathway analysis revealed that essential factors controlling vascular smooth muscle signaling and $[Ca^{++}]_i$ are regulated by (-)-epicatechin in the aorta of mice in vivo (Tab. 17) including the Ca^{++} -channel, CaM and IP₃R. In addition the enzymes phospholipase C, PKA and PKG are regulated by (-)-epicatechin, all which can regulate IP₃R mediated Ca^{++} -release from intracellular storage in smooth muscle (Murthy et al. 2003, Narayanan et al. 2012). On the other hand $[Ca^{++}]_i$ can be regulated by entry through voltage-dependent Ca^{++} -channel, and action of the endothelin receptor, both are targets also regulated by (-)-epicatechin. As downstream effectors microarray analysis together with western-blot analysis revealed a regulation of MLCK and MYPT.

This transcriptional study strongly indicate that oral administration of (-)-epicatechin regulates vascular reactivity also by modulating $[Ca^{++}]_i$ dependent signaling in smooth muscles of the vascular wall. This hypothesis is supported from in vitro findings using other catechin compounds but is not reported for (-)-epicatechin. In rat aortic smooth muscle cells (RASMC) EGCG increased cAMP and cGMP along with diminished $[Ca^{++}]_i$ increase to a contractile stimulus. This effect was accompanied by EGCG-mediated relaxation of endothelium-intact rat aortic rings (Alvarez et al. 2006). However earlier findings by the same group show a reverse response to EGCG with a transient $[Ca^{++}]_i$ increase in RASMC accompanied by a contraction of endothelium-denuded aortic rings (Alvarez-Castro et al. 2004). Measurements of actual currents in RASMC using the whole-cell voltage-clamp technique suggest that an increase in Ca^{++} -influx is responsible for the acute EGCG-induced increase in $[Ca^{++}]_i$ and the subsequent endothelium-independent contractile effect, while the Ca^{++} -antagonist activity of EGCG in long-term treatments is responsible for the vasorelaxant effect (Campos-Toimil et al. 2007). Downstream of $[Ca^{++}]_i$ regulation EGCG has been shown to activate MYPT and as a consequence decrease the phosphorylation state of myosin in colon cancer cells (Umeda et al. 2008). In general it seems important to distinguish between an initial transient smooth muscle contraction, which is mediated by Ca^{++}/CaM -dependent activation of MLCK/myosin phosphorylation and sustained long-term effects which are largely Ca^{++} -independent and involve regulation of MYPT (Murthy et al. 2003). In this work the phosphorylation state and herewith the activity of MCLK and MYPT in the aorta of the mice was not changed by (-)-epicatechin treatment (Fig. 35), but as described regulation of myosin phosphorylation is a rapid and transient mechanism rather than a constant inert biochemical state.

Taken together in vitro studies support the role of eNOS-cGMP-PKG, and regulation of Ca^{++} -signaling and myosin phosphorylation in flavanol mediated effects. However the exact regulation of the signaling cascade including $[Ca^{++}]_i$, MLCK, MYPT and myosin by (-)-epicatechin remains to be investigated, since there is no in vivo data about it, and/or in vitro data were done with cells of not vascular origin or applying EGCG, a not-comparable compound with different structure and potentially different effects.

This work in mice shows that in vivo vascular smooth muscle- and Ca^{++} -signaling pathways are potentially regulated by (-)-epicatechin in vascular tissue, and therefore interaction of NO- and Ca^{++} -signaling in the vessel wall may be an important mechanism by which oral (-)-epicatechin improves vascular function (Fig. 37).

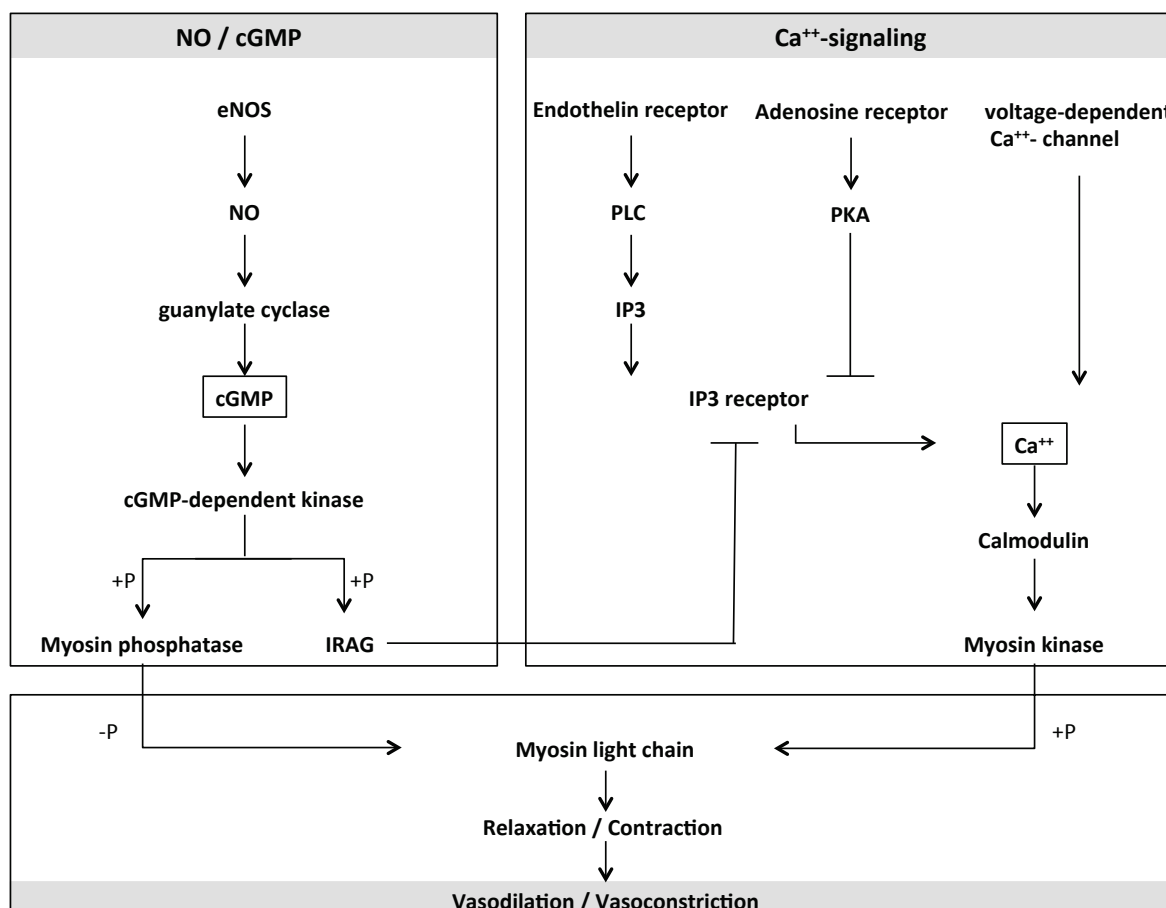


Fig. 37: Network of (-)-epicatechin regulated genes involved in the NO- and Ca^{++} -mediated process of vascular muscle relaxation / contraction.

IRAG = IP3R-associated cGMP kinase substrate, PLC = Phospholipase C, IP3 = Inositol trisphosphate, PKA = Protein kinase A.

In summary this is the first in vivo study to show that 1) (-)-epicatechin changes global gene expression in vascular tissue, 2) this regulation pattern is dependent on the dosage, 3) phosphoproteins regulating transcription are the top regulated gene cluster, 4) regulation of redox-signaling, Ca^{++} -signaling and vascular smooth muscle signaling can explain the reported in vivo effects, 5) many other targets are significantly regulated and deserve deeper analysis but were out of focus in this work.

Limitations of global gene expression analysis in this study is the lack of target verification by real-time PCR for all targets and lack of functional analysis but these are steps, which are currently under investigation. Since aorta lysates were used, the discrimination between gene regulation in endothelial cells and smooth muscle cells is not possible. However, it is important to consider that most of the template origins from smooth muscles because they outnumber endothelial cells in the aorta. Whether or not decreased $[Ca^{++}]_i$ in smooth muscle parallels increased vasorelaxation by (-)-epicatechin in vivo should be subject of future investigations.

Establishing a mouse model for assessment of vascular function

The establishment of methods for the non-invasive measurement of vascular function in living mice was an essential part of this work. Scanning LDPI together with high-resolution ultrasound has been introduced for the first time as a robust non-invasive method for the assessment of vascular function in mice in vivo. Determination of PORH in the hindlimb allowed the reproducible intra- and inter-individual measurements, which may be applied to evaluate vascular function in mice models of cardiovascular disease. In particular this study shows that, 1) changes in diameter and flow in the femoral artery in response to vasoactive drugs correlate with changes in MPU, 2) dilation of the femoral artery in response to reperfusion after transient ischemia (FMD) correlate with increased tissue reperfusion (PORH), 3) measurements of PORH by scanning LDPI are reproducible, depend on availability of endogenous vasodilators and decrease with increasing animal age.

What is the origin of the LDPI signal in mouse hindlimb?

The perfusion map obtained by scanning a defined area of the hindlimb shows a discrete region of very high signal intensity, which corresponds to the area of tissue with and around the femoral artery (see methods). According to the manufacturer's information the measurement depth of the system used in this study has been calculated to be around 1 mm in human skin. In mice the femoral artery can be

visualized at 0.4 cm penetration depth with high-resolution ultrasound. Thus, a major part of the measured “mean perfusion units” is dependent on blood flow in the femoral artery (macrocirculation) and less a measure of microcirculatory tissue perfusion. Therefore, the use of scanning LDPI in the mouse hindlimb is not comparable to its use in human skin, where – considering the penetration depth of the laser – it is applied to assess microcirculatory function.

Measurements of PORH: reproducibility and dependency on physiological stimuli.

Measurement of PORH with different methods is routinely applied in clinical settings to evaluate the endothelial functionality of different vessel beds, and it is known to be dependent on occlusion time and on endogenous vasodilators.

As a first step of scanning LDPI validation for assessment of hyperemic responses, this study shows that the LDPI signal is directly correlated to changes in diameter and blood flow in the femoral artery assessed by ultrasound (Fig. 11). Thus, administration of endothelium independent and endothelium dependent pharmacological vasodilators or a vasoconstrictor caused an increase or decrease in vessel diameter, and blood flow, which corresponded to a comparable response in MPU.

As a second step, it has been verified that PORH-induced changes in peak MPU corresponded to peak FMD of the femoral artery, which is a widely accepted parameter for determining endothelial function. The elevation of MPU lasted longer than the FMD response (Fig. 14), indicating a microvascular component of the LDPI signal. Interestingly, maximal MPU after PORH was comparable with the maximum NTG-induced MPU increase, and significantly higher than the ACh or adenosine induced response. Importantly, basal perfusion was blunted and PORH was absent in chronic hindlimb ischemia induced by surgical excision of the femoral artery (Fig. 13). In addition PORH-induced changes in MPU were dependent on the duration of the occlusion (Fig. 15) and increased with longer occlusion times, further validating this measurement approach.

As a third step, the reproducibility and variability of PORH assessed by LDPI has been analysed by repeated intra-individual and inter-individual measurements (Fig. 15). The

most robust parameter was the time to peak, which is an indicator of the rapidity of the response, and the ratio of maximum and baseline perfusion, which is an indicator of the magnitude of the response. Interestingly, the rapidity of the hyperemic response was dependent on synthesis of both NO and prostaglandins, as the NOS inhibitor L-NNA as well as the COX inhibitor indomethacin increased time to peak (Fig. 16).

As a fourth step the physiological significance of PORH has been proven. Vascular aging is known to induce endothelial dysfunction in humans (Seals et al. 2011) and in rats (Heiss et al. 2007) and is associated with impaired angiogenesis (Rivard et al. 1999) and aortic ring relaxation (Gendron et al. 2012) in mice. Here, it was found that 12 and 24 months old mice have a slower vascular responsiveness (time to peak), significantly decreased magnitude of response (perfusion reserve and AUC) and a less sustained hyperemia as compared to younger mice (Fig. 17).

Although the use of in vivo models of cardiovascular disease is widely spread, methods for evaluating endothelial function in rodents are mainly restricted to ex vivo techniques, or high resolution ultrasound in rats (Heiss et al. 2007). Even if a direct correlation between the changes in arterial diameter, arterial blood flow and changes in perfusion has been demonstrated in this study, the LDPI technique cannot fully substitute ultrasound for determination of FMD in vivo. As compared to ultrasound, scanning LDPI is less specific for endothelial function (i.e. does not measure diameter and flow velocity in the vessel) and cannot distinguish macrocirculation and microcirculation. However, it allows to measure tissue perfusion in a defined region of interest, is easier to use, requires less training time to achieve reproducibility, and it is more robust as additionally demonstrated for basal perfusion measurements in mouse hindlimb (Greco et al. 2013). Moreover it is less sensible than ultrasound to tiny changes in hindlimb position during inflation and deflation of the cuff, temperature and small changes in cardiac and circulatory parameters, and it is more affordable.

To conclude, in order to perform reliable measurements for assessing vascular function in mice in vivo both methods were applied – high-resolution ultrasound and

scanning LDPI. Both methods combined allow to test the effects of pathophysiological changes of vascular function in correlation to genetic or pharmacological manipulation, or physiological processes like aging both in a cross-sectional or longitudinal experimental settings in the living animal. Thus they permit an easier translation of the findings to the clinical application in humans.

Summary and Conclusion

The present work analysed the mechanisms underlying the vascular effects of oral (-)-epicatechin in vivo. The beneficial action of flavanols on cardiovascular health is widely reported but the mechanisms are not well understood and mechanistic studies are mainly limited to in vitro findings with (-)-epicatechin. This study demonstrates that in vivo effects of (-)-epicatechin are dependent on both eNOS-dependent regulation of NO production and Nrf2-dependent regulation of the redox state (Fig. 38).

The underlying mechanisms include an activation of the eNOS/cGMP/PKG pathway, downstream signaling in the vessel wall, regulation of the antioxidant defense and regulation of redox state in tissue of the cardiovascular system. Moreover transcriptional profiling in vascular tissue identified novel (-)-epicatechin targets in vivo including vascular smooth muscle and Ca^{++} signaling in interaction of NO-signaling.

Discussion

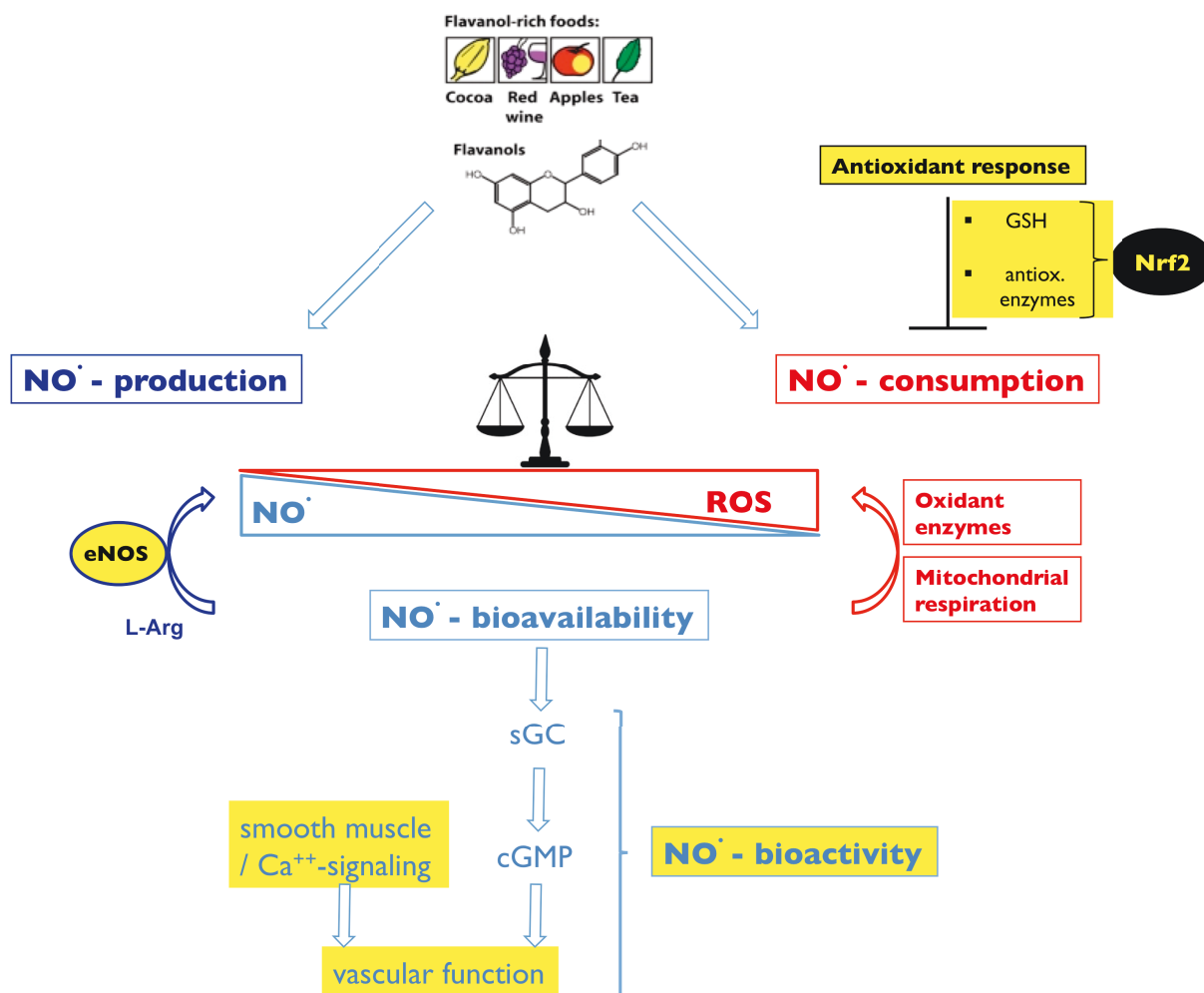


Fig. 38: (-)-Epicatechin increases vascular reactivity by regulation of eNOS/sGC/cGMP signaling and its effectors in smooth muscle cells.

Through a favourable impact on NO production and NO consumption through eNOS and Nrf2 (-)-epicatechin is able to increase NO-bioactivity and smooth muscle signalling and therefore improve vascular function (yellow = subject of investigation in this study).

In conclusion both, increased NO production by eNOS and reduced NO consumption by Nrf2 mediated antioxidant defense can increase NO-bioactivity in the vascular wall. Regulation of all, NO production within the endothelium, essential signaling cascades within smooth muscle and cellular antioxidant protection contribute to the beneficial effects of dietary (-)-epicatechin on cardiovascular health.

Why is this study relevant for translational flavanol research ?

This work provides significant contribution to translational flavanol research because it identified relevant underlying mechanisms, which are able to explain how flavanols improve vascular function *in vivo*. Analysis of biochemical and biological mechanisms involved in effects of a oral intervention is neither possible in tissue in humans, nor is reported in other *in vivo* models in this extent so far. There is cumulative evidence that flavanols can reverse or diminish the initiation and progression of cardiovascular disease. The identification of potential targets and regulated signaling cascades can help to develop and specify their application in dietary supplementation or medical treatment. In this study mice models were chosen to analyze the mechanisms in cardiovascular tissue because genetic models with a deletion in potential target genes were available. Importantly a dose of 2 mg/kg (-)-epicatechin was used in this study which improved vascular function in mice after five days, but was also demonstrated to improve FMD of the brachial artery in human in acute (2h) (Schroeter et al. 2006) and longer term conditions (1-7d) (Heiss et al. 2007) (Engler et al. 2004).

This study demonstrates that (-)-epicatechin is rapidly absorbed and metabolised in mice. HPLC-analysis of plasma samples revealed a dose-dependent absorption and metabolism of (-)-epicatechin in mice within one hour (Fig. 9). The saturation is reached at 4-10 mg/kg and up to 78 % of total (-)-epicatechin found in plasma is metabolized as methylated 3'- and 4'-O-methylepicatechin. In human the highest amount of circulating flavanols was found two hours after oral administration (Schroeter et al. 2006) and also the most abundant metabolite was methylated epicatechin while unmethylated (-)-epicatechin represented the minor part. Moreover it was shown that (-)-epicatechin is best absorbed, metabolised, and bioactive in human compared to other flavanol stereoisomers such as (+)-epicatechin, (-)-catechin, and (+)-catechin (Ottaviani et al. 2011). Interestingly compared to human total plasma flavanol concentration is threefold higher in mice (1500 nM vs. 600 nM) after administration of (-)-epicatechin. This underlines the importance of *in vivo* experiments to investigate flavanol mediated effects, as *in vitro* studies only rarely use

metabolites including the methylated derivatives of (-)-epicatechin for treatment of cells (Steffen et al. 2007).

Another phenomenon found in this study which is relevant for translational flavanol research, is a bell-shaped dose-dependence of (-)-epicatechin in vivo reported as dose-response curve measured as PORH and increased vascular reactivity and pulsatility with 2 mg/kg but not 10 mg/kg (-)-epicatechin measured as FMD, PWV and PORH. Similar to these findings in mice, treatment of healthy rats with 10 mg/kg (-)-epicatechin did not result in an increased aortic ring relaxation (Gomez-Guzman et al. 2012). The effects of different dose of dietary flavanols are reported but not satisfactory discussed in studies from animal models and also in human. Both dose of (-)-epicatechin, 2 mg/kg and 10 mg/kg, restored endothelial defects but only the higher dose reduced blood pressure and endothelin level in hypertensive rats (Gomez-Guzman et al. 2012). Moreover, this study provides further novel evidence for a bell-shaped action of (-)-epicatechin in vivo supporting the reverse effects: 1) The absorption and metabolism of (-)-epicatechin in mice reaches a plateau at 4 mg/kg (Fig. 9), this indicates a saturation effect where (-)-epicatechin can no longer be absorbed and metabolized. Importantly this resulting excess of unprocessed polyphenolic compounds in the organism may even have toxic effects for the organism (Takami et al. 2008, Eagle 2012); 2) Treatment with the higher (-)-epicatechin dose massively changes global gene regulation in vascular tissue compared to the lower dose and control conditions. This can be seen as a proof for the importance of the dose of flavanols used in in vivo studies, in particular when vascular effects are the matter of interest. Which mechanisms underlie the adverse effects on vascular function of higher dose of (-)-epicatechin in vivo, is current topic of research in our lab.

In summary this study provides new insights for mechanistic action, but also from metabolism and dose-dependence and thus helps to understand how (-)-epicatechin may mediate its beneficial cardiovascular effects in human and may therefore have relevant impact on future translational research in this field.

References

- Agouni, A., A. H. Lagrue-Lak-Hal, H. A. Mostefai, A. Tesse, P. Mulder, P. Rouet, F. Desmoulin, C. Heymes, M. C. Martinez and R. Andriantsitohaina (2009). "Red wine polyphenols prevent metabolic and cardiovascular alterations associated with obesity in Zucker fatty rats (Fa/Fa)." *PLoS One* **4**(5): e5557.
- Akata, T., M. Nakashima, K. Kodama, W. A. Boyle, 3rd and S. Takahashi (1995). "Effects of volatile anesthetics on acetylcholine-induced relaxation in the rabbit mesenteric resistance artery." *Anesthesiology* **82**(1): 188-204.
- Algotsson, A., A. Nordberg and B. Winblad (1995). "Influence of age and gender on skin vessel reactivity to endothelium-dependent and endothelium-independent vasodilators tested with iontophoresis and a laser Doppler perfusion imager." *J Gerontol A Biol Sci Med Sci* **50**(2): M121-127.
- Alvarez, E., M. Campos-Toimil, H. Justiniano-Basaran, C. Lugnier and F. Orallo (2006). "Study of the mechanisms involved in the vasorelaxation induced by (-)-epigallocatechin-3-gallate in rat aorta." *British journal of pharmacology* **147**(3): 269–280.
- Alvarez-Castro, E., M. Campos-Toimil and F. Orallo (2004). "(-)-Epigallocatechin-3-gallate induces contraction of the rat aorta by a calcium influx-dependent mechanism." *Naunyn-Schmiedeberg's archives of pharmacology* **369**(5): 496–506.
- Andriambelosen, E., A. L. Kleschyov, B. Muller, A. Beretz, J. C. Stoclet and R. Andriantsitohaina (1997). "Nitric oxide production and endothelium-dependent vasorelaxation induced by wine polyphenols in rat aorta." *British journal of pharmacology* **120**(6): 1053–1058.
- Arejian, M., Y. Li and M. B. Anand-Srivastava (2009). "Nitric oxide attenuates the expression of natriuretic peptide receptor C and associated adenylyl cyclase signaling in aortic vascular smooth muscle cells: role of MAPK." *Am J Physiol Heart Circ Physiol* **296**(6): H1859-1867.
- Auger, C., J.-H. Kim, P. Chabert, M. Chaabi, E. Anselm, X. Lanciaux, A. Lobstein and V. B. Schinikerth (2010). "The EGCg-induced redox-sensitive activation of endothelial nitric oxide synthase and relaxation are critically dependent on hydroxyl moieties." *Biochemical and biophysical research communications* **393**(1): 162–167.
- Baba, S., N. Osakabe, M. Natsume, Y. Muto, T. Takizawa and J. Terao (2001). "Absorption and urinary excretion of (-)-epicatechin after administration of different levels of cocoa powder or (-)-epicatechin in rats." *Journal of agricultural and food chemistry* **49**(12): 6050–6056.
- Baird, L. and A. T. Dinkova-Kostova (2011). "The cytoprotective role of the Keap1-Nrf2 pathway." *Arch Toxicol* **85**(4): 241-272.
- Balligand, J. L., O. Feron and C. Dessy (2009). "eNOS activation by physical forces: from short-term regulation of contraction to chronic remodeling of cardiovascular tissues." *Physiol Rev* **89**(2): 481-534.
- Balzer, J., T. Rassaf, C. Heiss, P. Kleinbongard, T. Lauer, M. Merx, N. Heussen, H. B. Gross, C. L. Keen, H. Schroeter and M. Kelm (2008). "Sustained benefits in vascular function through flavanol-containing cocoa in medicated diabetic patients a double-masked, randomized, controlled trial." *Journal of the American College of Cardiology* **51**(22): 2141–2149.
- Bassil, M. and M. B. Anand-Srivastava (2006). "Nitric oxide modulates Gi-protein expression and adenylyl cyclase signaling in vascular smooth muscle cells." *Free Radic Biol Med* **41**(7): 1162-1173.
- Benito, S., D. Lopez, M. P. Saiz, S. Buxaderas, J. Sanchez, P. Puig-Parellada and M. T. Mitjavila (2002). "A flavonoid-rich diet increases nitric oxide production in rat aorta." *Br J Pharmacol* **135**(4): 910-916.
- Bhupathiraju, S. N., N. M. Wedick, A. Pan, J. E. Manson, K. M. Rexrode, W. C. Willett, E. B. Rimm and F. B. Hu (2013). "Quantity and variety in fruit and vegetable intake and risk of coronary heart disease." *The American journal of clinical nutrition*.

References

- Brossette, T., C. Hundsdorfer, K. D. Kroncke, H. Sies and W. Stahl (2011). "Direct evidence that (-)-epicatechin increases nitric oxide levels in human endothelial cells." *Eur J Nutr* **50**(7): 595-599.
- Campos-Toimil, M. and F. Orallo (2007). "Effects of (-)-epigallocatechin-3-gallate in Ca²⁺ - permeable non-selective cation channels and voltage-operated Ca²⁺ channels in vascular smooth muscle cells." *Life sciences* **80**(23): 2147–2153.
- Cheung, P. Y. and R. Schulz (1997). "Glutathione causes coronary vasodilation via a nitric oxide- and soluble guanylate cyclase-dependent mechanism." *Am J Physiol* **273**(3 Pt 2): H1231-1238.
- Cooke, J. P., E. Rossitch, Jr., N. A. Andon, J. Loscalzo and V. J. Dzau (1991). "Flow activates an endothelial potassium channel to release an endogenous nitrovasodilator." *J Clin Invest* **88**(5): 1663-1671.
- Cornwell, T. L., E. Arnold, N. J. Boerth and T. M. Lincoln (1994). "Inhibition of smooth muscle cell growth by nitric oxide and activation of cAMP-dependent protein kinase by cGMP." *Am J Physiol* **267**(5 Pt 1): C1405-1413.
- Cortese-Krott, M. M., A. Rodriguez-Mateos, R. Sansone, G. G. Kuhnle, S. Thasian-Sivarajah, T. Krenz, P. Horn, C. Krisp, D. Wolters, C. Heiss, K. D. Kroncke, N. Hogg, M. Feelisch and M. Kelm (2012). "Human red blood cells at work: identification and visualization of erythrocytic eNOS activity in health and disease." *Blood* **120**(20): 4229-4237.
- Corti, R., A. J. Flammer, N. K. Hollenberg and T. F. Luscher (2009). "Cocoa and cardiovascular health." *Circulation* **119**(10): 1433-1441.
- Dauchet, L., P. Amouyel and J. Dallongeville (2009). "Fruits, vegetables and coronary heart disease." *Nature reviews. Cardiology* **6**(9): 599–608.
- Davies, J. I. and A. D. Struthers (2003). "Pulse wave analysis and pulse wave velocity: a critical review of their strengths and weaknesses." *J Hypertens* **21**(3): 463-472.
- Delom, F. and E. Chevet (2006). "Phosphoprotein analysis: from proteins to proteomes." *Proteome Sci* **4**: 15.
- Denison, M. S., A. A. Soshilov, G. He, D. E. DeGroot and B. Zhao (2011). "Exactly the same but different: promiscuity and diversity in the molecular mechanisms of action of the aryl hydrocarbon (dioxin) receptor." *Toxicol Sci* **124**(1): 1-22.
- Donovan, J. L., V. Crespy, M. Oliveira, K. A. Cooper, B. B. Gibson and G. Williamson (2006). "(+)-Catechin is more bioavailable than (-)-catechin: relevance to the bioavailability of catechin from cocoa." *Free Radic Res* **40**(10): 1029-1034.
- Doonan, R. J., P. Scheffler, A. Yu, G. Egiziano, A. Mutter, S. Bacon, F. Carli, M. E. Daskalopoulos and S. S. Daskalopoulou (2011). "Altered arterial stiffness and subendocardial viability ratio in young healthy light smokers after acute exercise." *PLoS One* **6**(10): e26151.
- Eagle, K. (2012). "Toxicological effects of red wine, orange juice, and other dietary SULT1A inhibitors via excess catecholamines." *Food Chem Toxicol* **50**(6): 2243-2249.
- Ellinger, S., N. Muller, P. Stehle and G. Ulrich-Merzenich (2011). "Consumption of green tea or green tea products: is there an evidence for antioxidant effects from controlled interventional studies?" *Phytomedicine* **18**(11): 903-915.
- Engler, M. B., M. M. Engler, C. Y. Chen, M. J. Malloy, A. Browne, E. Y. Chiu, H.-K. Kwak, P. Milbury, S. M. Paul, J. Blumberg and M. L. Mietus-Snyder (2004). "Flavonoid-rich dark chocolate improves endothelial function and increases plasma epicatechin concentrations in healthy adults." *Journal of the American College of Nutrition* **23**(3): 197–204.
- Enli, Y., M. Turk, R. Akbay, H. Evrengul, H. Tanriverdi, O. Kuru, D. Seleci, A. Kaftan, O. Ozer and H. Enli (2008). "Oxidative stress parameters in patients with slow coronary flow." *Adv Ther* **25**(1): 37-44.
- Erdman, J. W., Jr., D. Balentine, L. Arab, G. Beecher, J. T. Dwyer, J. Folts, J. Harnly, P. Hollman, C. L. Keen, G. Mazza, M. Messina, A. Scalbert, J. Vita, G. Williamson and J. Burrowes (2007).

References

- "Flavonoids and heart health: proceedings of the ILSI North America Flavonoids Workshop, May 31-June 1, 2005, Washington, DC." *J Nutr* **137**(3 Suppl 1): 718S-737S.
- Eyre, H., R. Kahn and R. M. Robertson (2004). "Preventing cancer, cardiovascular disease, and diabetes: a common agenda for the American Cancer Society, the American Diabetes Association, and the American Heart Association." *CA: a cancer journal for clinicians* **54**(4): 190-207.
- Farkas, K., E. Kolossváry, Z. Járai, J. Nemcsik and C. Farsang (2004). Non-invasive assessment of microvascular endothelial function by laser Doppler flowmetry in patients with essential hypertension. *Atherosclerosis*. **173**: 97-102.
- Figueroa, A., F. Vicil and M. A. Sanchez-Gonzalez (2011). "Acute exercise with whole-body vibration decreases wave reflection and leg arterial stiffness." *American journal of cardiovascular disease* **1**(1): 60-67.
- Forstermann, U., J. P. Boissel and H. Kleinert (1998). "Expressional control of the 'constitutive' isoforms of nitric oxide synthase (NOS I and NOS III)." *FASEB J* **12**(10): 773-790.
- Fratta Pasini, A., A. Albiero, C. Stranieri, M. Cominacini, A. Pasini, C. Mozzini, P. Vallerio, L. Cominacini and U. Garbin (2012). "Serum oxidative stress-induced repression of Nrf2 and GSH depletion: a mechanism potentially involved in endothelial dysfunction of young smokers." *PLoS One* **7**(1): e30291.
- Frick M, N. T. S. W. T. (2002). Flußvermittelte Vasodilatation (FMD) der Arteria brachialis: Methodik und klinischer Stellenwert. *Journal für Kardiologie*: 1-7.
- Fujii, N., M. C. Reinke, V. E. Brunt and C. T. Minson (2013). Impaired acetylcholine-induced cutaneous vasodilation in young smokers: roles of nitric oxide and prostanoids. *AJP: Heart and Circulatory Physiology*. **304**: H667-673.
- Fukuda, I., R. Mukai, M. Kawase, K. Yoshida and H. Ashida (2007). "Interaction between the aryl hydrocarbon receptor and its antagonists, flavonoids." *Biochem Biophys Res Commun* **359**(3): 822-827.
- Furchgott, R. F., M. H. Carvalho, M. T. Khan and K. Matsunaga (1987). "Evidence for endothelium-dependent vasodilation of resistance vessels by acetylcholine." *Blood Vessels* **24**(3): 145-149.
- Furchgott, R. F. and J. V. Zawadzki (1980). "The obligatory role of endothelial cells in the relaxation of arterial smooth muscle by acetylcholine." *Nature* **288**(5789): 373-376.
- Galleano, M., I. Bernatova, A. Puzserova, P. Balis, N. Sestakova, O. Pechanova and C. G. Fraga (2013). "(-)-Epicatechin reduces blood pressure and improves vasorelaxation in spontaneously hypertensive rats by NO-mediated mechanism." *IUBMB Life*.
- Galleano, M., S. V. Verstraeten, P. I. Oteiza and C. G. Fraga (2010). "Antioxidant actions of flavonoids: thermodynamic and kinetic analysis." *Arch Biochem Biophys* **501**(1): 23-30.
- Gelatt-Nicholson, K. J., K. N. Gelatt, E. O. MacKay, D. E. Brooks and S. M. Newell (1999). Comparative Doppler imaging of the ophthalmic vasculature in normal Beagles and Beagles with inherited primary open-angle glaucoma. *Vet Ophthalmol*. **2**: 97-105.
- Gendron, M. E., N. Thorin-Trescases, A. M. Mamarbachi, L. Villeneuve, J. F. Theoret, Y. Mehri and E. Thorin (2012). "Time-dependent beneficial effect of chronic polyphenol treatment with catechin on endothelial dysfunction in aging mice." *Dose Response* **10**(1): 108-119.
- Getz, G. S. and C. A. Reardon (2012). "Animal models of atherosclerosis." *Arterioscler Thromb Vasc Biol* **32**(5): 1104-1115.
- Godecke, A., U. K. Decking, Z. Ding, J. Hirchenhain, H. J. Bidmon, S. Godecke and J. Schrader (1998). "Coronary hemodynamics in endothelial NO synthase knockout mice." *Circ Res* **82**(2): 186-194.
- Gomez-Guzman, M., R. Jimenez, M. Sanchez, M. Romero, F. O'Valle, R. Lopez-Sepulveda, A. M. Quintela, P. Galindo, M. J. Zarzuelo, E. Bailon, E. Delpon, F. Perez-Vizcaino and J. Duarte (2011).

References

- "Chronic (-)-epicatechin improves vascular oxidative and inflammatory status but not hypertension in chronic nitric oxide-deficient rats." *Br J Nutr* **106**(9): 1337-1348.
- Gomez-Guzman, M., R. Jimenez, M. Sanchez, M. J. Zarzuelo, P. Galindo, A. M. Quintela, R. Lopez-Sepulveda, M. Romero, J. Tamargo, F. Vargas, F. Perez-Vizcaino and J. Duarte (2012). "Epicatechin lowers blood pressure, restores endothelial function, and decreases oxidative stress and endothelin-1 and NADPH oxidase activity in DOCA-salt hypertension." *Free Radic Biol Med* **52**(1): 70-79.
- Grassi, D., S. Necozione, C. Lippi, G. Croce, L. Valeri, P. Pasqualetti, G. Desideri, J. B. Blumberg and C. Ferri (2005). "Cocoa reduces blood pressure and insulin resistance and improves endothelium-dependent vasodilation in hypertensives." *Hypertension* **46**(2): 398-405.
- Greco, A., M. Ragucci, R. Liuzzi, S. Gargiulo, M. Gramanzini, A. R. D. Coda, S. Albanese, M. Mancini, M. Salvatore and A. Brunetti (2013). Repeatability, reproducibility and standardisation of a laser Doppler imaging technique for the evaluation of normal mouse hindlimb perfusion. *Sensors (Basel)*. **13**: 500-515.
- Gu, L., M. A. Kelm, J. F. Hammerstone, G. Beecher, J. Holden, D. Haytowitz, S. Gebhardt and R. L. Prior (2004). "Concentrations of proanthocyanidins in common foods and estimations of normal consumption." *J Nutr* **134**(3): 613-617.
- Guleria, R. S., A. Jain, V. Tiwari and M. K. Misra (2002). "Protective effect of green tea extract against the erythrocytic oxidative stress injury during mycobacterium tuberculosis infection in mice." *Mol Cell Biochem* **236**(1-2): 173-181.
- Han, S. G., S. S. Han, M. Toborek and B. Hennig (2012). "EGCG protects endothelial cells against PCB 126-induced inflammation through inhibition of AhR and induction of Nrf2-regulated genes." *Toxicol Appl Pharmacol* **261**(2): 181-188.
- He, F. J., C. A. Nowson, M. Lucas and G. A. MacGregor (2007). "Increased consumption of fruit and vegetables is related to a reduced risk of coronary heart disease: meta-analysis of cohort studies." *Journal of human hypertension* **21**(9): 717-728.
- Heiss, C., A. Dejam, P. Kleinbongard, T. Schewe, H. Sies and M. Kelm (2003). "Vascular effects of cocoa rich in flavan-3-ols." *JAMA* **290**(8): 1030-1031.
- Heiss, C., D. Finis, P. Kleinbongard, A. Hoffmann, T. Rassaf, M. Kelm and H. Sies (2007). "Sustained increase in flow-mediated dilation after daily intake of high-flavanol cocoa drink over 1 week." *J Cardiovasc Pharmacol* **49**(2): 74-80.
- Heiss, C., S. Jahn, M. Taylor, W. M. Real, F. S. Angeli, M. L. Wong, N. Amabile, M. Prasad, T. Rassaf, J. I. Ottaviani, S. Mihardja, C. L. Keen, M. L. Springer, A. Boyle, W. Grossman, S. A. Glantz, H. Schroeter and Y. Yeghiazarians (2010). "Improvement of endothelial function with dietary flavanols is associated with mobilization of circulating angiogenic cells in patients with coronary artery disease." *Journal of the American College of Cardiology* **56**(3): 218-224.
- Heiss, C., C. L. Keen and M. Kelm (2010). "Flavanols and cardiovascular disease prevention." *Eur Heart J* **31**(21): 2583-2592.
- Heiss, C., P. Kleinbongard, A. Dejam, S. Perré, H. Schroeter, H. Sies and M. Kelm (2005). "Acute consumption of flavanol-rich cocoa and the reversal of endothelial dysfunction in smokers." *Journal of the American College of Cardiology* **46**(7): 1276-1283.
- Heiss, C., T. Lauer, A. Dejam, P. Kleinbongard, S. Hamada, T. Rassaf, S. Matern, M. Feelisch and M. Kelm (2006). "Plasma nitroso compounds are decreased in patients with endothelial dysfunction." *J Am Coll Cardiol* **47**(3): 573-579.
- Heiss, C., R. E. Sievers, N. Amabile, T. Y. Momma, Q. Chen, S. Natarajan, Y. Yeghiazarians and M. L. Springer (2007). In vivo measurement of flow-mediated vasodilation in living rats using high-resolution ultrasound. *AJP: Heart and Circulatory Physiology*. **294**: H1086-H1093.

References

- Helisch, A., S. Wagner, N. Khan, M. Drinane, S. Wolfram, M. Heil, T. Ziegelhoeffer, U. Brandt, J. D. Pearlman, H. M. Swartz and W. Schaper (2006). "Impact of mouse strain differences in innate hindlimb collateral vasculature." *Arterioscler Thromb Vasc Biol* **26**(3): 520-526.
- Hendgen-Cotta, U., M. Grau, T. Rassaf, P. Gharini, M. Kelm and P. Kleinbongard (2008). "Reductive gas-phase chemiluminescence and flow injection analysis for measurement of the nitric oxide pool in biological matrices." *Methods Enzymol* **441**: 295-315.
- Hollman, P. C., A. Cassidy, B. Comte, M. Heinonen, M. Richelle, E. Richling, M. Serafini, A. Scalbert, H. Sies and S. Vidry (2011). "The biological relevance of direct antioxidant effects of polyphenols for cardiovascular health in humans is not established." *J Nutr* **141**(5): 989S-1009S.
- Holt, R. R., C. Heiss, M. Kelm and C. L. Keen (2012). "The potential of flavanol and procyanidin intake to influence age-related vascular disease." *J Nutr Gerontol Geriatr* **31**(3): 290-323.
- Hooper, L., C. Kay, A. Abdelhamid, P. A. Kroon, J. S. Cohn, E. B. Rimm and A. Cassidy (2012). "Effects of chocolate, cocoa, and flavan-3-ols on cardiovascular health: a systematic review and meta-analysis of randomized trials." *Am J Clin Nutr* **95**(3): 740-751.
- Hutchison, S. J., K. Sudhir, R. E. Sievers, B. Q. Zhu, Y. P. Sun, T. M. Chou, K. Chatterjee, P. C. Deedwania, J. P. Cooke, S. A. Glantz and W. W. Parmley (1999). "Effects of L-arginine on atherogenesis and endothelial dysfunction due to secondhand smoke." *Hypertension* **34**(1): 44-50.
- Ignarro, L. J., G. M. Buga, K. S. Wood, R. E. Byrns and G. Chaudhuri (1987). "Endothelium-derived relaxing factor produced and released from artery and vein is nitric oxide." *Proc Natl Acad Sci U S A* **84**(24): 9265-9269.
- Itoh, K., T. Chiba, S. Takahashi, T. Ishii, K. Igarashi, Y. Katoh, T. Oyake, N. Hayashi, K. Satoh, I. Hatayama, M. Yamamoto and Y. Nabeshima (1997). "An Nrf2/small Maf heterodimer mediates the induction of phase II detoxifying enzyme genes through antioxidant response elements." *Biochem Biophys Res Commun* **236**(2): 313-322.
- Jakobsson, A. and G. E. Nilsson (1993). Prediction of sampling depth and photon pathlength in laser Doppler flowmetry. *Med Biol Eng Comput.* **31**: 301-307.
- Janssen-Heininger, Y. M., J. D. Nolin, S. M. Hoffman, J. L. van der Velden, J. E. Tully, K. G. Lahue, S. T. Abdalla, D. G. Chapman, N. L. Reynaert, A. van der Vliet and V. Anathy (2013). "Emerging mechanisms of glutathione-dependent chemistry in biology and disease." *J Cell Biochem* **114**(9): 1962-1968.
- Jarnert, C., M. Kalani, L. Rydén and F. Böhm (2012). Strict glycaemic control improves skin microcirculation in patients with type 2 diabetes: a report from the Diabetes mellitus And Diastolic Dysfunction (DADD) study. *Diab Vasc Dis Res.* **9**: 287-295.
- Kanatsuka, H., N. Sekiguchi, K. Sato, K. Akai, Y. Wang, T. Komaru, K. Ashikawa and T. Takishima (1992). Microvascular sites and mechanisms responsible for reactive hyperemia in the coronary circulation of the beating canine heart. *Circ Res.* **71**: 912-922.
- Kaner, D., H. Zhao, H. Terheyden and A. Friedmann (2013). Submucosal implantation of soft tissue expanders does not affect microcirculation. *Clin. Oral Impl. Res.:* n/a-n/a.
- Kapakos, G., A. Bouallegue, G. B. Daou and A. K. Srivastava (2010). "Modulatory Role of Nitric Oxide/cGMP System in Endothelin-1-Induced Signaling Responses in Vascular Smooth Muscle Cells." *Current cardiology reviews* **6**(4): 247-254.
- Karayannopoulou, M., L. P, P. LG, V. Tsioli, A. TL, A. N, C. TC, A. AN, K. E and P. VP (2010). Naturally occurring isohexenylnaphthazarins and wound healing: experimental study in dogs. *J Cutan Med Surg.* **14**: 62-70.
- Kaspar, J. W., S. K. Niture and A. K. Jaiswal (2009). "Nrf2:INrf2 (Keap1) signaling in oxidative stress." *Free Radic Biol Med* **47**(9): 1304-1309.

References

- Keen, C. L., R. R. Holt, P. I. Oteiza, C. G. Fraga and H. H. Schmitz (2005). "Cocoa antioxidants and cardiovascular health." *Am J Clin Nutr* **81**(1 Suppl): 298S-303S.
- Kenny, T. P., C. L. Keen, H. H. Schmitz and M. E. Gershwin (2007). "Immune effects of cocoa procyanidin oligomers on peripheral blood mononuclear cells." *Exp Biol Med (Maywood)* **232**(2): 293-300.
- Keymel, S., J. Siewhardt, J. Balzer, E. Stegemann, T. Rassaf, P. Kleinbongard, M. Kelm, C. Heiss and T. Lauer (2010). Characterization of the Non-Invasive Assessment of the Cutaneous Microcirculation by Laser Doppler Perfusion Scanner. *Microcirculation*: no-no.
- Kleinbongard, P., A. Dejam, T. Lauer, T. Rassaf, A. Schindler, O. Picker, T. Scheeren, A. Gödecke, J. Schrader, R. Schulz, G. Heusch, G. A. Schaub, N. S. Bryan, M. Feelisch and M. Kelm (2003). "Plasma nitrite reflects constitutive nitric oxide synthase activity in mammals." *Free radical biology & medicine* **35**(7): 790–796.
- Kluz, J., R. Małeckı and R. Adamiec (2013). Practical importance and modern methods of the evaluation of skin microcirculation during chronic lower limb ischemia in patients with peripheral arterial occlusive disease and/or diabetes. *Int Angiol.* **32**: 42-51.
- Kolluru, G. K., J. H. Siamwala and S. Chatterjee (2010). "eNOS phosphorylation in health and disease." *Biochimie* **92**(9): 1186–1198.
- Korashy, H. M. and A. O. El-Kadi (2006). "The role of aryl hydrocarbon receptor in the pathogenesis of cardiovascular diseases." *Drug Metab Rev* **38**(3): 411-450.
- Kubli, S., B. Waeber, A. Dalle-Ave and F. Feihl (2000). Reproducibility of laser Doppler imaging of skin blood flow as a tool to assess endothelial function. *J. Cardiovasc. Pharmacol.* **36**: 640-648.
- Kumar, N., R. Kant and P. K. Maurya (2010). "Concentration-dependent effect of (-) epicatechin in hypertensive patients." *Phytother Res* **24**(10): 1433-1436.
- Lee, J. M., K. Chan, Y. W. Kan and J. A. Johnson (2004). "Targeted disruption of Nrf2 causes regenerative immune-mediated hemolytic anemia." *Proc Natl Acad Sci U S A* **101**(26): 9751-9756.
- Leikert, J. F., T. R. Rathel, P. Wohlfart, V. Cheynier, A. M. Vollmar and V. M. Dirsch (2002). "Red wine polyphenols enhance endothelial nitric oxide synthase expression and subsequent nitric oxide release from endothelial cells." *Circulation* **106**(13): 1614-1617.
- Leonardo, C. C., M. Agrawal, N. Singh, J. R. Moore, S. Biswal and S. Dore (2013). "Oral administration of the flavanol (-)-epicatechin bolsters endogenous protection against focal ischemia through the Nrf2 cytoprotective pathway." *Eur J Neurosci.*
- Levett, D. Z., B. O. Fernandez, H. L. Riley, D. S. Martin, K. Mitchell, C. A. Leckstrom, C. Ince, B. J. Whipp, M. G. Mythen, H. E. Montgomery, M. P. Grocott, M. Feelisch and G. Caudwell Extreme Everest Research (2011). "The role of nitrogen oxides in human adaptation to hypoxia." *Sci Rep* **1**: 109.
- Levy, A. S., C. Vigna and J. W. Rush (2012). "Glutathione enhances endothelium-mediated control of coronary vascular resistance via a ROS- and NO intermediate-dependent mechanism." *J Appl Physiol (1985)* **113**(2): 246-254.
- Li, H. and U. Forstermann (2000). "Nitric oxide in the pathogenesis of vascular disease." *J Pathol* **190**(3): 244-254.
- Liang, C. P. and A. R. Tall (2001). "Transcriptional profiling reveals global defects in energy metabolism, lipoprotein, and bile acid synthesis and transport with reversal by leptin treatment in ob/ob mouse liver." *J Biol Chem* **276**(52): 49066-49076.
- Lichtenstein, A. H., L. J. Appel, M. Brands, M. Carnethon, S. Daniels, H. A. Franch, B. Franklin, P. Kris-Etherton, W. S. Harris, B. Howard, N. Karanja, M. Lefevre, L. Rudel, F. Sacks, L. van Horn, M. Winston and J. Wylie-Rosett (2006). "Diet and lifestyle recommendations revision 2006: a

References

- scientific statement from the American Heart Association Nutrition Committee." Circulation **114**(1): 82–96.
- Limbourg, A., T. Korff, L. C. Napp, W. Schaper, H. Drexler and F. P. Limbourg (2009). Evaluation of postnatal arteriogenesis and angiogenesis in a mouse model of hind-limb ischemia. Nat Protoc. **4**: 1737-1746.
- Litterio, M. C., G. Jagers, G. Sagdicoglu Celep, A. M. Adamo, M. A. Costa, P. I. Oteiza, C. G. Fraga and M. Galleano (2012). "Blood pressure-lowering effect of dietary (-)-epicatechin administration in L-NAME-treated rats is associated with restored nitric oxide levels." Free Radic Biol Med **53**(10): 1894-1902.
- Loke, W. M., J. M. Hodgson, J. M. Proudfoot, A. J. McKinley, I. B. Puddey and K. D. Croft (2008). "Pure dietary flavonoids quercetin and (-)-epicatechin augment nitric oxide products and reduce endothelin-1 acutely in healthy men." Am J Clin Nutr **88**(4): 1018-1025.
- Long, J., S. Wang, Y. Zhang, X. Liu, H. Zhang and S. Wang (2013). "The therapeutic effect of vascular endothelial growth factor gene- or heme oxygenase-1 gene-modified endothelial progenitor cells on neovascularization of rat hindlimb ischemia model." J Vasc Surg **58**(3): 756-765 e752.
- Long, L. H., A. Hoi and B. Halliwell (2010). "Instability of, and generation of hydrogen peroxide by, phenolic compounds in cell culture media." Arch Biochem Biophys **501**(1): 162-169.
- Lu, Y., R. Yao, Y. Yan, Y. Wang, Y. Hara, R. A. Lubet and M. You (2006). "A gene expression signature that can predict green tea exposure and chemopreventive efficacy of lung cancer in mice." Cancer Res **66**(4): 1956-1963.
- Lüscher, T. F., Z. Yang, M. Tschudi, L. v. Segesser, P. Stulz, C. Boulanger, R. Siebenmann, M. Turina and F. R. Bühler (1990). "Interaction between endothelin-1 and endothelium-derived relaxing factor in human arteries and veins." Circulation research **66**(4): 1088–1094.
- Mantovani, A., F. Bussolino and M. Introna (1997). "Cytokine regulation of endothelial cell function: from molecular level to the bedside." Immunol Today **18**(5): 231-240.
- Martin, M. A., S. Ramos, R. Mateos, M. Izquierdo-Pulido, L. Bravo and L. Goya (2010). "Protection of human HepG2 cells against oxidative stress by the flavonoid epicatechin." Phytother Res **24**(4): 503-509.
- Martin, S., E. Gonzalez-Burgos, M. E. Carretero and M. P. Gomez-Serranillos (2013). "Protective effects of Merlot red wine extract and its major polyphenols in PC12 cells under oxidative stress conditions." J Food Sci **78**(1): H112-118.
- Mattace-Raso F, H. A., Verwoert GC, Wittemana JC, Wilkinson I, Cockcroft J, McEniery C, Yasmin, Laurent S, Boutouyrie P, Bozec E, Hansen TW, Torp-Pedersen C, Ibsen H, Jeppesen J, Vermeersch SJ, Rietzschel E, De Buyzere M, Gillebert TC, Van Bortel L, Segers P, Vlachopoulos C, Aznaouridis C, Stefanadis C, Benetos A, Labat C, Lacolley P, Stehouwer C, Nijpels G, Dekker JM, Stehouwer C, Ferreira I, Twisk JW, Czernichow S, Galan P, Hercberg S, Pannier B, Guérin A, London G, Cruickshank JK, Anderson SG, Paini A, Agabiti Rosei E, Muiesan ML, Salvetti M, Filipovsky J, Seidlerova J, Dolejsova M. (2010). "Determinants of pulse wave velocity in healthy people and in the presence of cardiovascular risk factors: 'establishing normal and reference values'." European heart journal **31**(19): 2338–2350.
- Mauskar, N. A., S. Sood, T. E. Travis, S. E. Matt, M. J. Mino, M.-S. Burnett, L. T. Moffatt, P. Fidler, S. E. Epstein, M. H. Jordan and J. W. Shupp (2013). Donor Site Healing Dynamics: Molecular, Histological, and Noninvasive Imaging Assessment in a Porcine Model. J Burn Care Res.
- Mc Clean, C. M., J. Mc Laughlin, G. Burke, M. H. Murphy, T. Trinick, E. Duly and G. W. Davison (2007). "The effect of acute aerobic exercise on pulse wave velocity and oxidative stress following postprandial hypertriglyceridemia in healthy men." European journal of applied physiology **100**(2): 225–234.

References

- McCullough, M. L., J. J. Peterson, R. Patel, P. F. Jacques, R. Shah and J. T. Dwyer (2012). "Flavonoid intake and cardiovascular disease mortality in a prospective cohort of US adults." Am J Clin Nutr **95**(2): 454-464.
- Morgado, M., E. Cairrão, A. J. Santos-Silva and I. Verde (2012). "Cyclic nucleotide-dependent relaxation pathways in vascular smooth muscle." Cellular and molecular life sciences : CMLS **69**(2): 247–266.
- Mukai, R., I. Fukuda, S. Nishiumi, M. Natsume, N. Osakabe, K. Yoshida and H. Ashida (2008). "Cacao polyphenol extract suppresses transformation of an aryl hydrocarbon receptor in C57BL/6 mice." J Agric Food Chem **56**(21): 10399-10405.
- Mukai, R., Y. Shirai, N. Saito, I. Fukuda, S. Nishiumi, K. Yoshida and H. Ashida (2010). "Suppression mechanisms of flavonoids on aryl hydrocarbon receptor-mediated signal transduction." Arch Biochem Biophys **501**(1): 134-141.
- Mulvihill, E. E. and M. W. Huff (2010). "Antiatherogenic properties of flavonoids: implications for cardiovascular health." Can J Cardiol **26 Suppl A**: 17A-21A.
- Murthy, K. S. and H. Zhou (2003). "Selective phosphorylation of the IP3R-I in vivo by cGMP-dependent protein kinase in smooth muscle." American journal of physiology. Gastrointestinal and liver physiology **284**(2): G221-230.
- Narayanan, D., A. Adebisi and J. H. Jaggard (2012). "Inositol trisphosphate receptors in smooth muscle cells." American journal of physiology. Heart and circulatory physiology **302**(11): H2190-2210.
- Nausch, L. W. M., J. Ledoux, A. D. Bonev, M. T. Nelson and W. R. Dostmann (2008). "Differential patterning of cGMP in vascular smooth muscle cells revealed by single GFP-linked biosensors." Proceedings of the National Academy of Sciences of the United States of America **105**(1): 365–370.
- Ndiaye, M., M. Chataigneau, I. Lobysheva, T. Chataigneau and V. B. Schini-Kerth (2005). "Red wine polyphenol-induced, endothelium-dependent NO-mediated relaxation is due to the redox-sensitive PI3-kinase/Akt-dependent phosphorylation of endothelial NO-synthase in the isolated porcine coronary artery." FASEB J **19**(3): 455-457.
- Njike, V. Y., Z. Faridi, K. Shuval, S. Dutta, C. D. Kay, S. G. West, P. M. Kris-Etherton and D. L. Katz (2011). "Effects of sugar-sweetened and sugar-free cocoa on endothelial function in overweight adults." International journal of cardiology **149**(1): 83–88.
- Ohtsuji, M., F. Katsuoka, A. Kobayashi, H. Aburatani, J. D. Hayes and M. Yamamoto (2008). "Nrf1 and Nrf2 play distinct roles in activation of antioxidant response element-dependent genes." J Biol Chem **283**(48): 33554-33562.
- Oppermann, M., T. Suvorava, T. Freudenberger, V. T. Dao, J. W. Fischer, M. Weber and G. Kojda (2011). "Regulation of vascular guanylyl cyclase by endothelial nitric oxide-dependent posttranslational modification." Basic Res Cardiol **106**(4): 539-549.
- Ostertag, L. M., N. O'Kennedy, P. A. Kroon, G. G. Duthie and B. de Roos (2010). "Impact of dietary polyphenols on human platelet function--a critical review of controlled dietary intervention studies." Mol Nutr Food Res **54**(1): 60-81.
- Ottaviani, J. I., T. Y. Momma, C. Heiss, C. Kwik-Urbe, H. Schroeter and C. L. Keen (2011). "The stereochemical configuration of flavanols influences the level and metabolism of flavanols in humans and their biological activity in vivo." Free Radic Biol Med **50**(2): 237-244.
- Palmer, R. M., D. S. Ashton and S. Moncada (1988). "Vascular endothelial cells synthesize nitric oxide from L-arginine." Nature **333**(6174): 664-666.
- Palmer, R. M., A. G. Ferrige and S. Moncada (1987). "Nitric oxide release accounts for the biological activity of endothelium-derived relaxing factor." Nature **327**(6122): 524-526.
- Petschke, F. T., T. O. Engelhardt, H. Ulmer and H. Piza-Katzer (2006). [Effect of cigarette smoking on skin perfusion of the hand]. Chirurg. **77**: 1022-1026.

References

- Piskula, M. K. and J. Terao (1998). "Accumulation of (-)-epicatechin metabolites in rat plasma after oral administration and distribution of conjugation enzymes in rat tissues." The Journal of nutrition **128**(7): 1172–1178.
- Prasad, A., N. P. Andrews, F. A. Padder, M. Husain and A. A. Quyyumi (1999). "Glutathione reverses endothelial dysfunction and improves nitric oxide bioavailability." J Am Coll Cardiol **34**(2): 507-514.
- Pyke, K. E. and M. E. Tschakovsky (2005). The relationship between shear stress and flow-mediated dilatation: implications for the assessment of endothelial function. The Journal of Physiology. **568**: 357-369.
- Pyke, K. E. and M. E. Tschakovsky (2007). "Peak vs. total reactive hyperemia: which determines the magnitude of flow-mediated dilation?" J Appl Physiol (1985) **102**(4): 1510-1519.
- Ramirez-Sanchez, I., L. Maya, G. Ceballos and F. Villarreal (2010). "(-)-epicatechin activation of endothelial cell endothelial nitric oxide synthase, nitric oxide, and related signaling pathways." Hypertension **55**(6): 1398-1405.
- Ramirez-Sanchez, I., L. Maya, G. Ceballos and F. Villarreal (2011). "(-)-Epicatechin induces calcium and translocation independent eNOS activation in arterial endothelial cells." Am J Physiol Cell Physiol **300**(4): C880-887.
- Rassaf, T., C. Heiss, U. Hendgen-Cotta, J. Balzer, S. Matern, P. Kleinbongard, A. Lee, T. Lauer and M. Kelm (2006). "Plasma nitrite reserve and endothelial function in the human forearm circulation." Free radical biology & medicine **41**(2): 295–301.
- Redmond, E. M., P. A. Cahill, R. Hodges, S. Zhang and J. V. Sitzmann (1996). "Regulation of endothelin receptors by nitric oxide in cultured rat vascular smooth muscle cells." Journal of cellular physiology **166**(3): 469–479.
- Rein, D., S. Lotito, R. R. Holt, C. L. Keen, H. H. Schmitz and C. G. Fraga (2000). "Epicatechin in human plasma: in vivo determination and effect of chocolate consumption on plasma oxidation status." J Nutr **130**(8S Suppl): 2109S-2114S.
- Rice-Evans, C. A., N. J. Miller and G. Paganga (1996). "Structure-antioxidant activity relationships of flavonoids and phenolic acids." Free Radic Biol Med **20**(7): 933-956.
- Ried, K., T. R. Sullivan, P. Fakler, O. R. Frank and N. P. Stocks (2012). "Effect of cocoa on blood pressure." Cochrane Database Syst Rev **8**: CD008893.
- Rivard, A., J. E. Fabre, M. Silver, D. Chen, T. Murohara, M. Kearney, M. Magner, T. Asahara and J. M. Isner (1999). "Age-dependent impairment of angiogenesis." Circulation **99**(1): 111-120.
- Rizvi, S. I. and M. A. Zaid (2001). "Intracellular reduced glutathione content in normal and type 2 diabetic erythrocytes: effect of insulin and (-)-epicatechin." J Physiol Pharmacol **52**(3): 483-488.
- Rodriguez-Mateos, A., C. Rendeiro, T. Bergillos-Meca, S. Tabatabaee, T. W. George, C. Heiss and J. P. Spencer (2013). "Intake and time dependence of blueberry flavonoid-induced improvements in vascular function: a randomized, controlled, double-blind, crossover intervention study with mechanistic insights into biological activity." Am J Clin Nutr **98**(5): 1179-1191.
- Rodriguez-Ramiro, I., M. A. Martin, S. Ramos, L. Bravo and L. Goya (2011). "Comparative effects of dietary flavanols on antioxidant defences and their response to oxidant-induced stress on Caco2 cells." Eur J Nutr **50**(5): 313-322.
- Romeo, L., M. Intriери, V. D'Agata, N. G. Mangano, G. Oriani, M. L. Ontario and G. Scapagnini (2009). "The major green tea polyphenol, (-)-epigallocatechin-3-gallate, induces heme oxygenase in rat neurons and acts as an effective neuroprotective agent against oxidative stress." J Am Coll Nutr **28** Suppl: 492S-499S.

References

- Ruijters, E. J., A. R. Weseler, C. Kicken, G. R. Haenen and A. Bast (2013). "The flavanol (-)-epicatechin and its metabolites protect against oxidative stress in primary endothelial cells via a direct antioxidant effect." *Eur J Pharmacol* **715**(1-3): 147-153.
- Ruiz-Nuno, A., A. Rosado, A. G. Garcia, M. G. Lopez and M. Villarroya (2004). "Differences in the vascular selectivity and tolerance between the NO donor/beta-blocker PF9404C and nitroglycerin." *Eur J Pharmacol* **498**(1-3): 203-210.
- Sachdev, U., X. Cui and E. Tzeng (2013). HMGB1 and TLR4 mediate skeletal muscle recovery in a murine model of hindlimb ischemia. *J. Vasc. Surg.* **58**: 460-469.
- Scapagnini, G., S. Vasto, N. G. Abraham, C. Caruso, D. Zella and G. Fabio (2011). "Modulation of Nrf2/ARE pathway by food polyphenols: a nutritional neuroprotective strategy for cognitive and neurodegenerative disorders." *Mol Neurobiol* **44**(2): 192-201.
- Scheid, L., A. Reusch, P. Stehle and S. Ellinger (2010). "Antioxidant effects of cocoa and cocoa products ex vivo and in vivo: is there evidence from controlled intervention studies?" *Curr Opin Clin Nutr Metab Care* **13**(6): 737-742.
- Schroeter, H., C. Heiss, J. Balzer, P. Kleinbongard, C. L. Keen, N. K. Hollenberg, H. Sies, C. Kwik-Uribe, H. H. Schmitz and M. Kelm (2006). "(-)-Epicatechin mediates beneficial effects of flavanol-rich cocoa on vascular function in humans." *Proc Natl Acad Sci U S A* **103**(4): 1024-1029.
- Seals, D. R., K. L. Jablonski and A. J. Donato (2011). "Aging and vascular endothelial function in humans." *Clin Sci (Lond)* **120**(9): 357-375.
- Seymour, E. M., M. R. Bennink and S. F. Bolling (2013). "Diet-relevant phytochemical intake affects the cardiac AhR and nrf2 transcriptome and reduces heart failure in hypertensive rats." *J Nutr Biochem* **24**(9): 1580-1586.
- Shah, Z. A., R. C. Li, A. S. Ahmad, T. W. Kensler, M. Yamamoto, S. Biswal and S. Dore (2010). "The flavanol (-)-epicatechin prevents stroke damage through the Nrf2/HO1 pathway." *J Cereb Blood Flow Metab* **30**(12): 1951-1961.
- Sies, H. (1993). "Strategies of antioxidant defense." *Eur J Biochem* **215**(2): 213-219.
- Sies, H. (1999). "Glutathione and its role in cellular functions." *Free Radic Biol Med* **27**(9-10): 916-921.
- Smiesko, V. and P. C. Johnson (1993). The arterial lumen is controlled by flow-related shear stress. *Physiology*, Am Physiological Soc. **8**: 34-38.
- Smolenski, A., C. Bachmann, K. Reinhard, P. Honig-Liedl, T. Jarchau, H. Hoschuetzky and U. Walter (1998). "Analysis and regulation of vasodilator-stimulated phosphoprotein serine 239 phosphorylation in vitro and in intact cells using a phosphospecific monoclonal antibody." *J Biol Chem* **273**(32): 20029-20035.
- Steffen, Y., T. Schewe and H. Sies (2007). "(-)-Epicatechin elevates nitric oxide in endothelial cells via inhibition of NADPH oxidase." *Biochem Biophys Res Commun* **359**(3): 828-833.
- Stephanie J. Muga, P. T., Qixia Zhang, Paula Martin, R. Scott Hudson, Lee Mangiante, and Elisabeth McCauley (2004). "Effect of dietary conjugated linoleic acid on apoptosis and gene expression in mouse colon and human colon cancer cell lines." *AACR Meeting Abstracts*.
- Stoen, R., K. Lossius, A. A. Persson and J. O. Karlsson (2001). "Relative significance of the nitric oxide (NO)/cGMP pathway and K⁺ channel activation in endothelium-dependent vasodilation in the femoral artery of developing piglets." *Acta Physiol Scand* **171**(1): 29-35.
- Sugamura, K. and J. F. Keaney, Jr. (2011). "Reactive oxygen species in cardiovascular disease." *Free Radic Biol Med* **51**(5): 978-992.
- Swain, J. H., A. M. Kresak and T. P. Pretiow (2007). "Tumor number and comparative microarray analysis of tumor and adjacent non-tumor intestinal tissue after iron supplementation in ApcMin/+ mice." *Faseb Journal* **21**(5): A384-A384.

References

- Takami, S., T. Imai, M. Hasumura, Y. M. Cho, J. Onose and M. Hirose (2008). "Evaluation of toxicity of green tea catechins with 90-day dietary administration to F344 rats." Food Chem Toxicol **46**(6): 2224-2229.
- Tannenbaum, S. R. (1979). "Nitrate and nitrite: origin in humans." Science **205**(4413): 1332, 1334-1337.
- Toh, J. Y., V. M. Tan, P. C. Lim, S. T. Lim and M. F. Chong (2013). "Flavonoids from fruit and vegetables: a focus on cardiovascular risk factors." Curr Atheroscler Rep **15**(12): 368.
- Umeda, D., S. Yano, K. Yamada and H. Tachibana (2008). "Involvement of 67-kDa laminin receptor-mediated myosin phosphatase activation in antiproliferative effect of epigallocatechin-3-O-gallate at a physiological concentration on Caco-2 colon cancer cells." Biochemical and biophysical research communications **371**(1): 172-176.
- Unosson, J., A. Blomberg, T. Sandström, A. Muala, C. Boman, R. Nyström, R. Westerholm, N. L. Mills, D. E. Newby, J. P. Langrish and J. A. Bosson (2013). "Exposure to wood smoke increases arterial stiffness and decreases heart rate variability in humans." Particle and fibre toxicology **10**(1): 20.
- Vlachopoulos, C., K. Aznaouridis, N. Alexopoulos, E. Economou, I. Andreadou and C. Stefanadis (2005). "Effect of dark chocolate on arterial function in healthy individuals." American journal of hypertension **18**(6): 785-791.
- Wakabayashi, N., S. L. Slocum, J. J. Skoko, S. Shin and T. W. Kensler (2010). "When NRF2 talks, who's listening?" Antioxid Redox Signal **13**(11): 1649-1663.
- Wallerath, T., D. Poleo, H. Li and U. Forstermann (2003). "Red wine increases the expression of human endothelial nitric oxide synthase: a mechanism that may contribute to its beneficial cardiovascular effects." J Am Coll Cardiol **41**(3): 471-478.
- Wang, J. and M. E. Widlansky (2009). "Lifestyle choices and endothelial function: risk and relevance." Current vascular pharmacology **7**(2): 209-224.
- Wang, J. F., D. D. Schramm, R. R. Holt, J. L. Ensunsa, C. G. Fraga, H. H. Schmitz and C. L. Keen (2000). "A dose-response effect from chocolate consumption on plasma epicatechin and oxidative damage." J Nutr **130**(8S Suppl): 2115S-2119S.
- Wang, S. I. and H. Mukhtar (2002). "Gene expression profile in human prostate LNCaP cancer cells by (-) epigallocatechin-3-gallate." Cancer Lett **182**(1): 43-51.
- Wardell, K., A. Jakobsson and G. E. Nilsson (1993). Laser Doppler perfusion imaging by dynamic light scattering. Biomedical Engineering, IEEE Transactions on, IEEE. **40**: 309-316.
- Weinreb, O., S. Mandel and M. B. Youdim (2003). "cDNA gene expression profile homology of antioxidants and their antiapoptotic and proapoptotic activities in human neuroblastoma cells." Faseb Journal **17**(8): 935-937.
- Weseler, A. R. and A. Bast (2010). "Oxidative stress and vascular function: implications for pharmacologic treatments." Curr Hypertens Rep **12**(3): 154-161.
- Weseler, A. R., E. J. Ruijters, M. J. Drittij-Reijnders, K. D. Reesink, G. R. Haenen and A. Bast (2011). "Pleiotropic benefit of monomeric and oligomeric flavanols on vascular health--a randomized controlled clinical pilot study." PLoS One **6**(12): e28460.
- Widlansky, M. E., N. Gokce, J. F. Keane, Jr. and J. A. Vita (2003). "The clinical implications of endothelial dysfunction." J Am Coll Cardiol **42**(7): 1149-1160.
- Wood, K. C., M. M. Cortese-Krott, J. C. Kovacic, A. Noguchi, V. B. Liu, X. Wang, N. Raghavachari, M. Boehm, G. J. Kato, M. Kelm and M. T. Gladwin (2013). "Circulating blood endothelial nitric oxide synthase contributes to the regulation of systemic blood pressure and nitrite homeostasis." Arteriosclerosis, thrombosis, and vascular biology **33**(8): 1861-1871.
- Woodman, O. L., O. Wongsawatkul and C. G. Sobey (2000). "Contribution of nitric oxide, cyclic GMP and K⁺ channels to acetylcholine-induced dilatation of rat conduit and resistance arteries." Clin Exp Pharmacol Physiol **27**(1-2): 34-40.

References

- Ying, L., X. Xu, J. Liu, D. Dou, X. Yu, L. Ye, Q. He and Y. Gao (2012). "Heterogeneity in relaxation of different sized porcine coronary arteries to nitrovasodilators: role of PKG and MYPT1." Pflügers Archiv : European journal of physiology **463**(2): 257–268.
- Zhu, B. Q., R. E. Sievers, A. E. Browne, R. J. Lee, K. Chatterjee, W. Grossman, J. S. Karliner and W. W. Parmley (2003). "Comparative effects of aspirin with ACE inhibitor or angiotensin receptor blocker on myocardial infarction and vascular function." J Renin Angiotensin Aldosterone Syst **4**(1): 31-37.
- Zhu, H., Z. Jia, L. Zhang, M. Yamamoto, H. P. Misra, M. A. Trush and Y. Li (2008). "Antioxidants and phase 2 enzymes in macrophages: regulation by Nrf2 signaling and protection against oxidative and electrophilic stress." Exp Biol Med (Maywood) **233**(4): 463-474.

Acknowledgment

This work was supported by the VIVID (in vivo investigations in metabolic pathomechanisms and diseases in Düsseldorf) graduate program funded by the Heinrich-Heine University of Düsseldorf, by the Deutsche Forschungsgemeinschaft (DFG KE405/5-1), as well as by the Susanne-Bunnenberg- Stiftung at Düsseldorf Heart Center to Prof. Dr. med. Malte Kelm.

As a result of four years of hard scientific work this dissertation would not be possible without the direct involvement of the persons I am going to thank. Nevertheless I would like to excuse in advance that not all persons that deserve an acknowledgment will be mentioned in this place.

I would like to thank:

Prof. Dr. med. Malte Kelm, director of the Department of Cardiology, Pneumology and Angiology, for giving me the opportunity to work in these exiting conditions of translational research. Further I appreciate his outstanding expertise and support to my work and I thank him for reviewing and examine this dissertation.

Prof. Dr. rer. nat. Eckhard Lammert, director of the Institute of Metabolic Physiology and spokesperson of VIVID, for being my supervisor, for the essential recommendations he gave me during progression and completion of this project and for review of the final examination.

A special thank is dedicated to Dr. rer. nat. Miriam M. Cortese-Krott for the supervision during the entire process of being a PhD candidate. She taught me how to deal with success and failure in daily laboratory work, how to manage the pressure of a young scientist and helped me to be independent and to develop my own ideas in interesting discussions. Also her practical experimental help was unalienable for this work. Finally I thank her for reviewing this dissertation and for the help in preparation of the final examination.

Acknowledgment

Dr. med. Christian Heiss, for giving me an insight into the field of flavanol research. He helped me to better understand the physiological complexity of the human cardiovascular system and supported the establishment of methods for assessment of vascular function in mice. I thank him for all the ideas, tips and discussions.

I sincerely thank all members of the cardiology lab. In particular I would like to thank Sivatharsini Thasian-Sivarajah for the experimental help in the establishment of the staining conditions for Western-blot analysis, assessment of NO metabolites in plasma and many others. Leena, you know that without you I would have never come this far. I am thanking you not only for the work you have done for me in the lab but in first place for your understanding and for being who you are. Please, never change your character, its unique.

I further thank Kim Weber for performing Western-Blot and real-time PCR analysis of targets in the mice tissues, Matthias Weidenbach for the help in establishment of in vivo methods and performing the measurement of blood pressure in mice and Dr. Ana Rodriguez-Mateos for measurement of metabolites in plasma of the mice.

Further special acknowledgement is dedicated to the stuff of our "mice-lab", in particular Steffi, Dominik and Rabia for the patient, detailed and comprehensive introduction into the difficult methodology of animal handling and experiments.

I additionally thank meanwhile called "Dr. rer. nat." Simone Zander, Rainer Windler and Martina Kropp, but also Dr. rer. nat. Margarete Lukosz and Sonja Ecken who helped me with all kind of questions, gave me the motivation and guided me the way on this difficult road.

I do not have to especially thank my family, my mother and my brother, they know that my life and all that I do would be worthless without them. The same is true for the other half of me and for my friends.

Curriculum Vitae

Personal Details

First Name: Tomasz

Family Name: Krenz

Date of Birth: September, 3th, 1983

Place of Birth: Lukow (Poland)

Current Address: Eichenkreuzstr. 19, 40589 Düsseldorf, Germany

Contact: thomas.krenz@uni-duesseldorf.de

Family Status: single

Nationality: German



Academic Studies

03/02/2014

Final exam. Title of PhD thesis: “*Role of eNOS and Nrf2 in the vascular effects of (-)-epicatechin*“

06/2012 – 02/2012

Membership of the VIVID graduate school (in vivo models for human metabolic diseases Düsseldorf).

Membership of iGRAD (Interdisciplinary Graduate and Research Academy Düsseldorf)

12/2009 –

PhD Candidate

Heinrich-Heine-Universität Düsseldorf

Division of Cardiology, Pulmonology and Angiology

WS 2007/2008 – SS 2009:

Master Biology

Heinrich-Heine-Universität Düsseldorf

Course specialization: Cell and Molecular Biology, Biochemistry

Master thesis: „Generation and characterization of clonal Unrestricted Somatic Stem Cells (USSC) from cord blood and analysis of the mesodermal differentiation potential“

Institute for Transplantation Diagnostics and Cell Therapeutics (ITZ)

Qualification: Master of Science (“excellent”)

WS 2004/2005 – SS 2007:

Bachelor Biology

Heinrich-Heine-Universität Düsseldorf

Bachelor thesis: „A comparison of methods for the qualitative and quantitative determination of RNA molecules in living cells “

Institute: Institute for Biophysics

Qualification: Bachelor of Science (Final grade:
"very good")

Civilien Service

09/2003 – 06/2004: Central Laboratory of the Community Hospital
in Solingen

Education

06/1994 – 06/2003: Secondary School August-Dicke in Solingen
Qualification: Abitur (Final grade: 2,8)

09/1991 – 05/1994: Primary School Meigen in Solingen

Work Experience

07/2007 – 09/2009: José Carreras Stem Cell Bank, Düsseldorf

02/2007 – 03/2007: During Bachelor Study at a laboratory for
hematology of the St.Lukas hospital in Solingen

10/2001 – 11/2001: DuPont® Performance Coatings

Publications / Abstracts

T. Krenz*, M. Weidenbach*, M. Cortese-Krott, and M. Kelm. *Endothelial dysfunction in mice lacking nuclear factor (erythroid-derived 2)-like 2*. Submitted for presentation in DGK's 80th Annual Meeting (2014)

T. Krenz, M. Cortese-Krott, M. Weidenbach, M. Totzeck, T. Rassaf, M. Kelm, C. Heiss. - *Laser Doppler perfusion imaging for non-invasive assessment of vascular responses in living mice*. Submitted for presentation in DGK's 79th Annual Meeting. Clin Res Cardiol 102, Suppl 1, (2013)

M. Cortese-Krott*, T. Krenz*, A. Rodriguez-Mateos, F. Oberle, K. Weber, D. Pullman, M. Haerberlein, S. Thasian-Sivarajah, J. Spencer, M. Kelm, M. W. Merx, C. Heiss. - *Analysis of acute and chronic effects of (-)-epicatechin on NO bioavailability and organ redox state in the cardiovascular system in vivo*. Submitted for presentation in DGK's 79th Annual Meeting. Clin Res Cardiol 102, Suppl 1, (2013)

Miriam M. Cortese-Krott, Ana Rodriguez-Mateos, Roberto Sansone, Gunter G. C. Kuhnle, Sivatharsini Thasian-Sivarajah, Thomas Krenz, Patrick Horn, Christoph Krisp, Dirk Wolters, Christian Heiß, Klaus-Dietrich Kröncke, Neil Hogg, Martin Feelisch and Malte Kelm. *Human red blood cells at work: identification and visualization of erythrocytic eNOS activity in health and disease*. Blood (2012).

Thomas Krenz, Miriam M Cortese-Krott, Malte Kelm, and Christian Heiss. *Non-Invasive Assessment of Vascular Responses in Living Mice Using Laser Doppler Perfusion Imaging*. Submitted for presentation in SFRBM's 19th Annual Meeting. Free Radical Biology and Medicine, Volume 53, Supplement 2, Page S45, (2012).

M.M. Cortese-Krott*, T. Krenz*, A. Rodriguez-Mateos, F. Oberle, S. Sivarajah, M. Kelm. *(-)-Epicatechin increases systemic Nrf2-dependent response and vascular function in mice*. Submitted for

Curriculum Vitae

presentation in SFRBM's 19th Annual Meeting. Free Radical Biology and Medicine, Volume 53, Supplement 1, Page S167, (2012).

Miriam M Cortese-Krott*, Thomas Krenz*, Ana Rodriguez-Mateos, Friederike Oberle, Kim Weber, Sivatharsini Thasian-Sivarajah, Malte Kelm, and Christian Heiss. *(-)-Epicatechin Increases NO Bioavailability and Nrf2- Dependent Response in the Vessel Wall in Vivo*. Submitted for presentation in SFRBM's 19th Annual Meeting. Free Radical Biology and Medicine, Volume 53, Supplement 2, Page S179, (2012).

Cortese-Krott, MM.*, Krenz, T.*, Rodriguez-Mateos, A., Oberle, F., Sivarajah, S., Heiss, C. and Kelm, M. *Molecular mechanisms involved in cocoa-induced vascular protection: a role of Nrf2*, submitted for presentation in DGK's 78th Annual Meeting. Clin Res Cardiol 101, Suppl 1. (2012).

Cortese-Krott, MM., Sansone, R., Sivarajah, S., Rodriguez-Mateos, A., Kuhnle, G., Krenz, T., Krisp, C., Horn, P., Wolters, D., Heiss, C. and Kelm, M. *Decreased expression and activity of red cell eNOS correlate with endothelial dysfunction in humans*, submitted for presentation in SFRBM's 18th Annual Meeting. Free Radical Biology and Medicine, Volume 51, Supplement 1, Page S157, (2011).

Cortese-Krott, MM., Horn, P., Krenz, T., Krisp, C., Sivarajah, S., Lysaja, K., Strigl, F., Kröncke, K-D., Heiss, C. and Kelm, M. *Isolation, Characterisation, and Activity of an Endothelial Nitric Oxide Synthase in Human Red Blood Cells*, submitted for presentation in SFRBM's 17th Annual Meeting. Free Radical Biology and Medicine, Volume 49, Supplement, (2010)

Kluth, S., Buchheiser, A., Houben, A., Geyh, S., Krenz, T., Radke, TF., Wiek, C., Hanenberg, H., Reinecke, P., Wernet, P., Kögler, G. *DLK-1 as a marker to distinguish unrestricted somatic stem cells and mesenchymal stromal cells in cord blood*, Stem Cells Dev. 2010

Krenz, T., Geyh, S., Kluth, S., Wernet, P., Wiek, C. Hanenberg, H., Buchheiser, A. and Kögler, G. *Generation of clonal derived Unrestricted Somatic Stem Cells (USSC) from cord blood and analysis of their expression and differentiation potential*, submitted for poster presentation in Stem Cell Network North Rhine-Westphalia (2009).

Additional

Language skills: English (written and spoken)
Polish (native language)
Spanish (school knowledge)
French (school knowledge)

Achievements

during studies: VIVID scholarship funded by the Heinrich-Heine-Universität Düsseldorf
Grant from the Dr. Jost Henkel Stiftung
Poster-Award (5th International Meeting, Stem Cell Network North Rhine-Westphalia)

Additional Courses and

“Time Management-Get more done with less Effort”
“Writing workshop – research paper”

Curriculum Vitae

Workshops

“Presenting science 1 – comprehensive, competent and convincing”

“Good Scientific Practice”

“Felasa - Federation for Laboratory Animal Science Associations

“English – Grammar I“

“English – Grammar II“

“Adobe Photoshop – workshop“

Interests:

sportive activities in privacy as well as at college
(Soccer, Swimming, Running, Bicycling)

Music, Cinema, Movies